Microphysical (activation and mixing) impact on shallow cumulus convection

Joanna Slawinska, University of Warsaw
Wojciech Grabowski, NCAR
Andrzej Wyszogrodzki, NCAR
Hugh Morrison, NCAR
Hanna Pawlowska, University of Warsaw

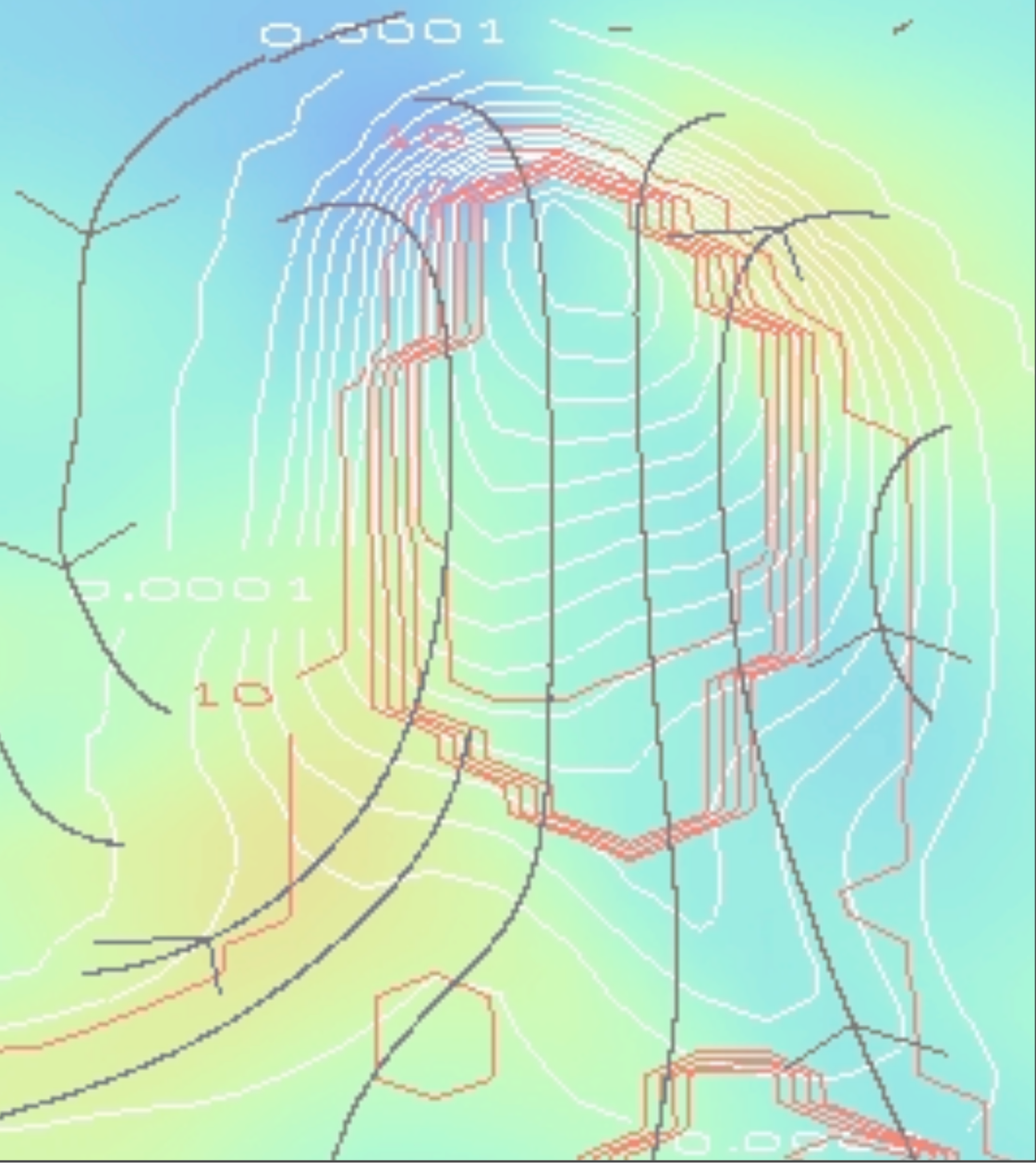

Tools and settings

- numerical model EULAG: http://www.mmm.ucar.edu/eulag/
- 3-dimensional LES
- EULERIAN version, Cartesian mesh
- parallel computing, supercomputer frost (NCAR)
- Two-moment bulk scheme (*Morrison and Grabowski 2007, 2008*)

Prognostic variables:

- supersaturation
- concentration of activated CCN
- cloud water mixing ratio, q_c
- cloud droplet concentration, n_c
- rain water mixing ratio, q_r
- rain drops concentration, n_r

$$\frac{\partial N}{\partial t} + \frac{1}{\rho_a}\nabla \cdot [\rho_a(\mathbf{u} - V_N\mathbf{k})N] = \mathcal{F}_N \equiv$$

$$\equiv \left(\frac{\partial N}{\partial t}\right)_{act} + \left(\frac{\partial N}{\partial t}\right)_{cond} + \left(\frac{\partial N}{\partial t}\right)_{acc} + \left(\frac{\partial N}{\partial t}\right)_{auto} + \left(\frac{\partial N}{\partial t}\right)_{self} + \mathcal{D}(N)$$

$$\frac{\partial q}{\partial t} + \frac{1}{\rho_a}\nabla \cdot [\rho_a(\mathbf{u} - V_q\mathbf{k})q] = \mathcal{F}_q \equiv$$

$$\equiv \left(\frac{\partial q}{\partial t}\right)_{act} + \left(\frac{\partial q}{\partial t}\right)_{cond} + \left(\frac{\partial q}{\partial t}\right)_{acc} + \left(\frac{\partial q}{\partial t}\right)_{auto} + \mathcal{D}(q)$$

Microphysics

- Gamma size distributions: $N(D)=N_0 D^{\mu} e^{-\lambda D}$
- The parameter $\mu=\eta^{-2}-1$ uses parametrizations of Martin et al. (1994):

$$\eta = 0.0005714 N_c + 0.2714.$$

- The droplet effective radius, $r_{e,f,}$ is equal to:

$$r_{e,f} = \frac{\Gamma(\mu_f + 4)}{2\lambda_f \Gamma(\mu_f + 3)}$$

where Γ - Euler gamma function

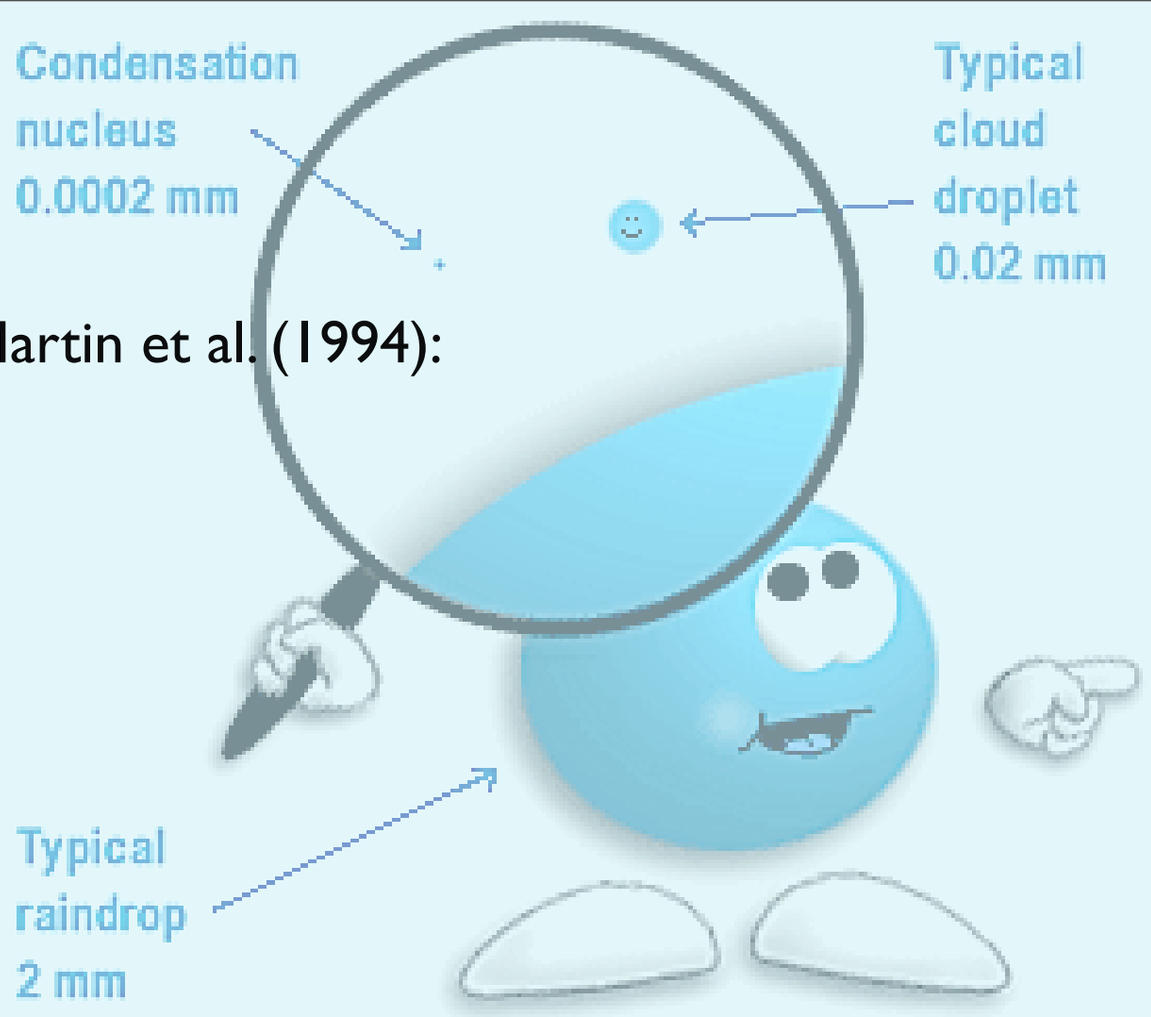

Photosource: http://www.bom.gov.au/

- Kohler theory is applied to determine the concentration of activated CCN, with locally predicted supersaturation and assumed homogeneous concentration of background aerosol.
- Changes in water vapour and cloud water mixing ratios, are determined with the assumption of a 1μm radius for freshly activated CCN.
- The condensation/evaporation rate is calculated for cloud water and rain as:

$$S_{q_v,2} = -S_{\varphi_1,2} = \frac{q_v - q_{vs}}{\tau_{\varphi_1}} \left(1 + \frac{dq}{dT}\frac{L_v}{c_p}\right)^{-1}$$

- Possible three different parametrizations for the coalescence processes: Beheng (1994), Seifert and Beheng (2001), Khairoutdinov and Kogan (2000)

Subgrid scale mixing

Mixing scenario depends on the time scale of mixing and the time scale of evaporation.

- *extremely inhomogeneous:*

Time scale of cloud droplet evaporation is significantly larger than time scale of turbulent mixing

Cloud droplet concentration decreases

Mean cloud droplet radius does not change

- *inhomogeneous:*

Concentration and mean cloud droplet radius decrease

- *homogeneous:*

Time scale of turbulent mixing is significantly larger than time scale of cloud droplet evaporation

Cloud droplet concentration "constant" (affected only by dilution)

Mean cloud droplet radius decreases

Subgrid scale mixing

Microphysical adjustment for tendencies due to mixing:

$$N_f = N_i \left(\frac{q_f}{q_i} \right)^{\alpha}$$

- Mixing scenarios:

  - extremely inhomogeneous: ($\alpha = 1$)
  - inhomogeneous: ($0 < \alpha < 1$)
  - homogeneous: ($\alpha = 0$)

- i - initial value (after turbulent mixing, before evaporation)
- f - final values (after turbulent mixing and evaporation)

Bomex case

Simulated case: BOMEX

- Barbados Oceanographic and Meteorological Experiment
- Date: summer 1969
- Place: Atlantic East of Barbados

Setup

- Computational domain:
  - 6.4 km × 6.4 km × 3 km
  - nx=ny=128 nz=151
  - dx=dy=2.5 × dz = 100 m
  - dt =1s

The simulations are run for 6 h.
Data are stored every 10 minutes.
The last 3 hours are used in the analysis.

Initial profiles, boundary conditions, surface fluxes and large-scale forcings follows Siebesma et al. (2003).

Background aerosol concentration, either:
100 mg^{-1} (PRISTINE case)
1000 mg^{-1} (POLLUTED case)

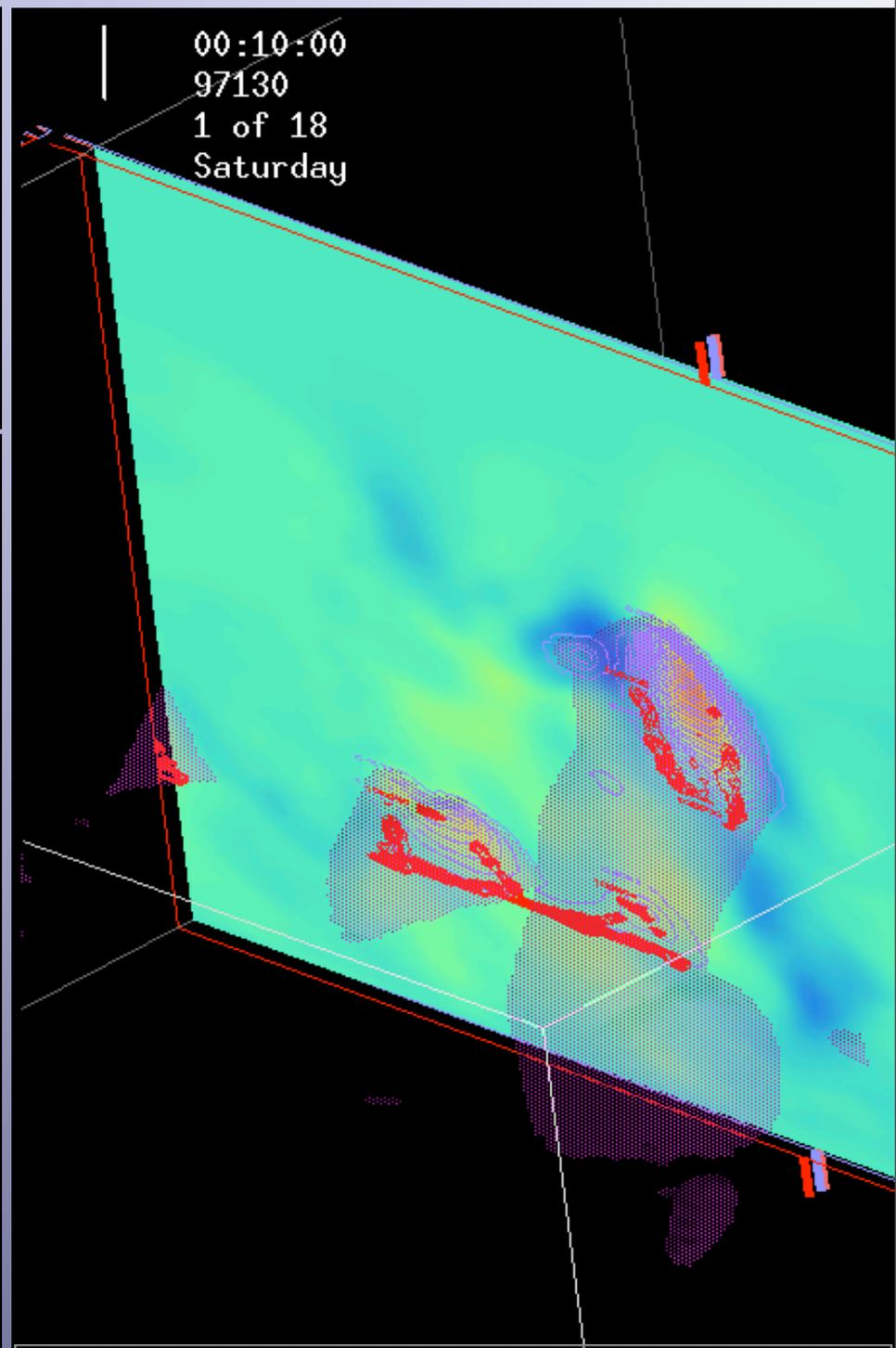

background color of the slice: vertical velocity
violet isosurfaces: qc = 0.01 g kg^{-1}
violet contours: qc every 0.1 g kg^{-1}
pink contours: cloud droplet activation forcing

Rico (Rain in Cumulus Over the Ocean) case

Setup

- **DATE:** winter 2004/2005
  PLACE: Antigua i Barbuda
- Computational domain:
  - 6.4 km × 6.4 km × 4 km
  - nx=ny=128 nz=201
  - dx=dy=2.5 × dz = 100 m
  - dt =1s
- The simulations are run for 21 h.
  Data are stored every 10 minutes.
  Hours 3-6, 18-21 and 21-24 are used in the analysis.
- Background aerosol concentration, either:
  - 100 mg^{-1} (PRISTINE case)
  - 1000 mg^{-1} (POLLUTED case)
- Initial profiles, boundary conditions, surface fluxes and large-scale forcings follows that of the Large Eddy Simulation intercomparison:
  http://www.knmi.nl/samenw/rico/setup3d.html

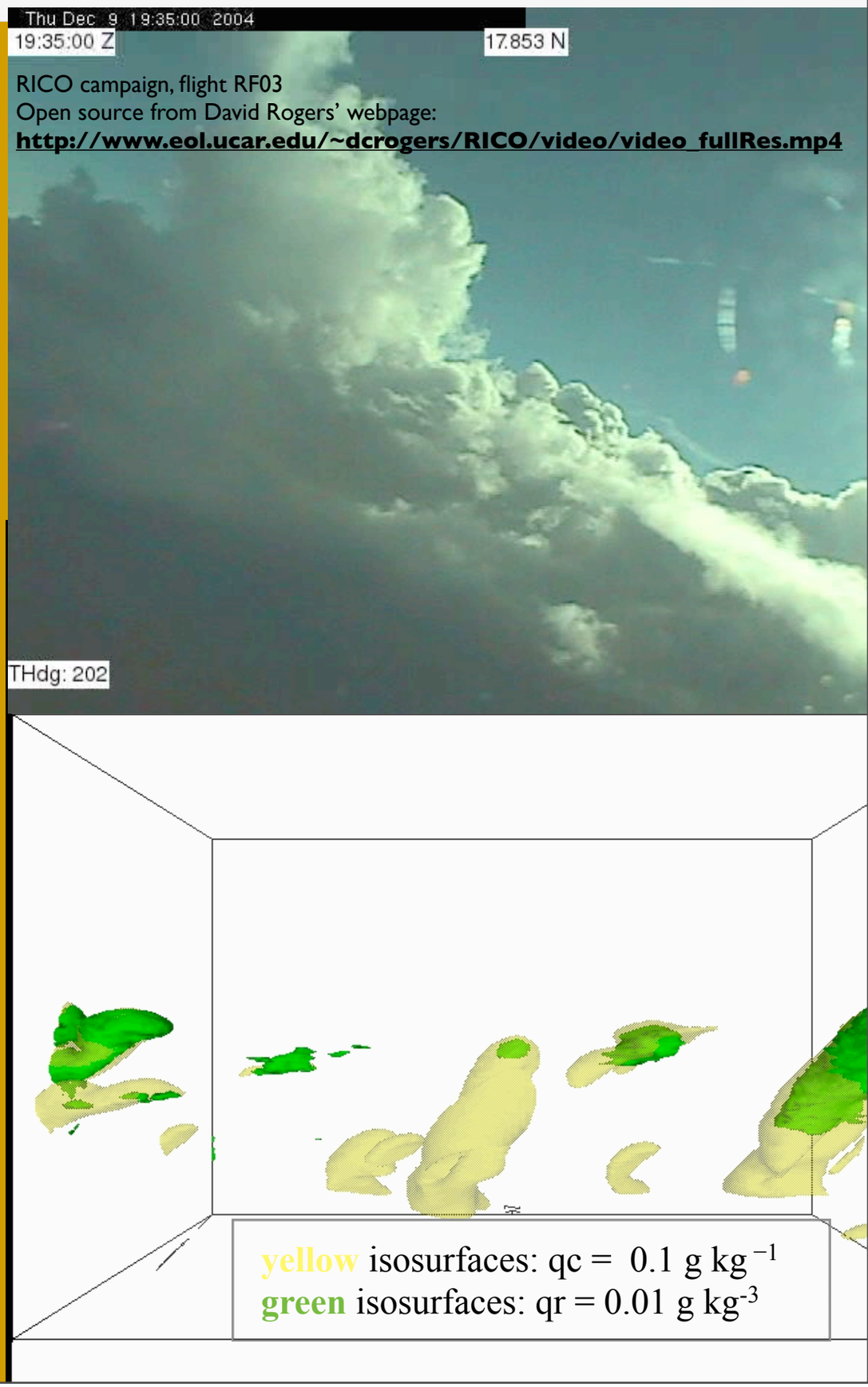

Cloud field versus activation

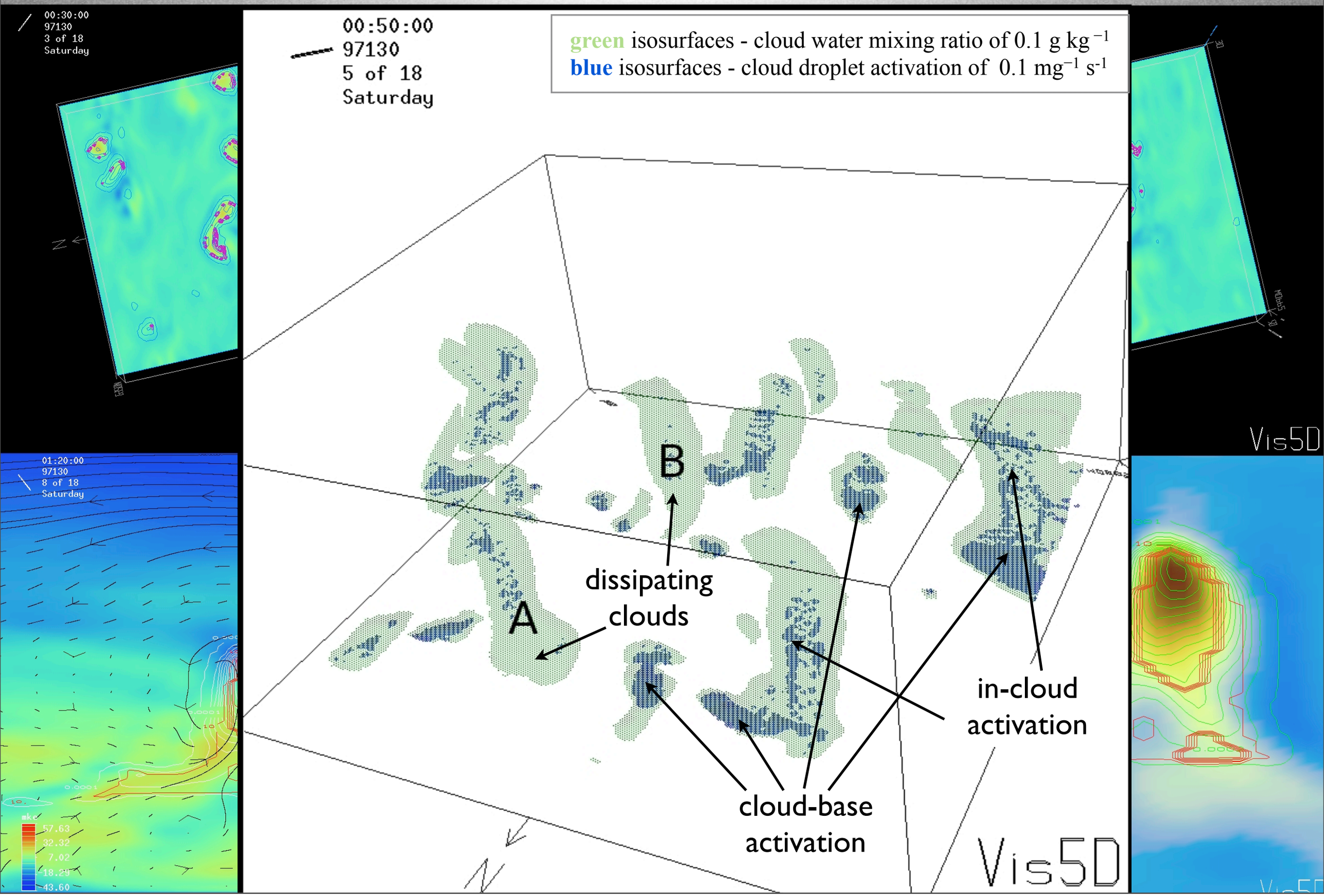

Cloud field versus activation

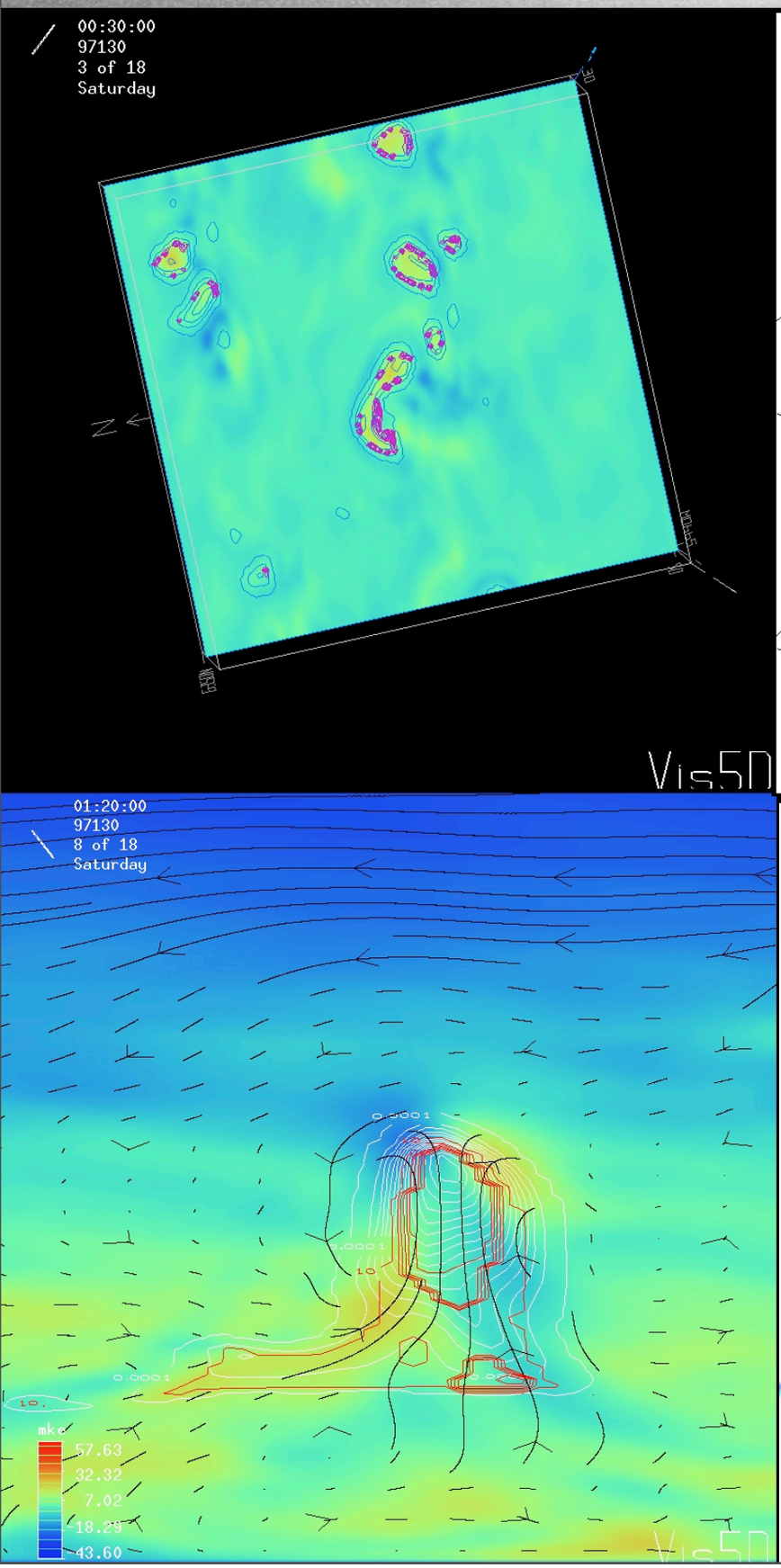

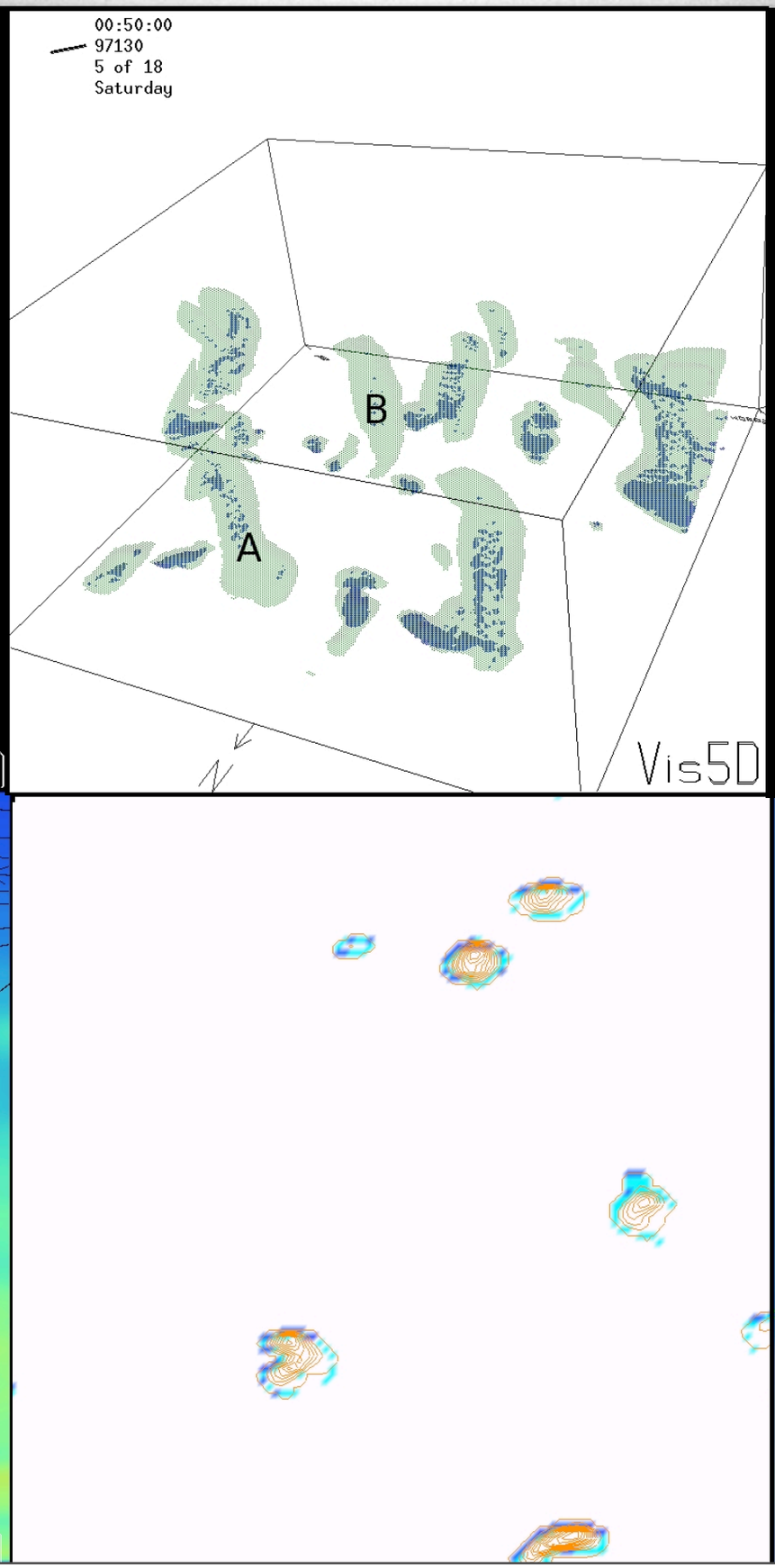

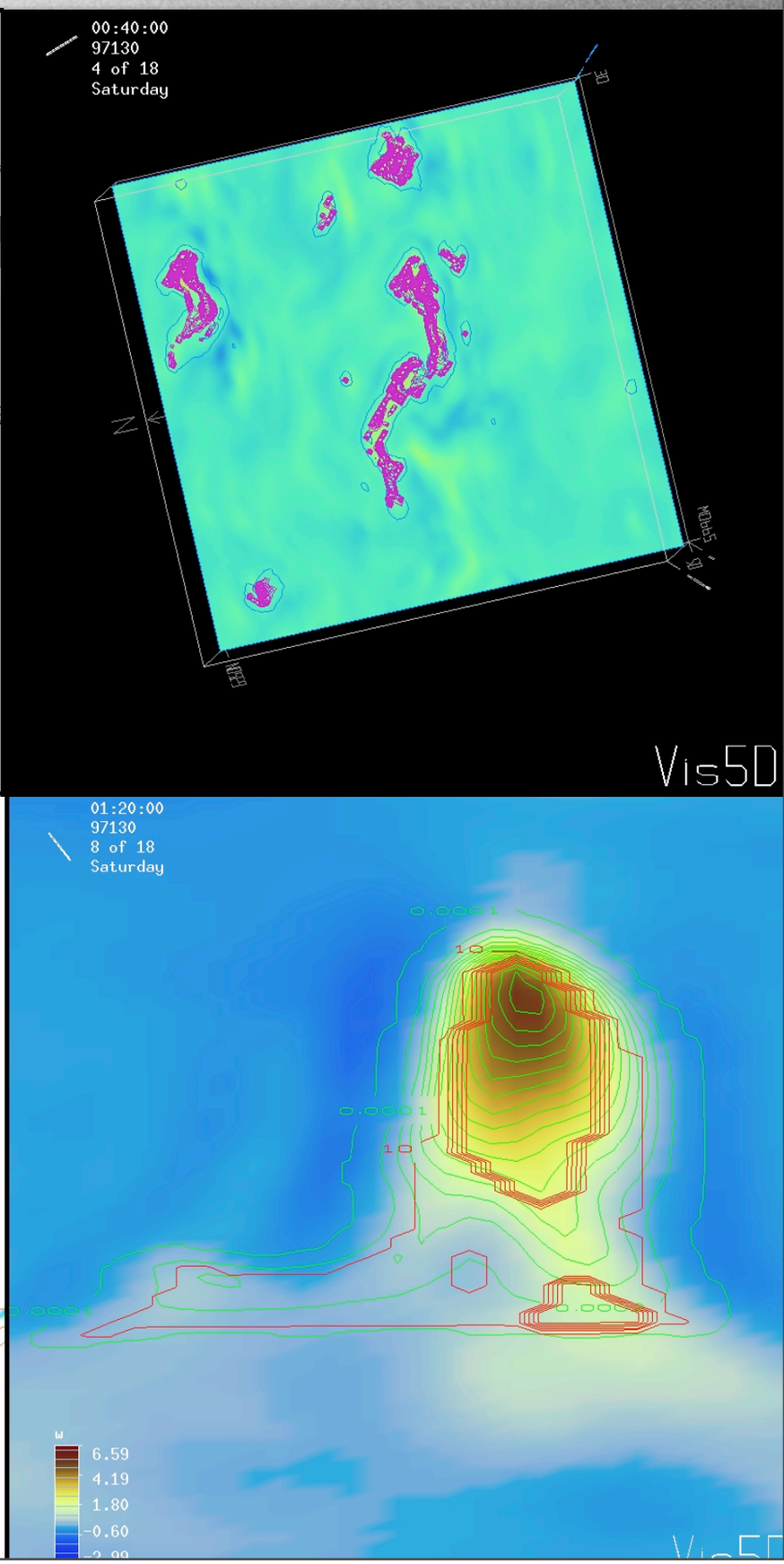

Cloud field versus activation

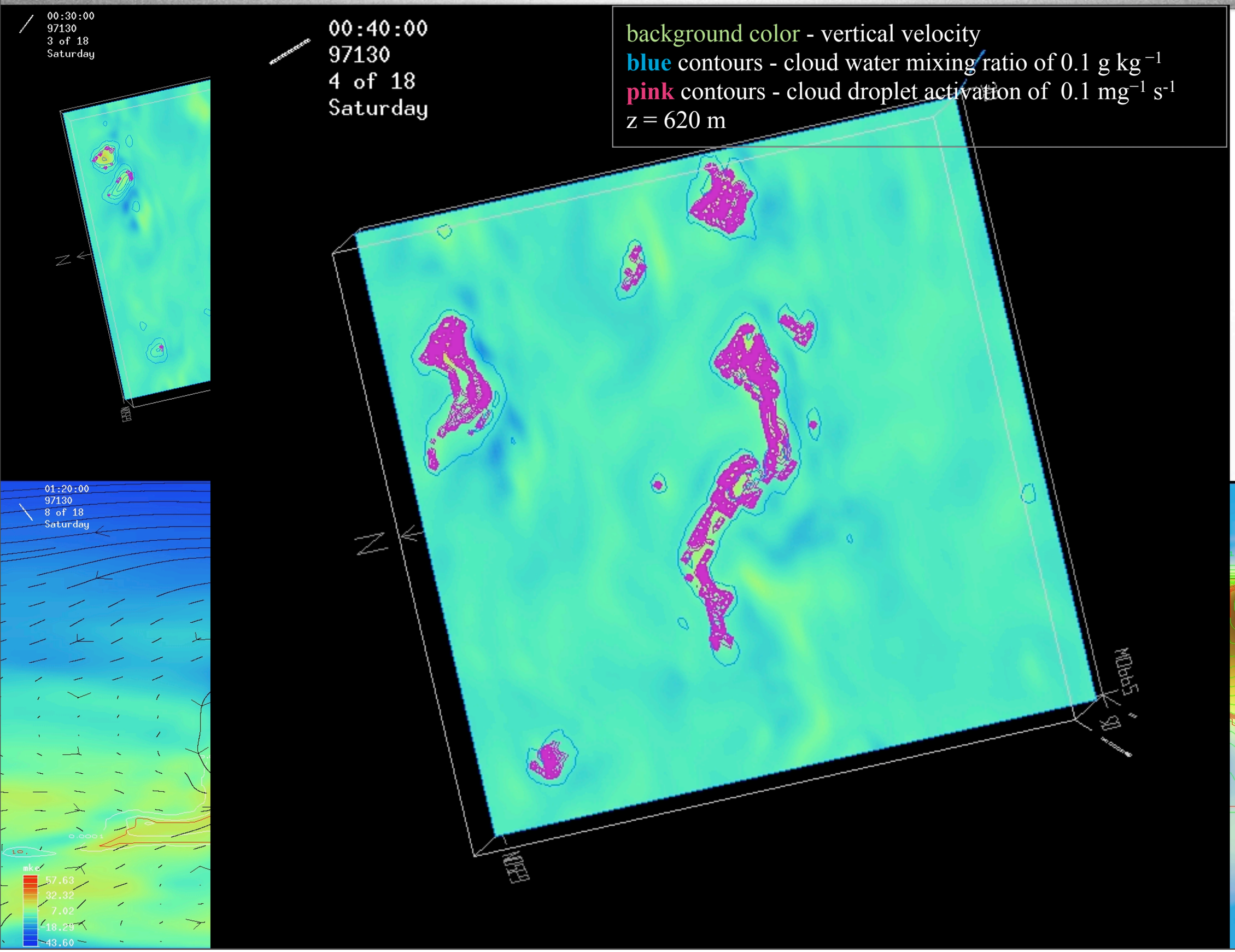

Cloud field versus activation

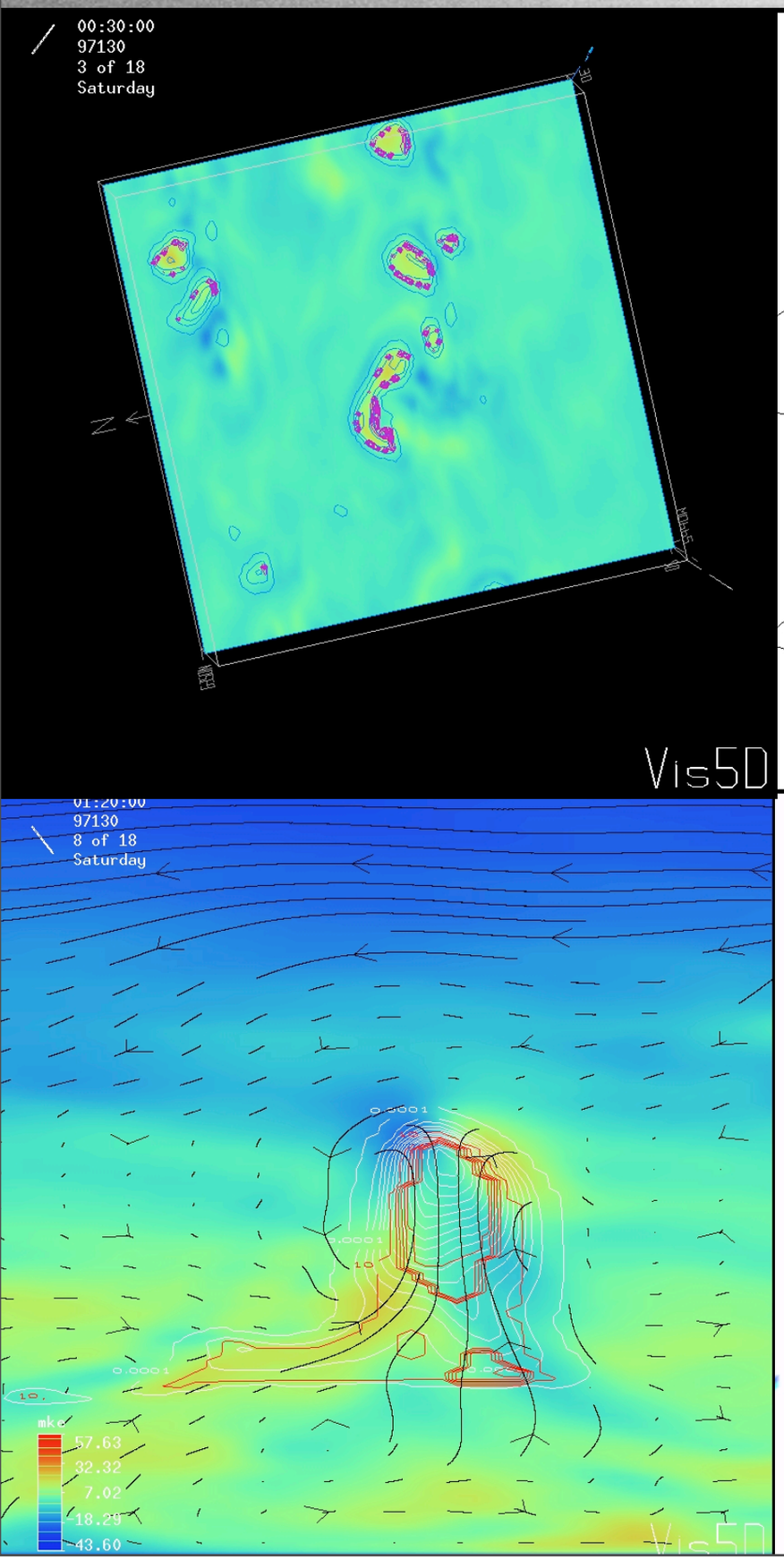

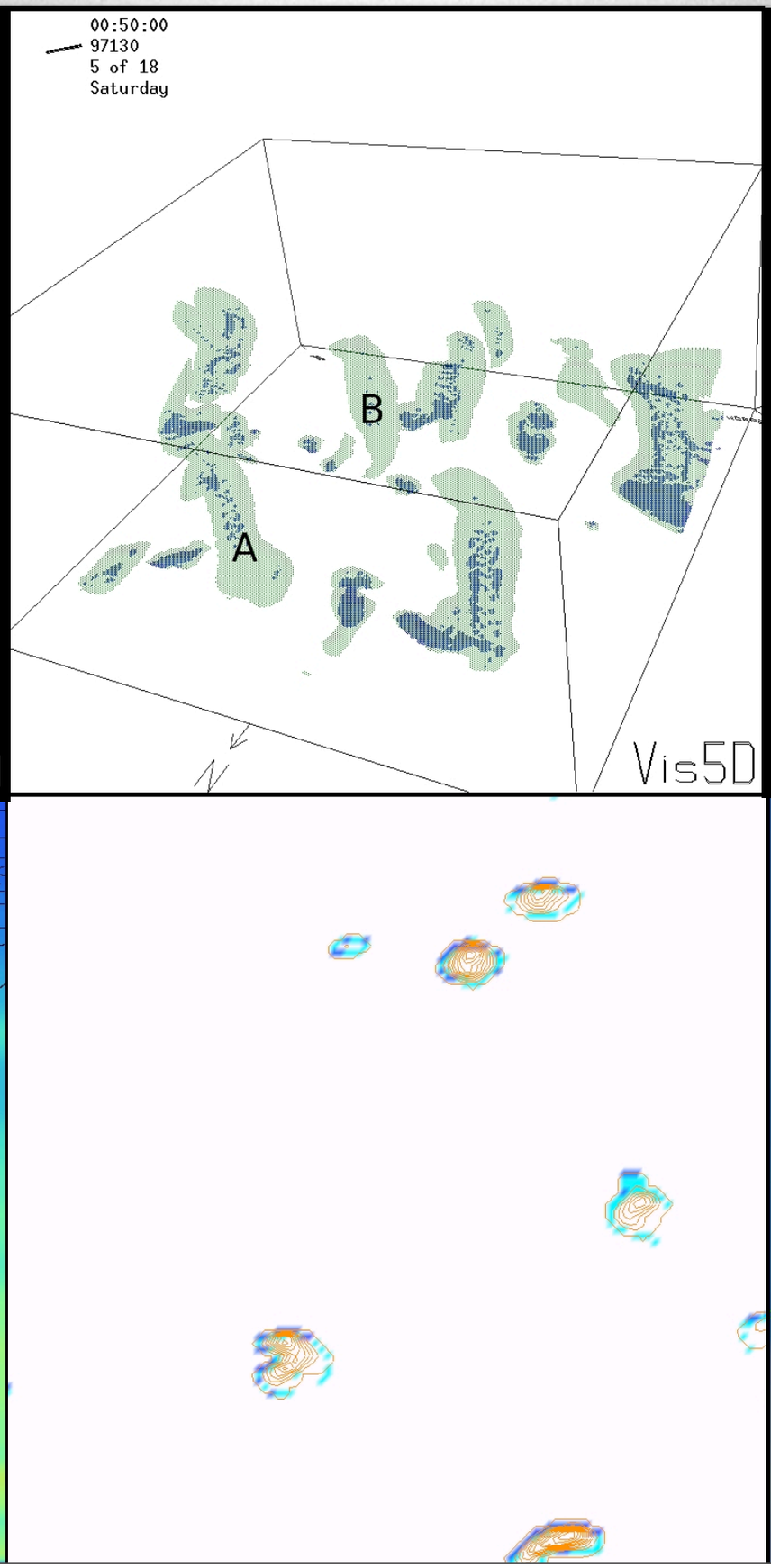

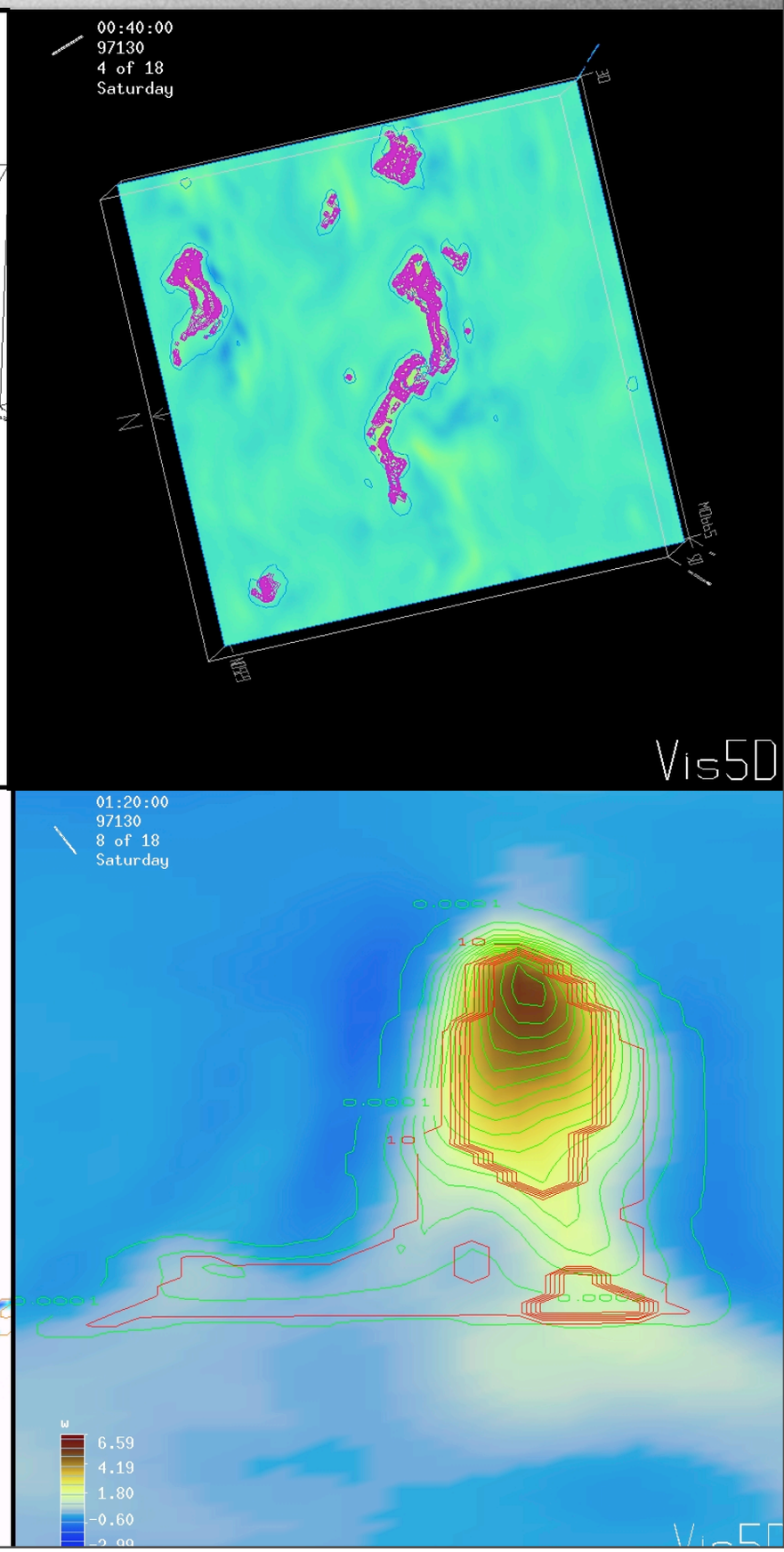

Cloud field versus activation

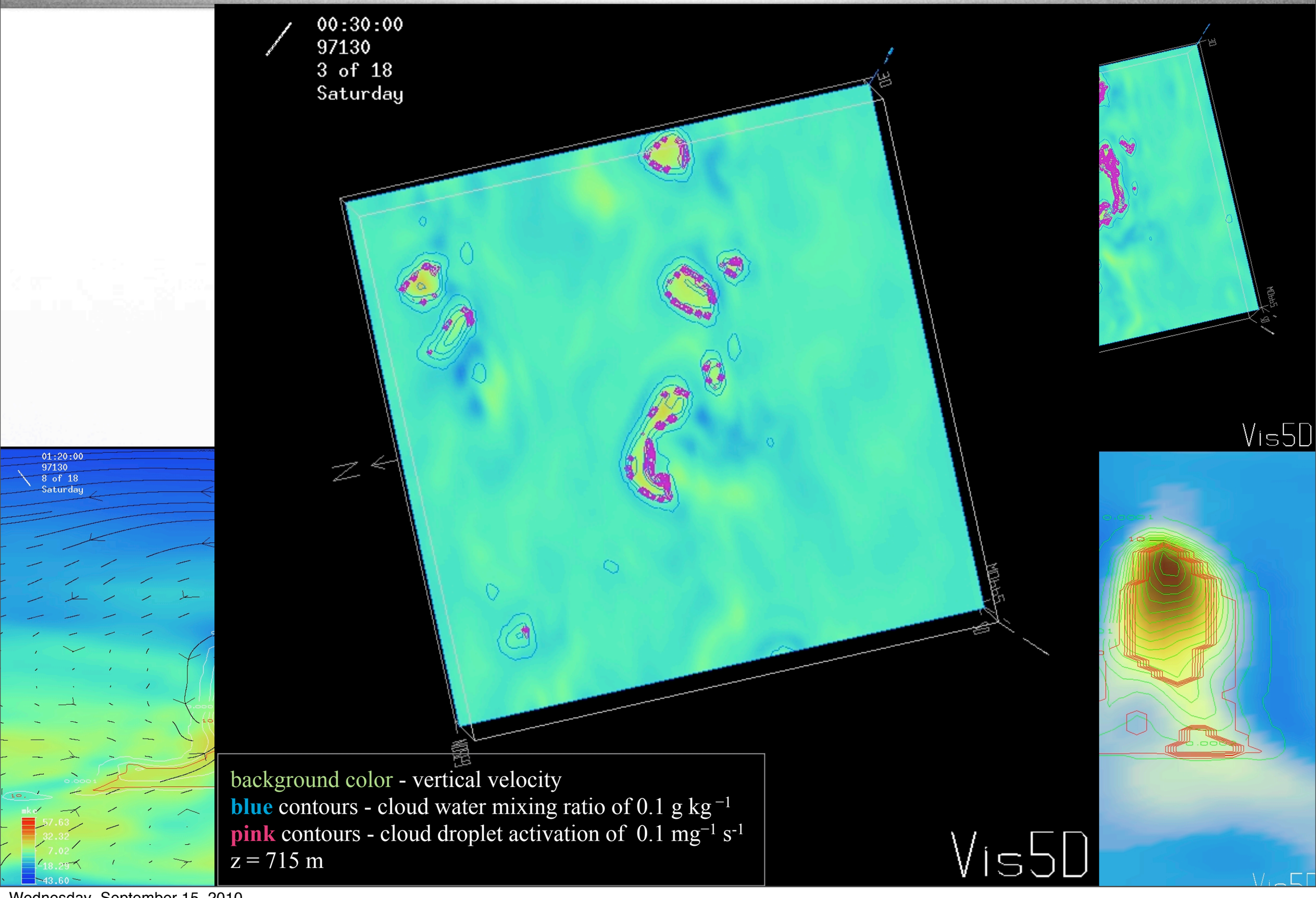

background color - vertical velocity
blue contours - cloud water mixing ratio of 0.1 g kg $^{-1}$
pink contours - cloud droplet activation of 0.1 mg^{-1} s^{-1}
z = 715 m

Cloud field versus activation

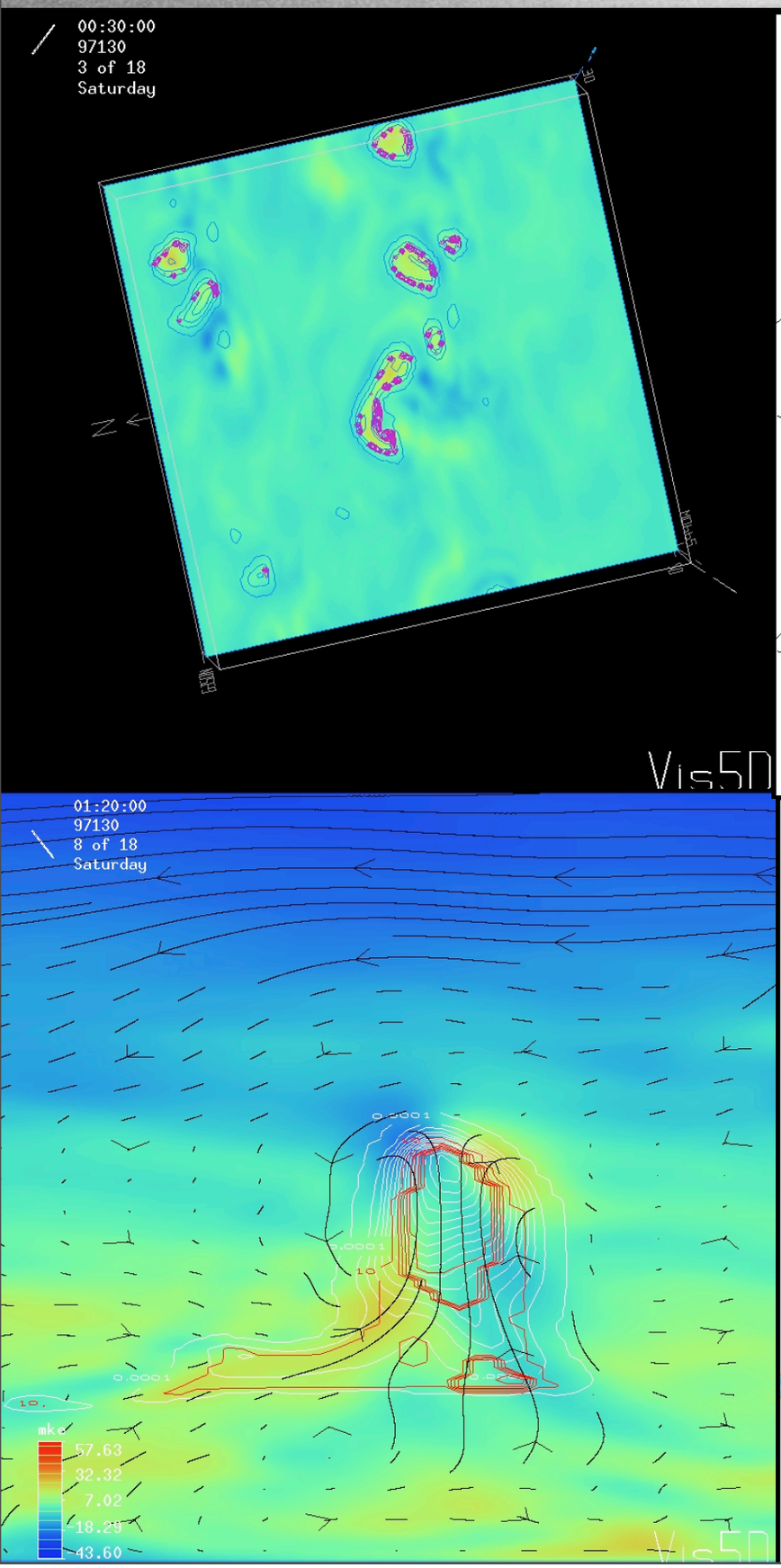

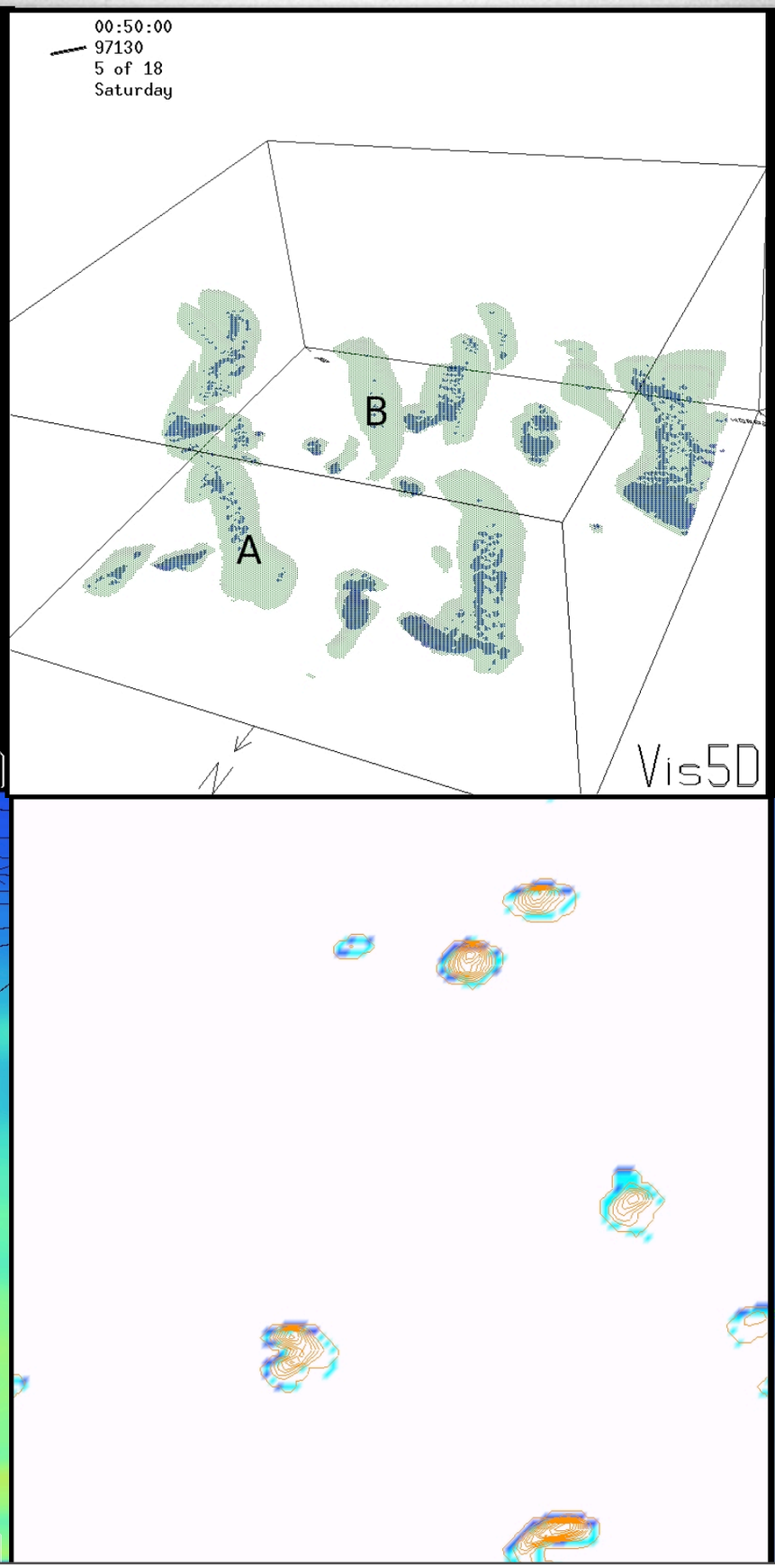

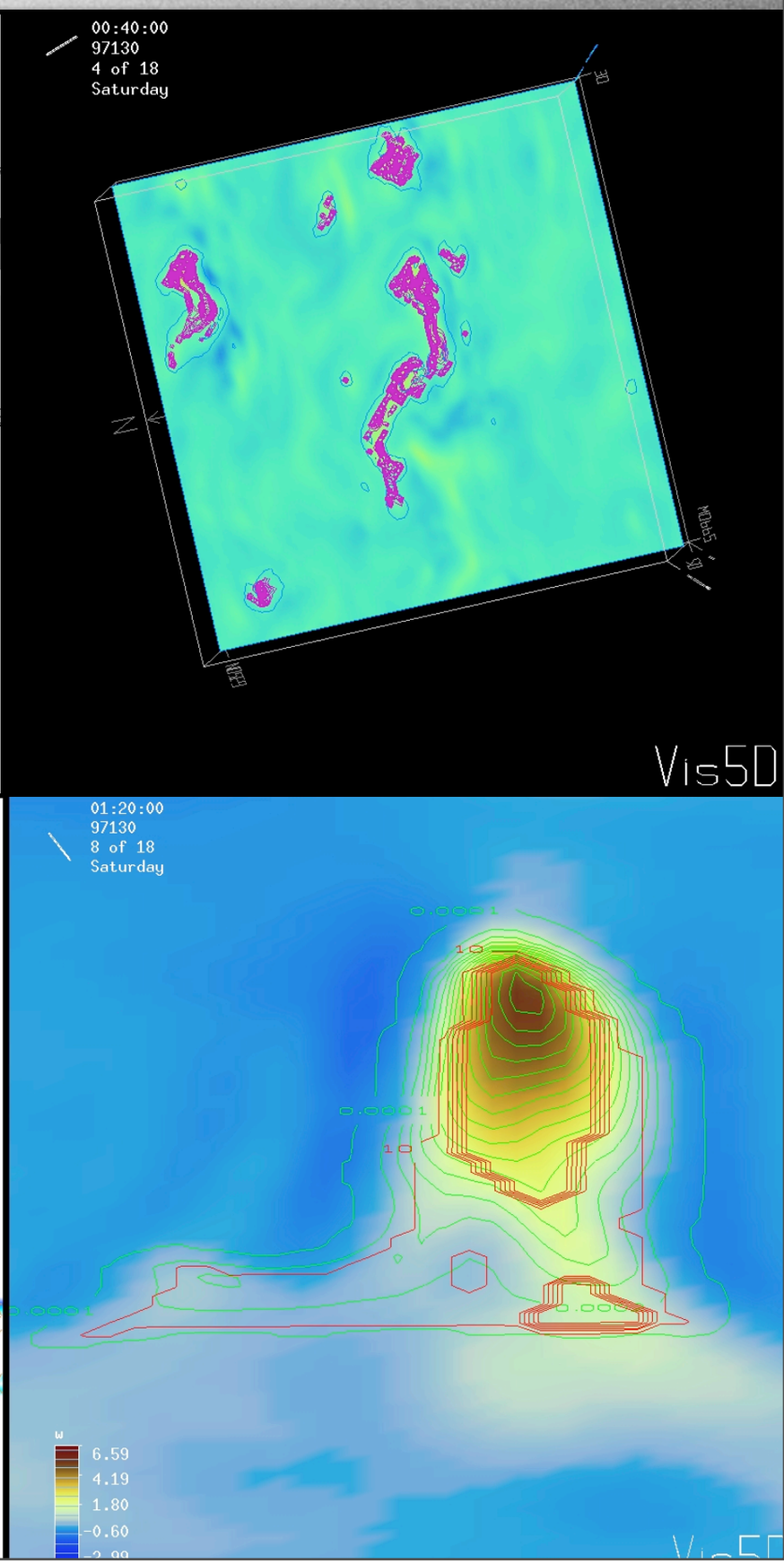

Cloud field versus activation

orange contours - cloud water mixing ratio of 0.1 g kg^{-1}
background color - supersaturation gradient inside cloud
z = 1208 m

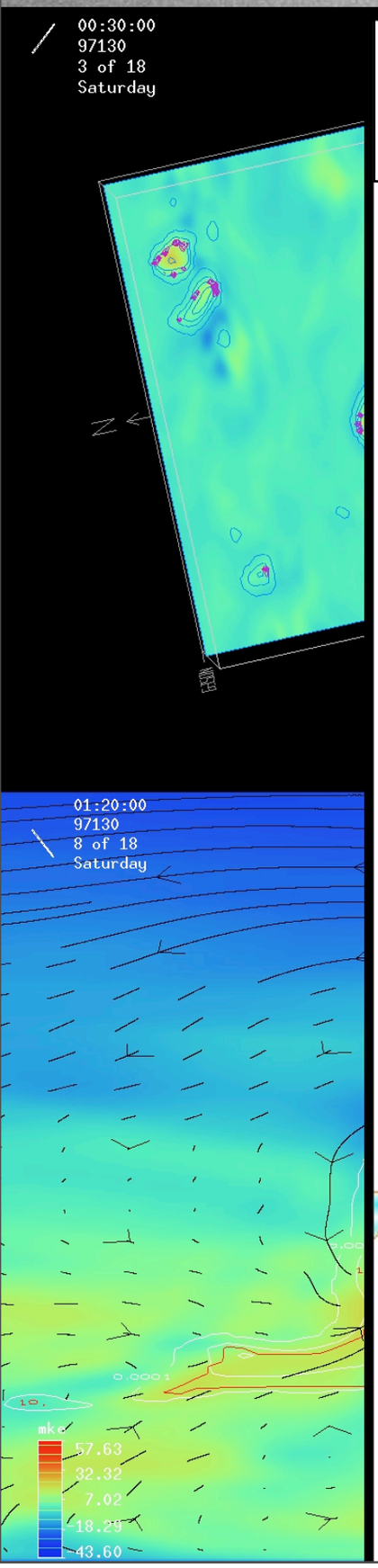

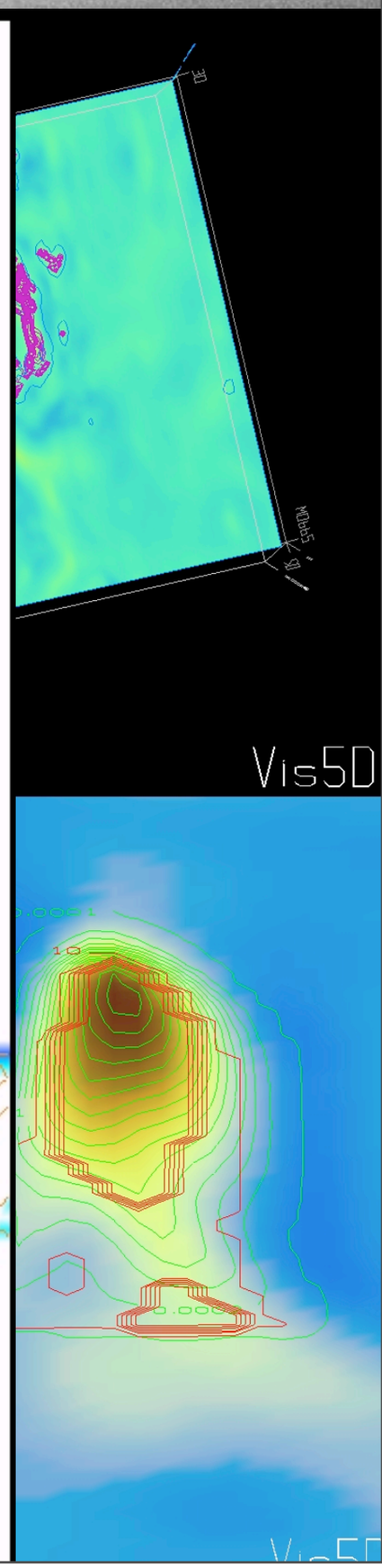

Wednesday, September 15, 2010

Cloud field versus activation

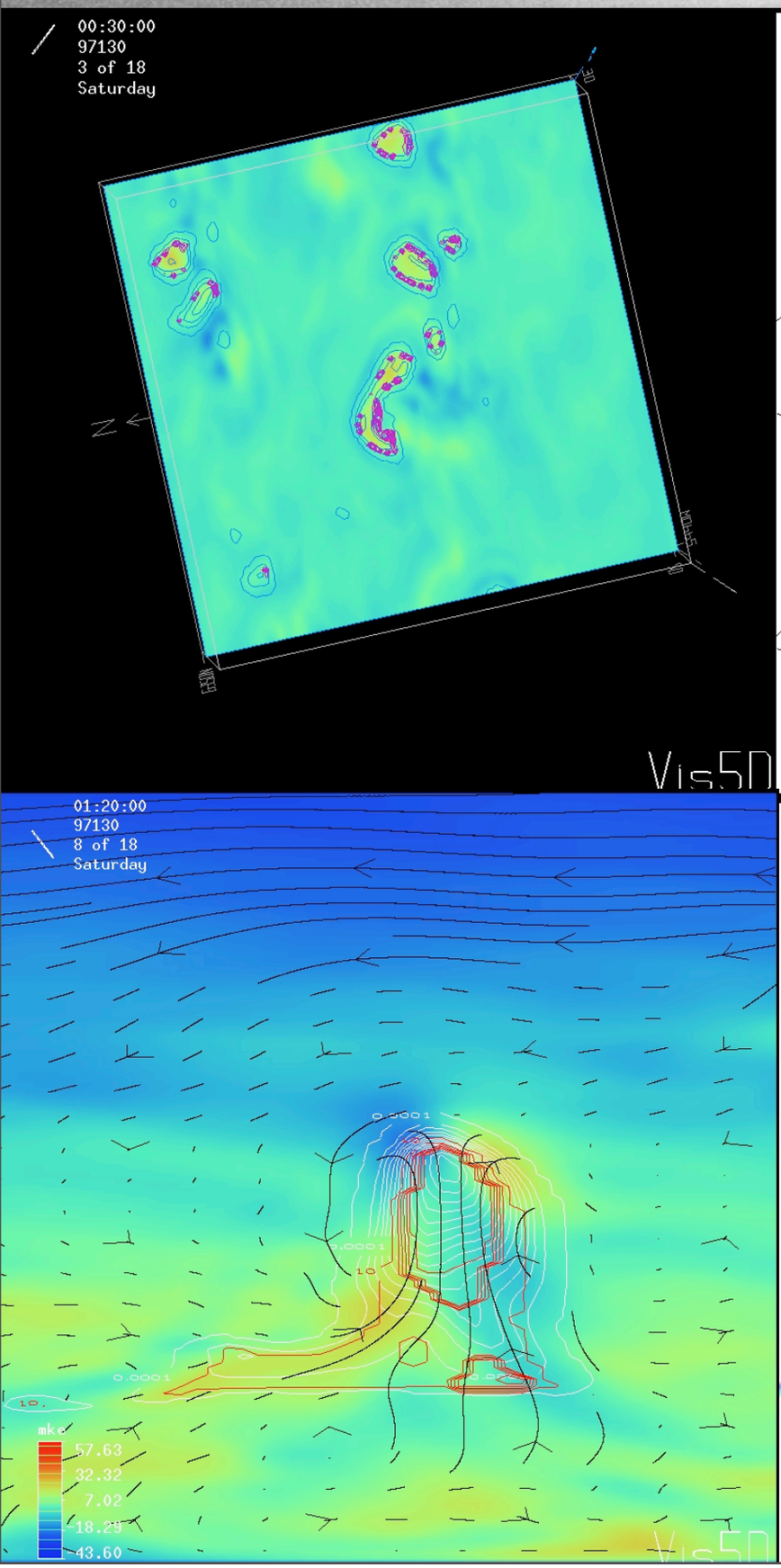

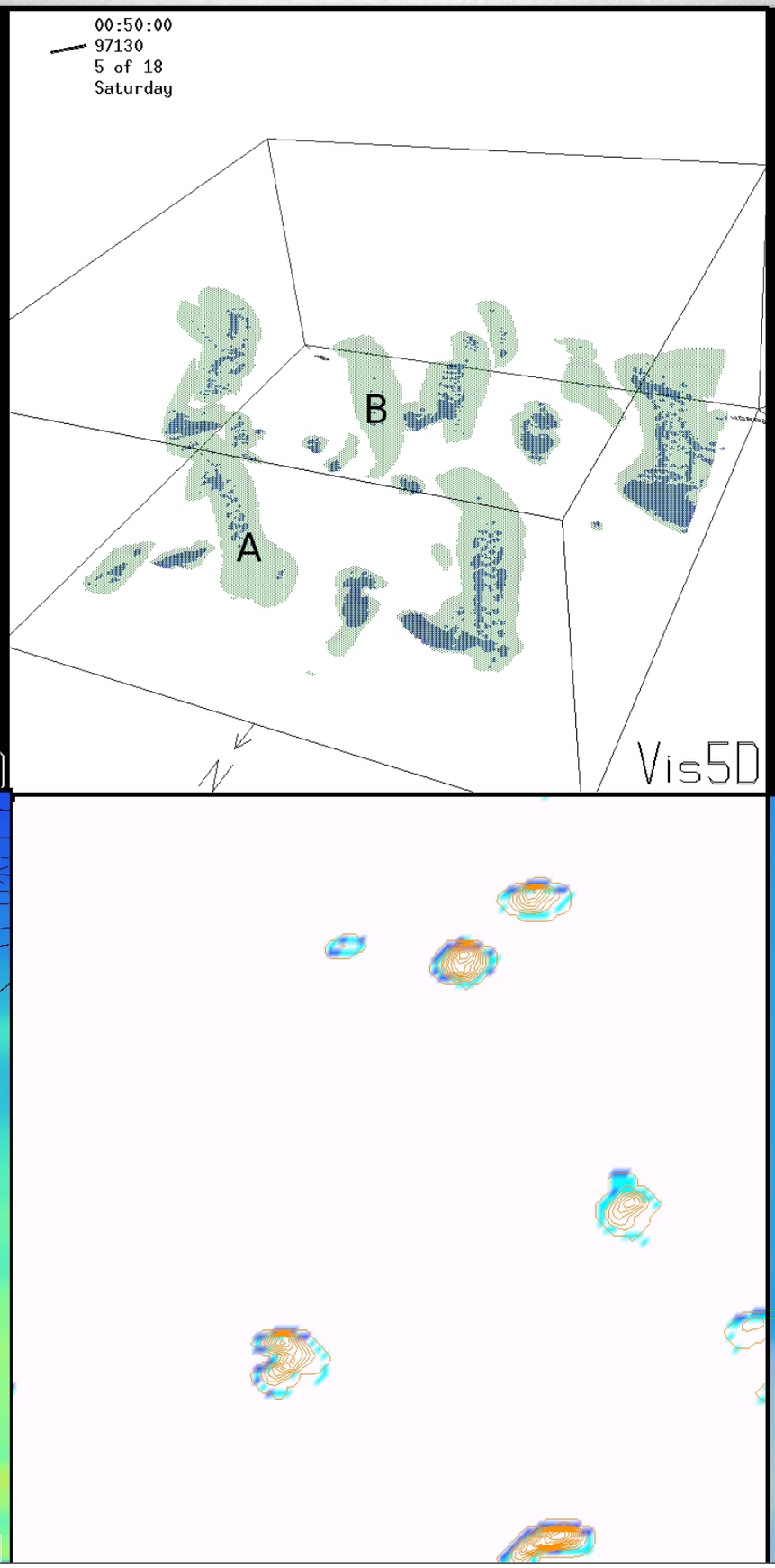

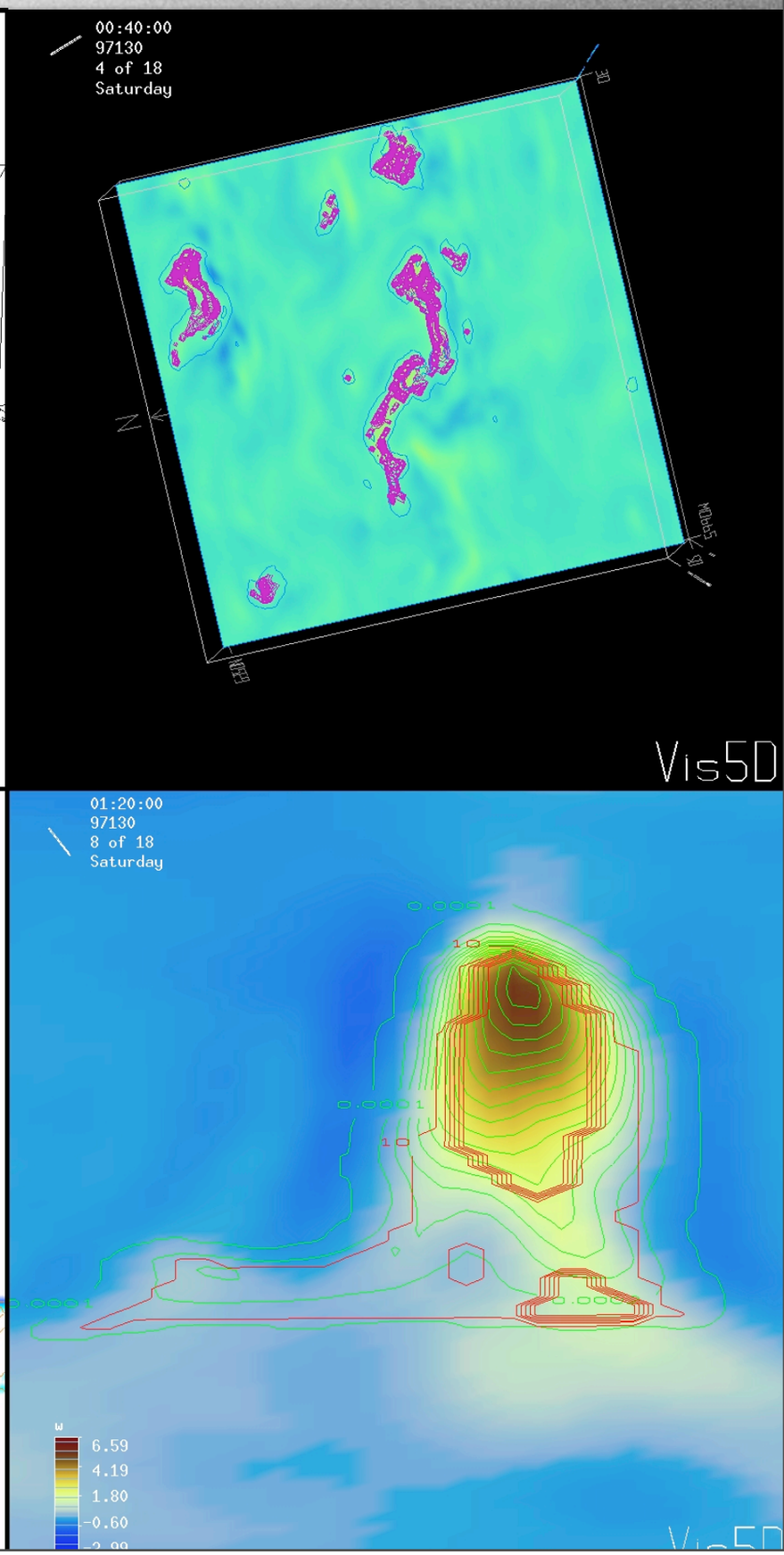

Cloud field versus activation

LEFT PLOT

background color - u^2+v^2

white contours - isolines of cloud water mixing ratio with interval of 0.1 g kg^{-1}

red contours - isolines of supersaturation

black curves - streamfunctions

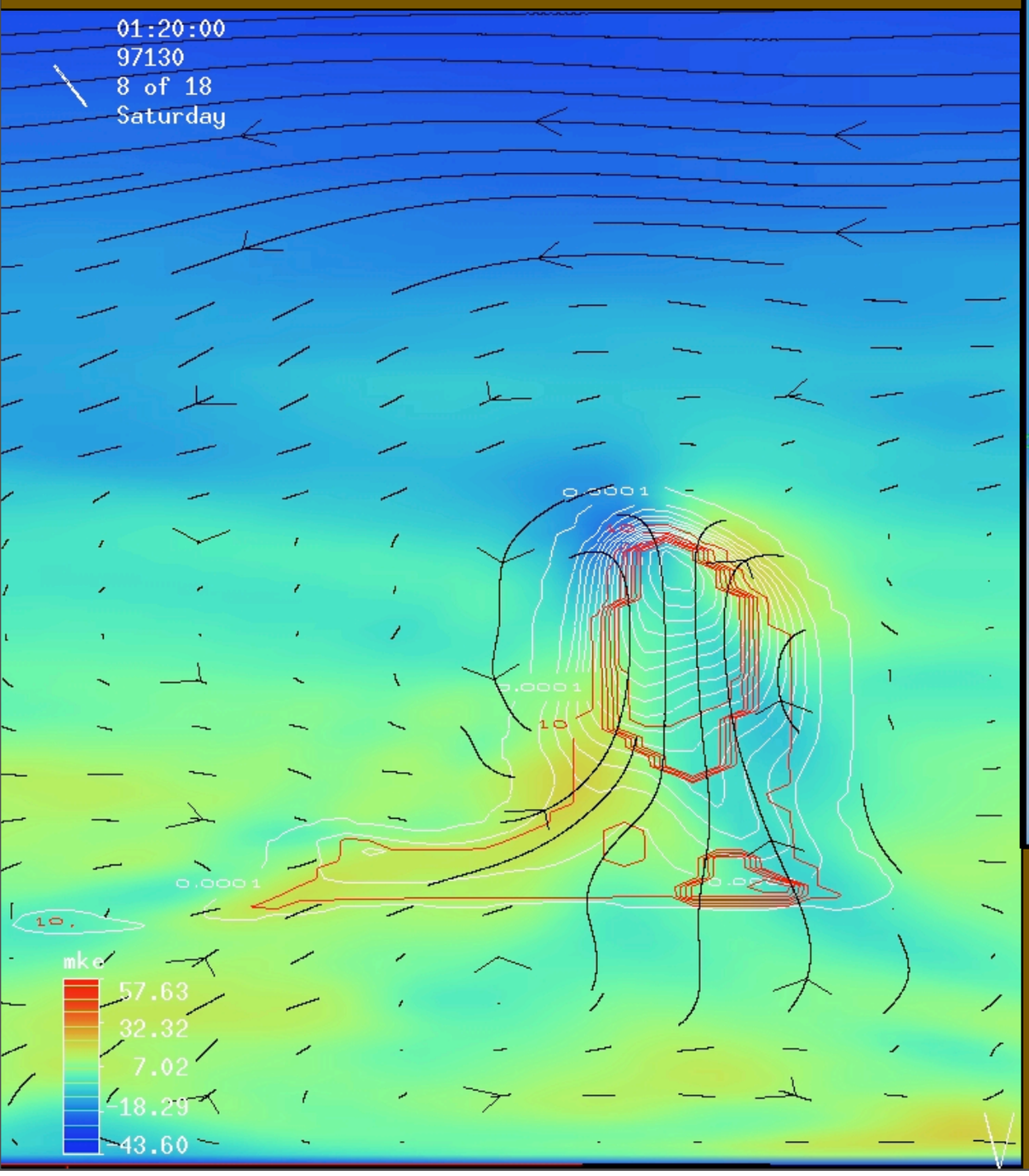

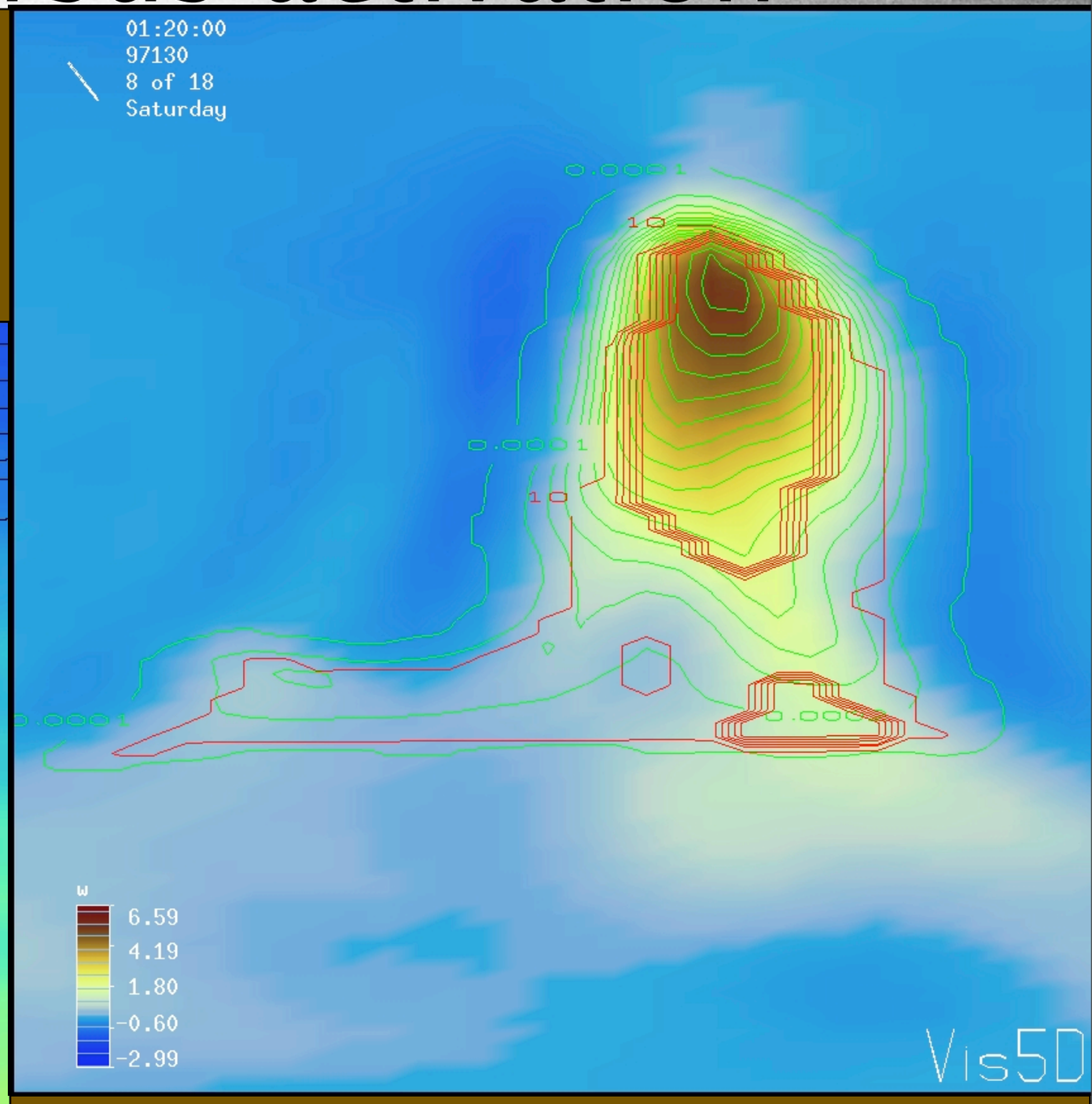

RIGHT PLOT

background color - vertical velocity

green contours - isolines of cloud water mixing ratio with interval of 0.1 g kg^{-1}

red contours - isolines of supersaturation

Average profiles

Normalized mean horizontal profile through cloud field
of width 300, 500 and 700 m
in the layer 700-800 m (dashed line), 900-1000 m (solid line) and 1300-1400 m (dashed dotted line)
for the PRISTINE homogeneous case

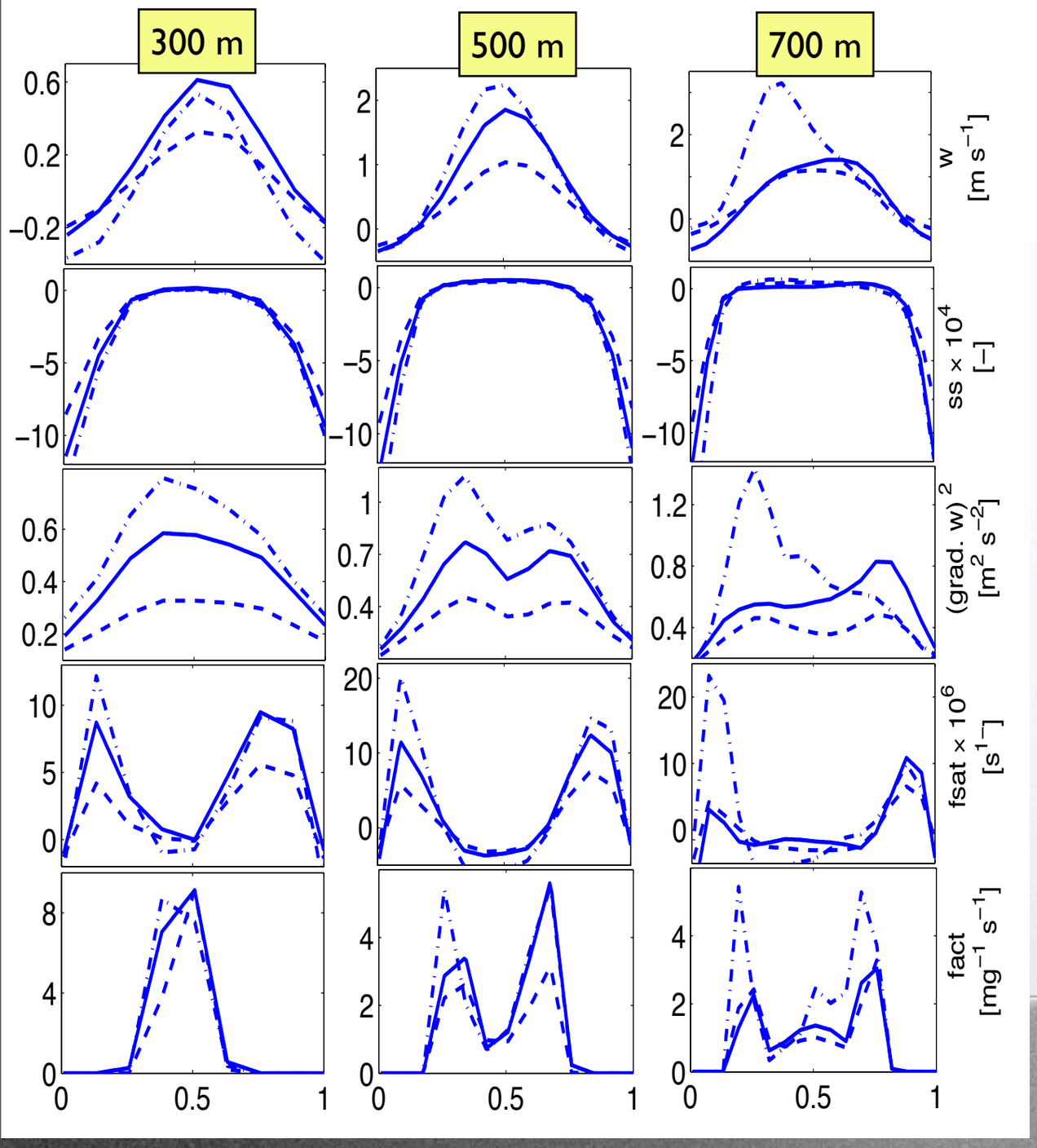

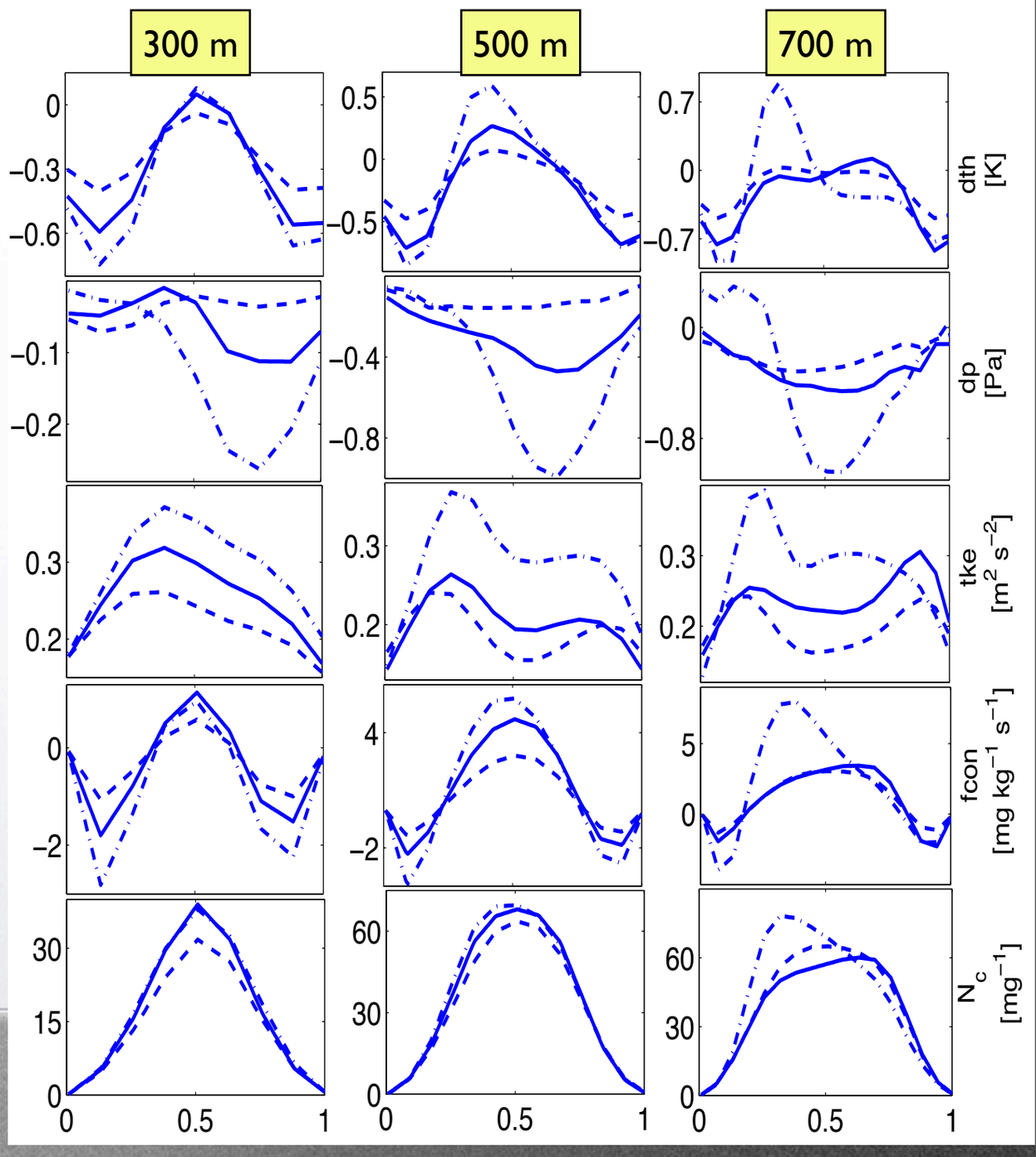

Average profiles

Normalized mean horizontal profile through cloud field
of width 300, 500 and 700 m
in the layer 700-800 m (dashed line), 900-1000 m (solid line) and 1300-1400 m (dashed dotted line)
for the PRISTINE homogeneous case

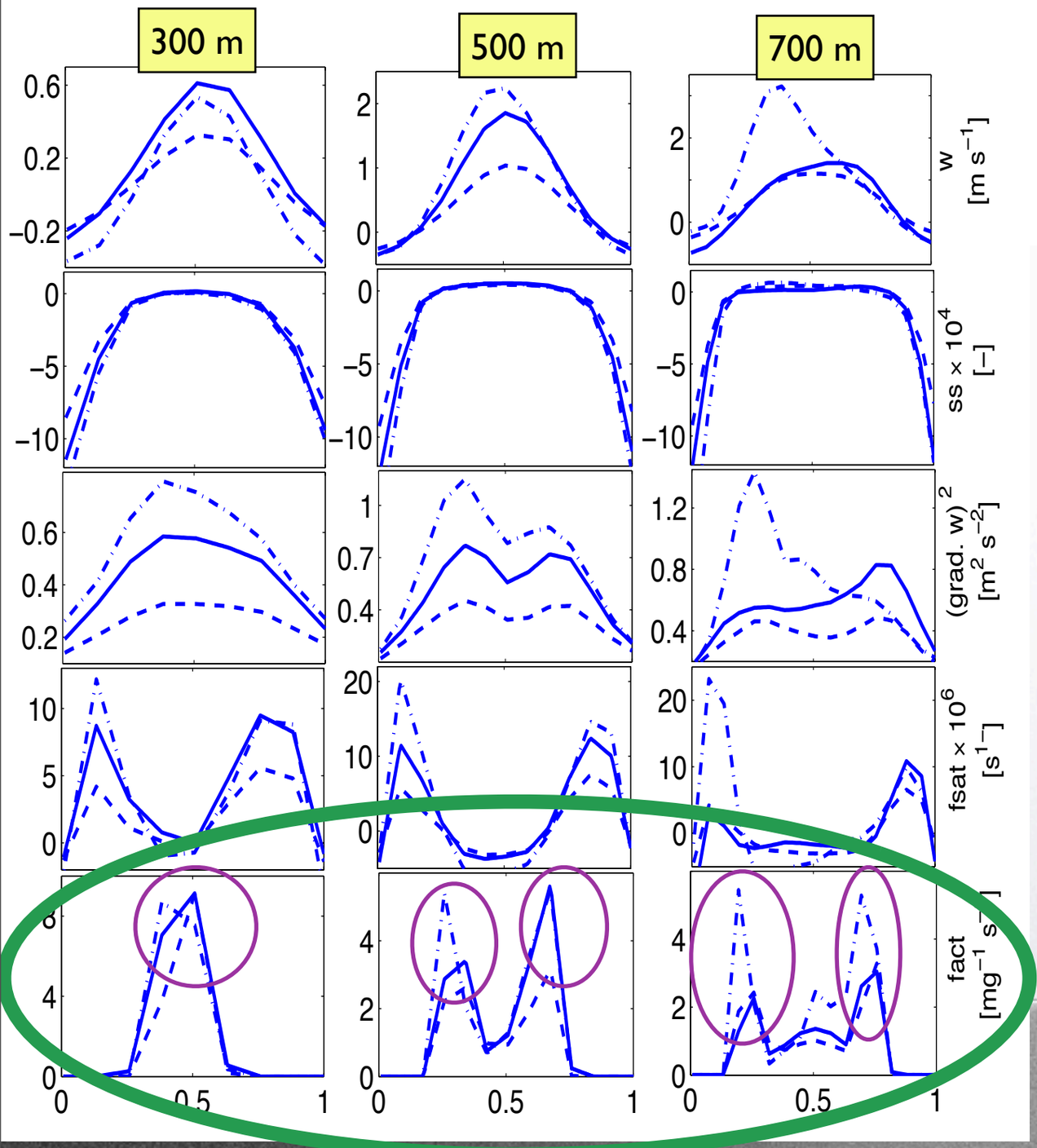

- **Activation tendency peaks** in a cloud are found at the edge of the cloud core.

Average profiles

Normalized mean horizontal profile through cloud field
of width 300, 500 and 700 m
in the layer 700-800 m (dashed line), 900-1000 m (solid line) and 1300-1400 m (dashed dotted line)
for the PRISTINE homogeneous case

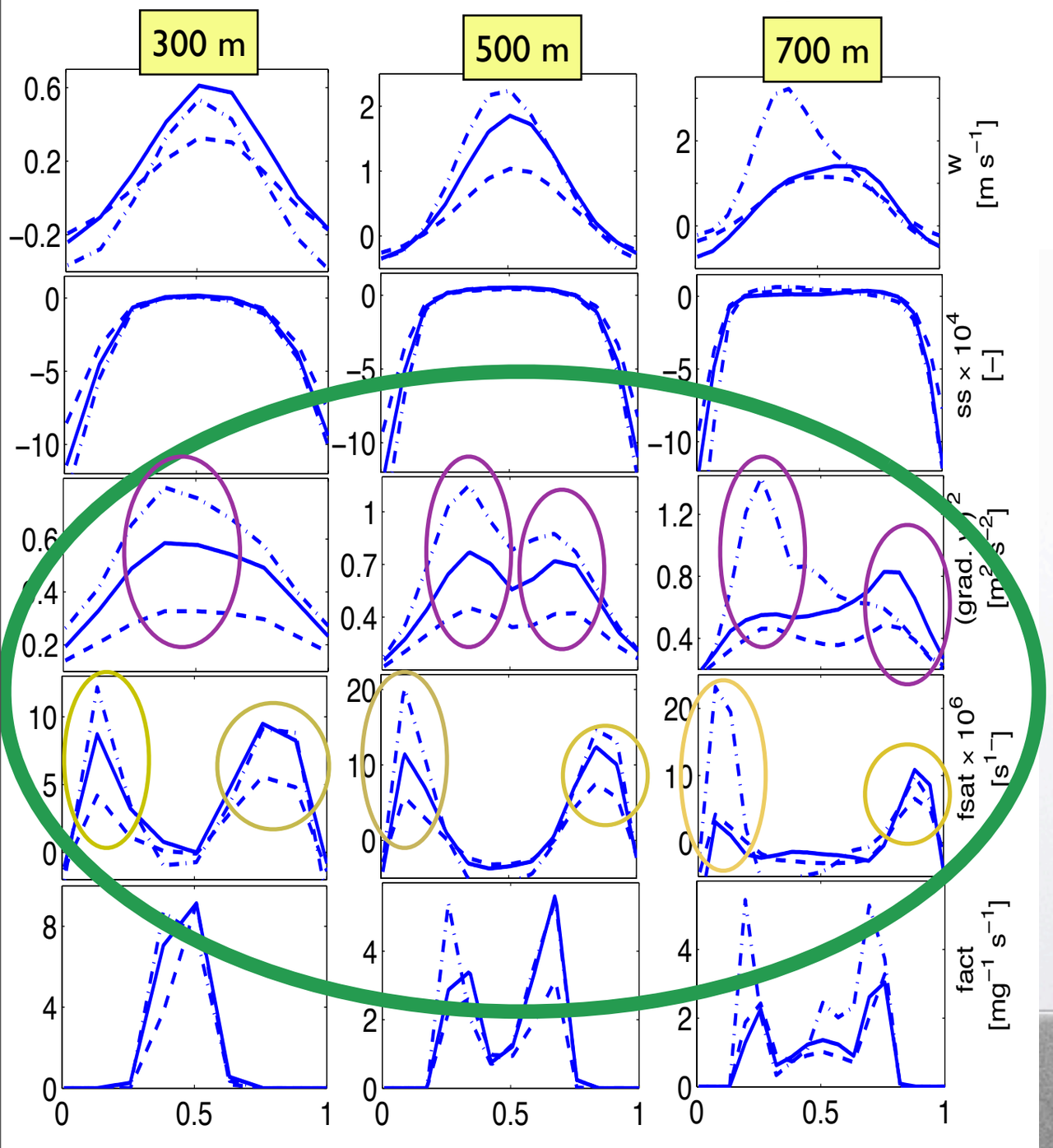

- **Activation tendency peaks** in a cloud are found at the edge of the cloud core.
- This is where vertical velocity gradient and subsequently supersaturation gradient are large.

Average profiles

Normalized mean horizontal profile through cloud field
of width 300, 500 and 700 m
in the layer 700-800 m (dashed line), 900-1000 m (solid line) and 1300-1400 m (dashed dotted line)
for the PRISTINE homogeneous case

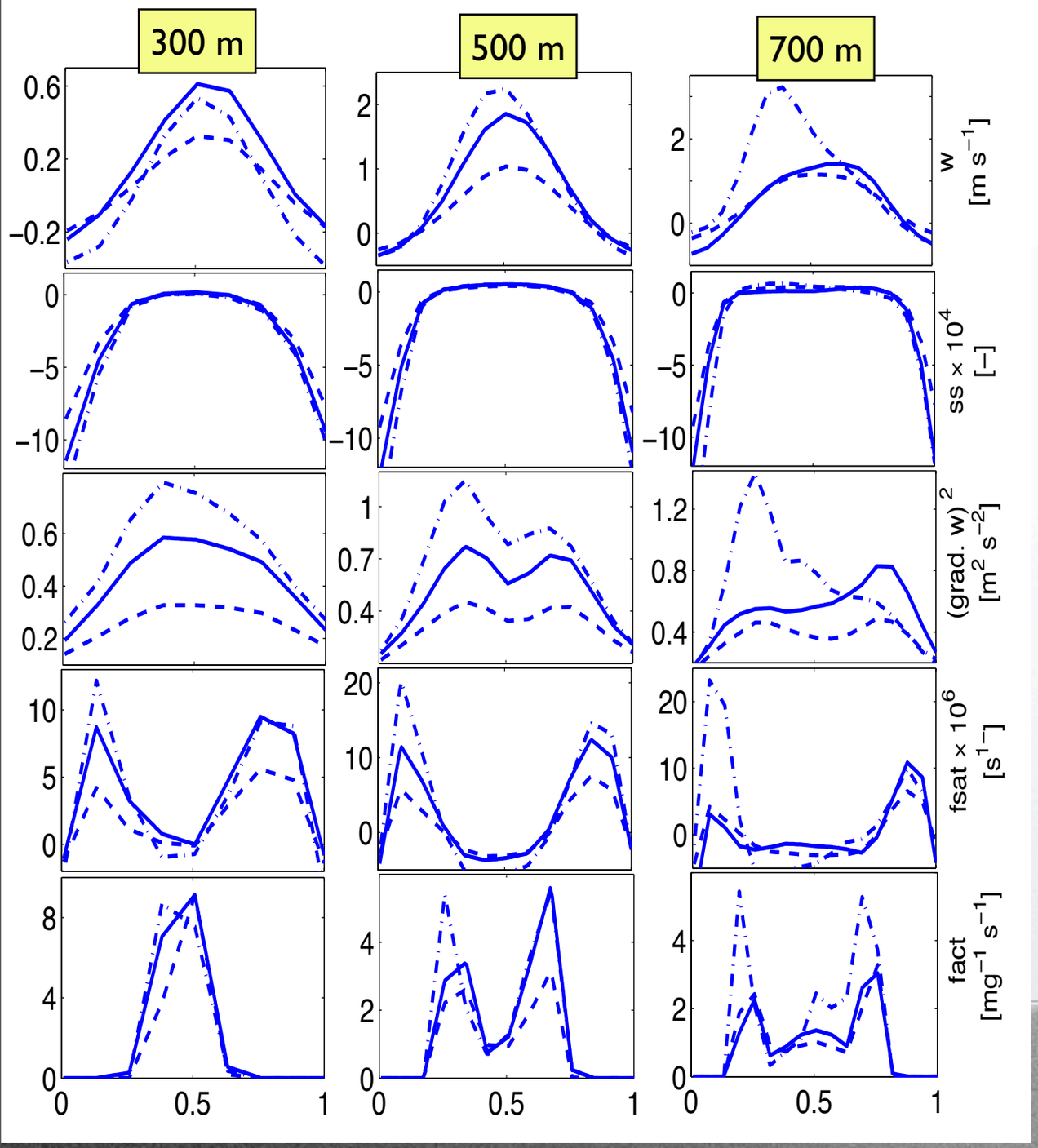

- **Activation tendency peaks** in a cloud are found at the edge of the cloud core.
- This is where vertical velocity gradient and subsequently supersaturation gradient are large.
- In-cloud activation happens in the area of large gradients, when air is accelerated strongly during entrainment / inflow into the cloud core.

Sensitivity tests

- In order to check the sensitivity of microphysical as well as macrophysical properties of in-cloud activation, additional tests have been conducted.
- Activation has been turned off above the level of 700 m.

Sensitivity tests

- In order to check the sensitivity of microphysical as well as macrophysical properties of in-cloud activation, additional tests have been conducted.
- Activation has been turned off above the level of 700 m.
- Similar to base run macrophysical properties, however, much more abundant precipitation occurs, with a peak at 1.6 km.

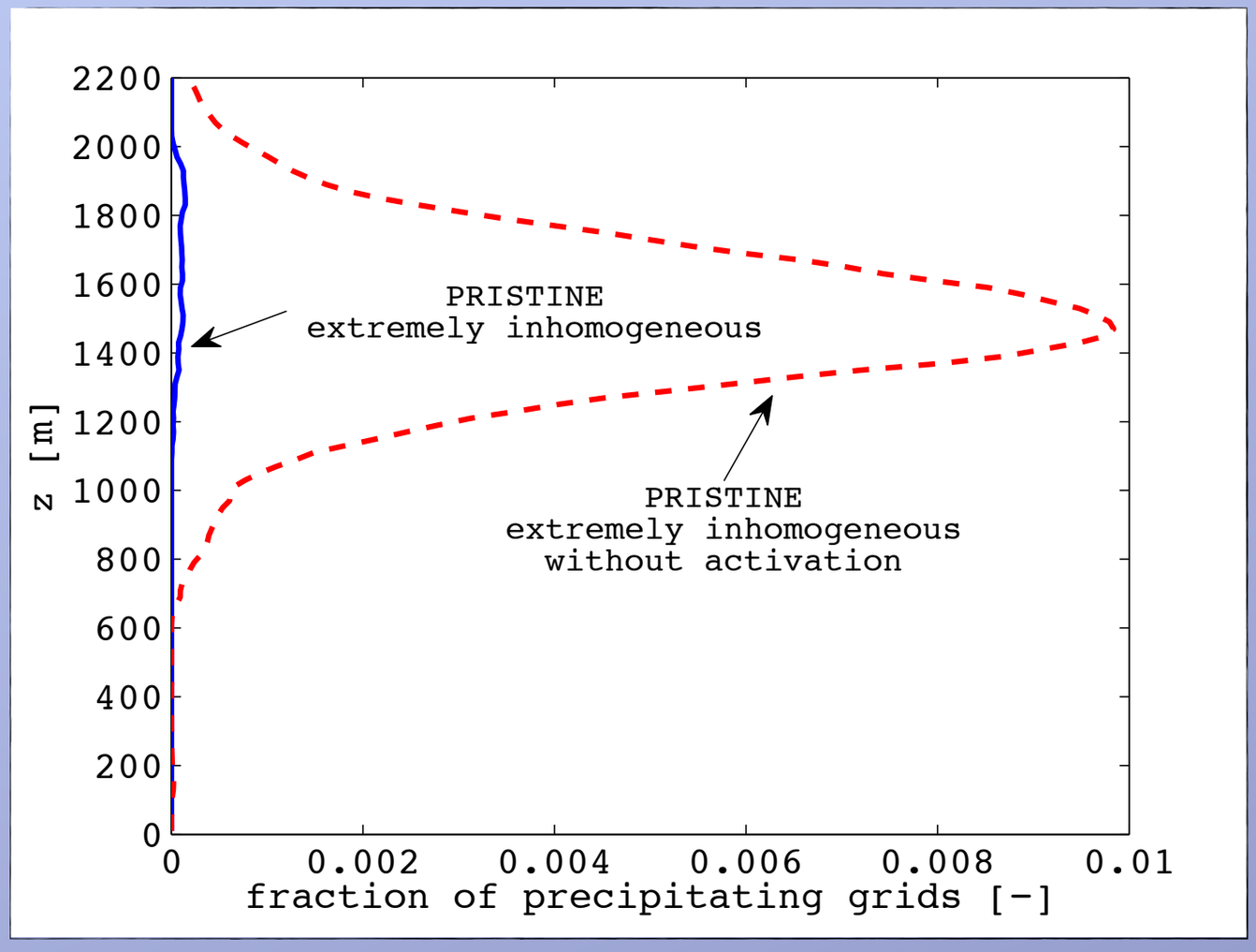

Sensitivity tests

- In order to check the sensitivity of microphysical as well as macrophysical properties of in-cloud activation, additional tests have been conducted.
- Activation has been turned off above the level of 700 m.
- Similar to base run macrophysical properties, however, much more abundant precipitation occurs, with a peak at 1.6 km.
- Additional peak of liquid water content, along with the increase of the total water variance at 1.6 km.

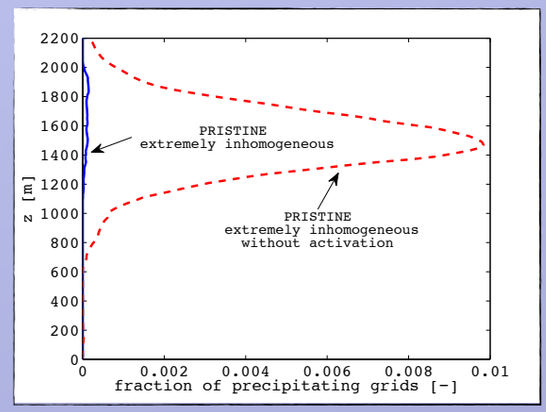

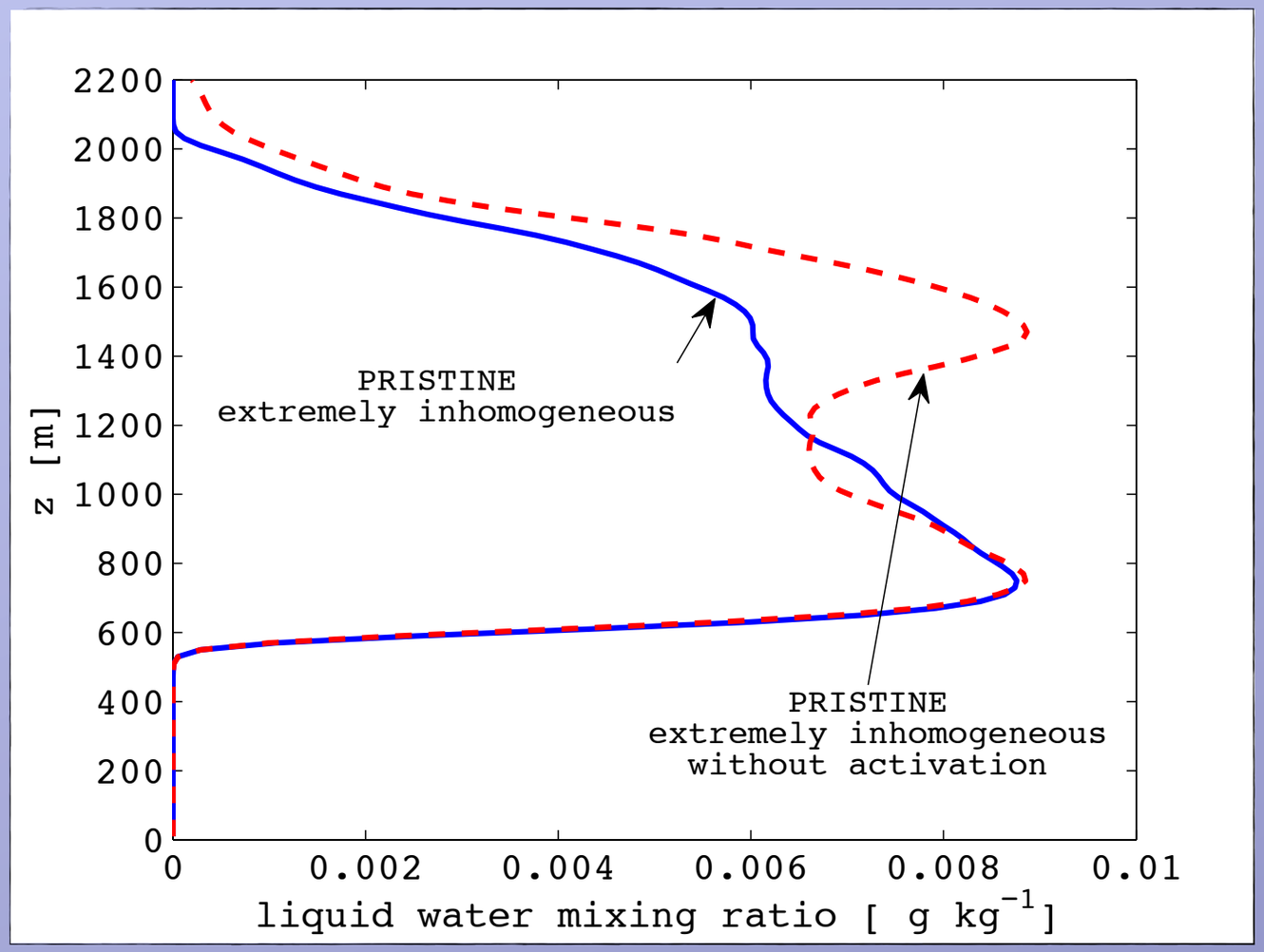

Sensitivity tests

- In order to check the sensitivity of microphysical as well as macrophysical properties of in-cloud activation, additional tests have been conducted.
- Activation has been turned off above the level of 700 m.
- Similar to base run macrophysical properties, however, much more abundant precipitation occurs, with a peak at 1.6 km.
- Additional peak of liquid water content, along with the increase of the total water variance at 1.6 km.
- Vertical velocity inside the cloud is lower, than for the base run: a mean velocity peak of 0.7 m s $^{-1}$ at 1.1 km (0.78 m s $^{-1}$ for the base run).

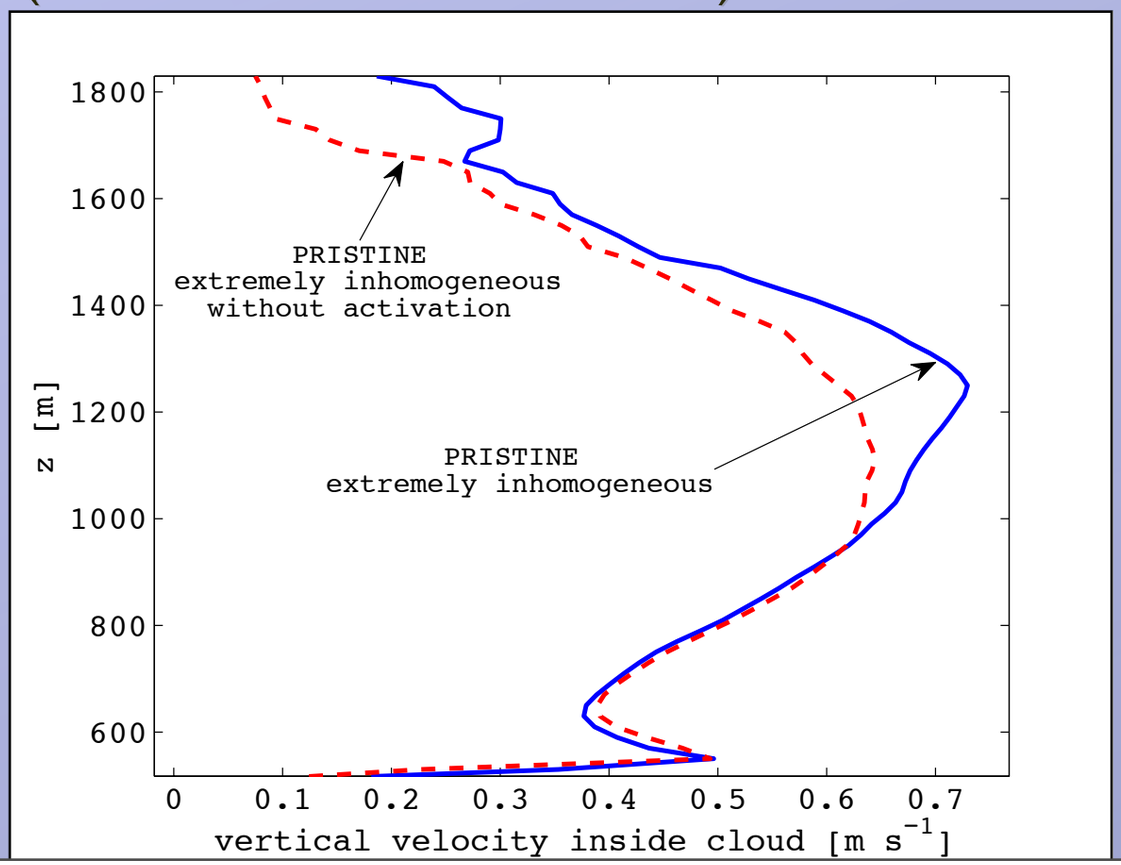

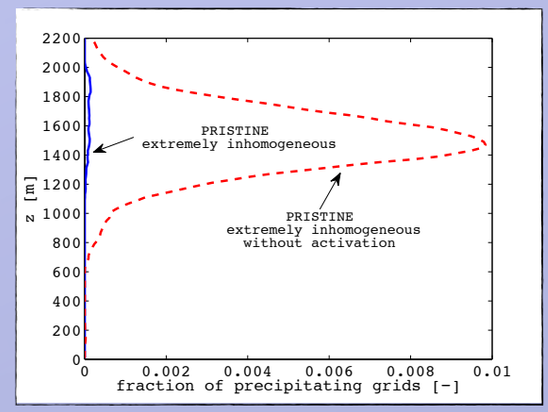

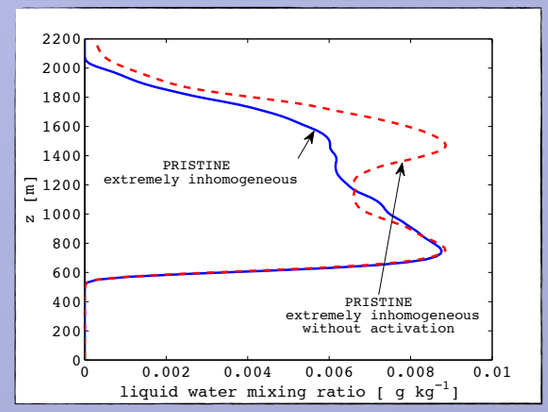

Sensitivity tests

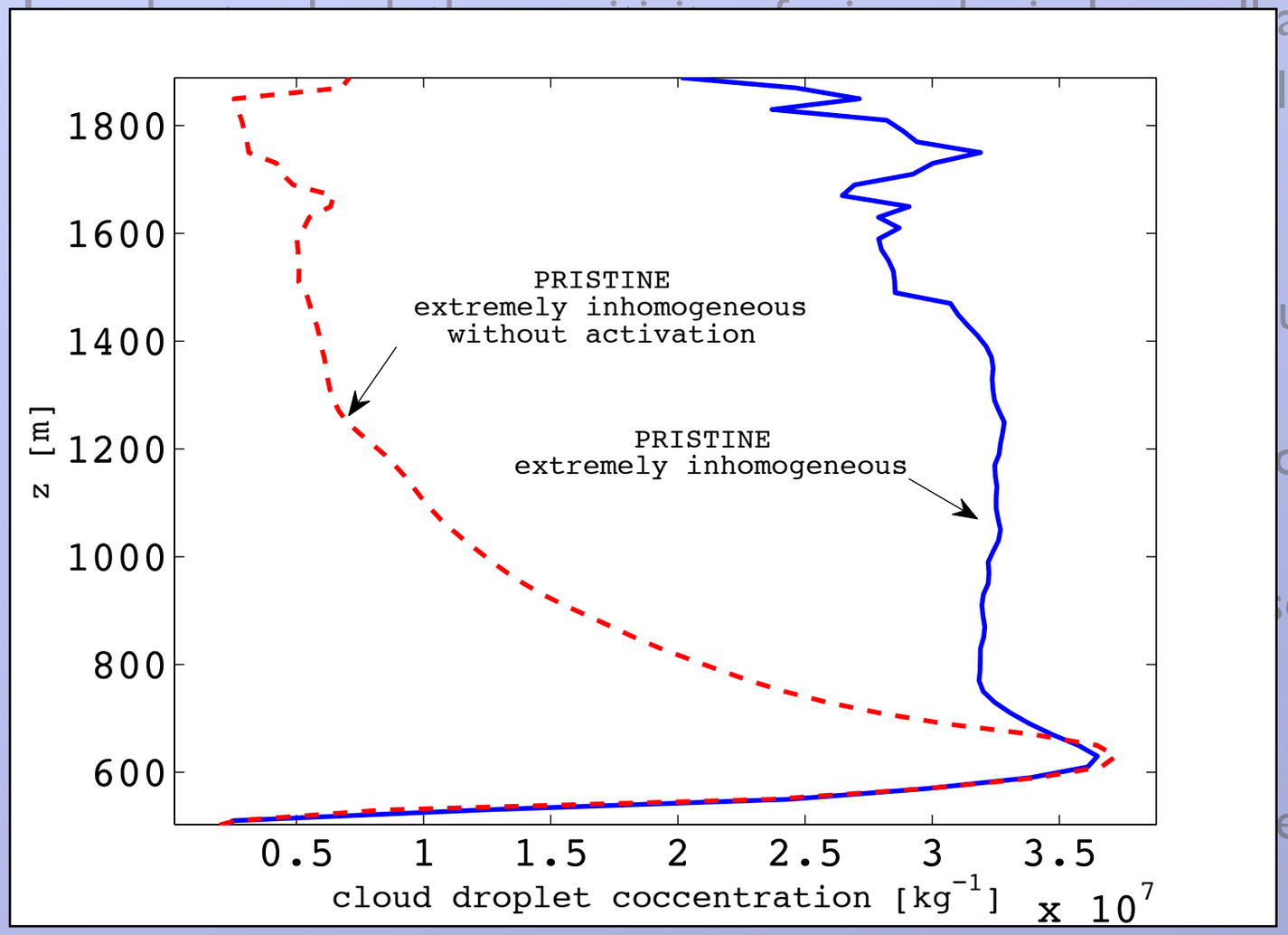

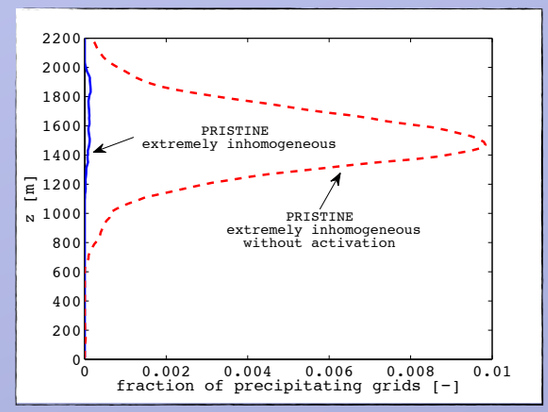

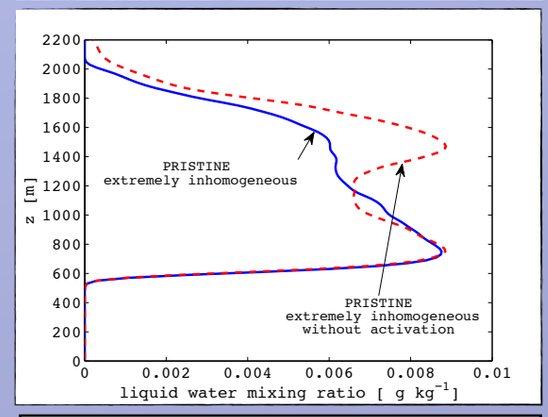

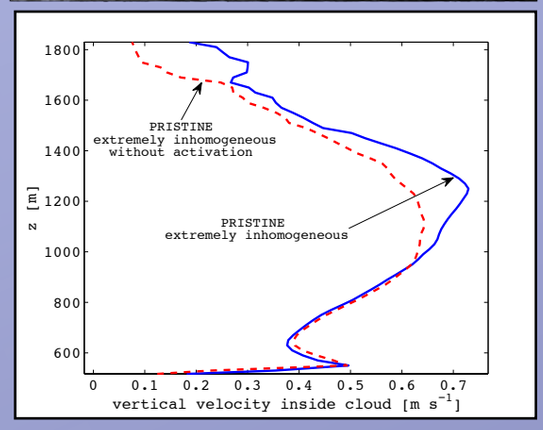

- Cloud droplet concentration decreases with height down to 5 mg $^{-1}$ (15 percent of Nc for the base run) at 2 km.

Sensitivity tests

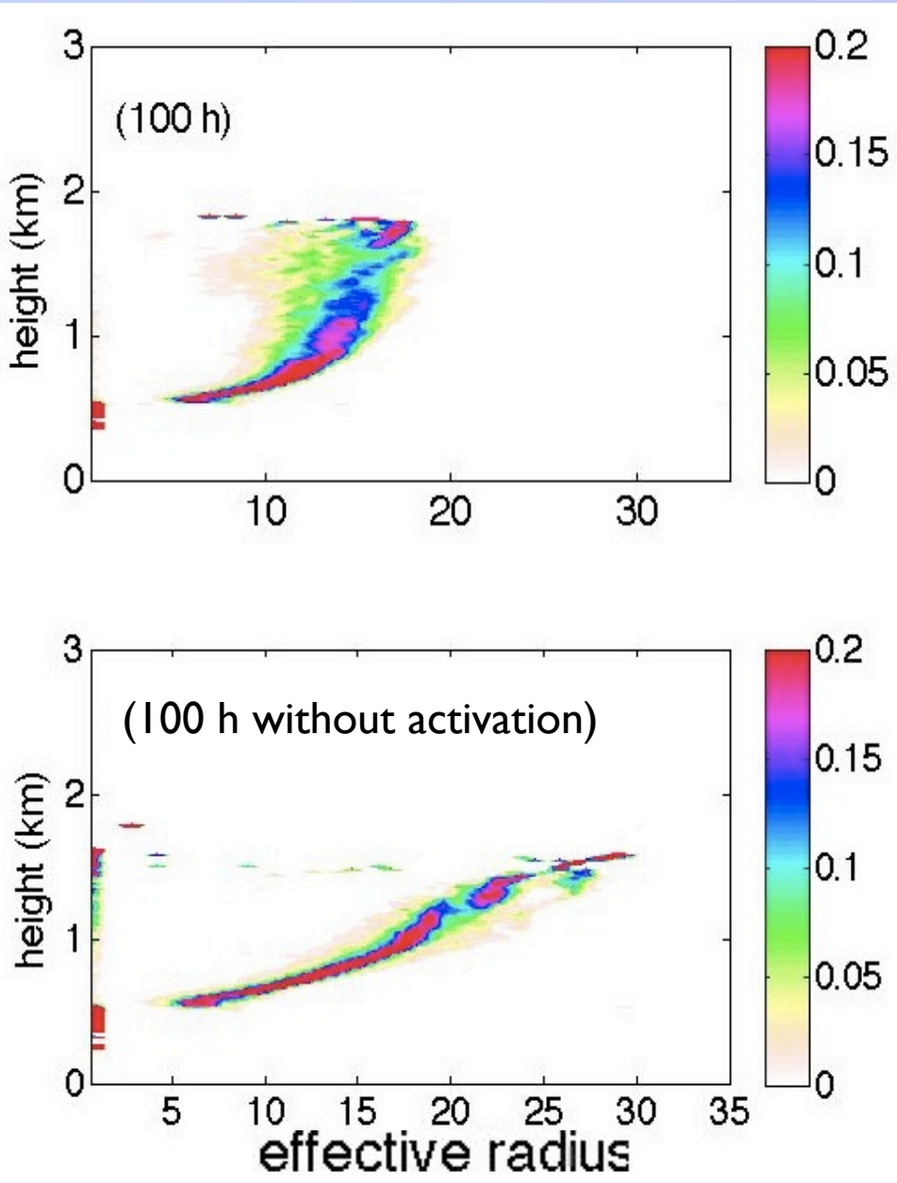

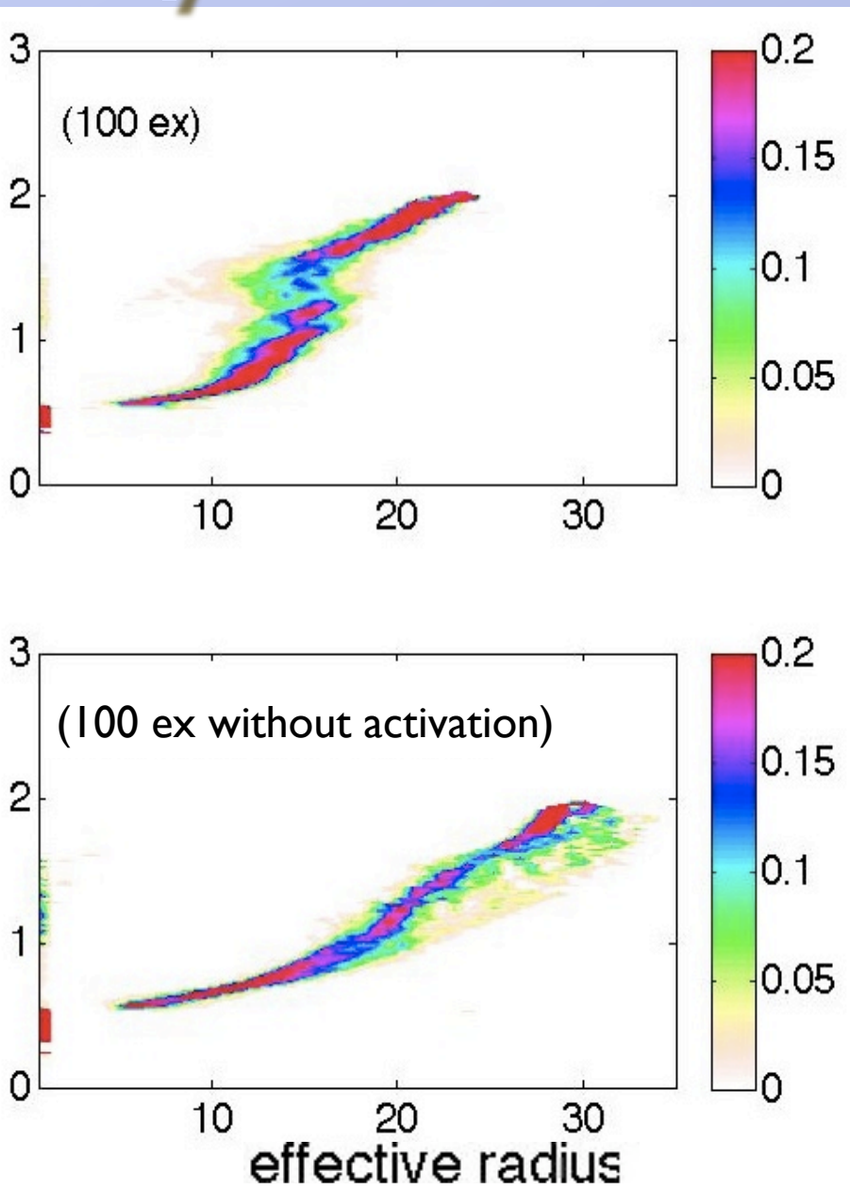

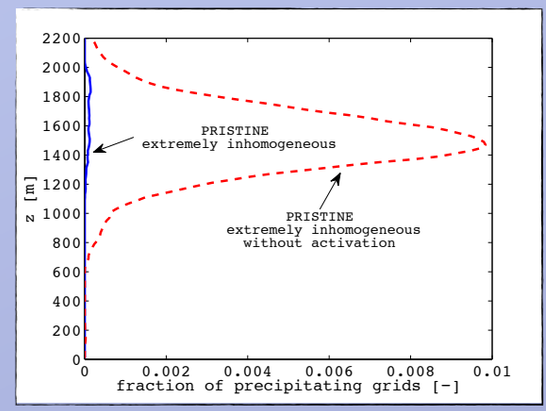

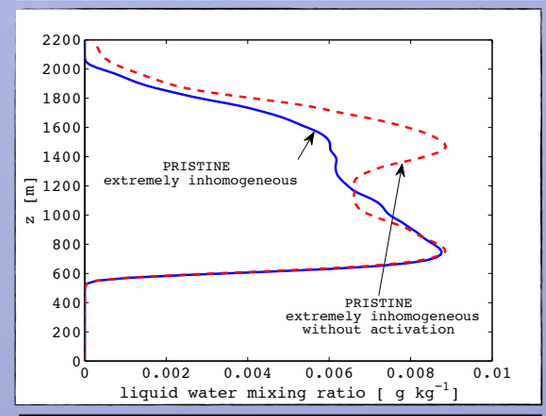

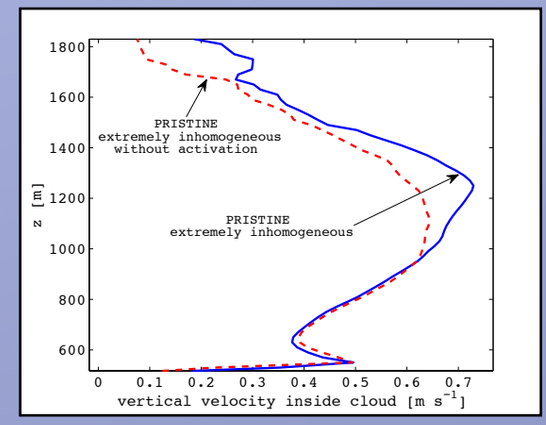

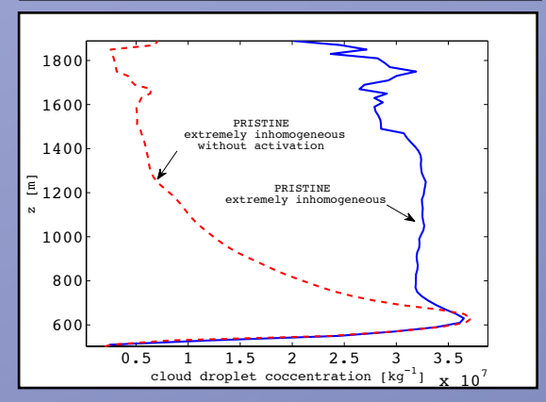

- The contour frequency of altitude diagram of effective radius is much narrower for a given height and broadening of cfad towards lower effective radii does not occur.
- In-cloud mean effective radius increases with height from 2-3 micrometers at the cloud base to above 30 micrometers at 2 km, which is much alike adiabatic radius.

Cloud droplet lifetime

- To quantify the role of activation, the time needed to activate the total number of the droplets has been calculated:

$$\tau = \frac{< \sum(N_c) >}{< \sum((\frac{\partial N}{\partial t})_{act}) >},$$

averaging is performed over time and points, where:
$q_c > 0.01$ g kg^{-1} or $N_c > 5$ cm^{-3}

- τ can be interpreted as the timescale of the cloud droplet lifetime, since it specifies how fast existing droplets are to be replaced by the one to be activated.

- For the non-precipitating cases, similar timescale of the cloud droplet lifetime should be found when calculating the time needed to deplete the total number of droplets through evaporation due to dilution and mixing.

Cloud droplet lifetime [min]	BOMEX 3-6	BOMEX 3-6 without activation	RICO 3-6	RICO 18-21	RICO 21-24 without activation
PRISTINE, homogeneous	4.00	4.20	4.70	4.18	
PRISTINE, extremely inhomogeneous	3.20	3.48	3.86	3.07	
POLLUTED, homogeneous	3.48	4.53	4.18	4.10	5.70
POLLUTED, extremely inhomogeneous	2.91	3.71	3.48	3.77	4.40

Cloud droplet lifetime

- For base simulation, timescale is in the range of about 3-5 minutes.

Cloud droplet lifetime [min]	BOMEX 3-6	BOMEX 3-6 without activation	RICO 3-6	RICO 18-21	RICO 21-24 without activation
PRISTINE, homogeneous	4.00	4.20	4.70	4.18	
PRISTINE, extremely inhomogeneous	3.20	3.48	3.86	3.07	
POLLUTED, homogeneous	3.48	4.53	4.18	4.10	5.70
POLLUTED, extremely inhomogeneous	2.91	3.71	3.48	3.77	4.40

Cloud droplet lifetime

- For base simulation, timescale is in the range of 3-5 minutes.
- Lower values for the extremely inhomogeneous mixing than for the homogeneous mixing.

Cloud droplet lifetime [min]	BOMEX 3-6	BOMEX 3-6 without activation	RICO 3-6	RICO 18-21	RICO 21-24 without activation
PRISTINE, homogeneous	4.00	4.20	4.70	4.18	
PRISTINE, extremely inhomogeneous	3.20	3.48	3.86	3.07	
POLLUTED, homogeneous	3.48	4.53	4.18	4.10	5.70
POLLUTED, extremely inhomogeneous	2.91	3.71	3.48	3.77	4.40

Cloud droplet lifetime

- For base simulation, timescale is in the range of 3-5 minutes.
- Lower values for the extremely inhomogeneous mixing than for the homogeneous mixing.
- Larger values and differences in timescale for cases without cloud droplet activation above 700m.

Cloud droplet lifetime [min]	BOMEX 3-6	BOMEX 3-6 without activation	RICO 3-6	RICO 18-21	RICO 21-24 without activation
PRISTINE, homogeneous	4.00	4.20	4.70	4.18	
PRISTINE, extremely inhomogeneous	3.20	3.48	3.86	3.07	
POLLUTED, homogeneous	3.48	4.53	4.18	4.10	5.70
POLLUTED, extremely inhomogeneous	2.91	3.71	3.48	3.77	4.40

Cloud droplet lifetime

- For base simulation, timescale is in the range of 3-5 minutes.
- Lower values for the extremely inhomogeneous mixing than for the homogeneous mixing.
- Larger values and differences in timescale for cases without cloud droplet activation above 700m.
- Lower value for the POLLUTED case than for the PRISTINE case, although not for cases that differ with precipitation.

Cloud droplet lifetime [min]	BOMEX 3-6	BOMEX 3-6 without activation	RICO 3-6	RICO 18-21	RICO 21-24 without activation
PRISTINE, homogeneous	4.00	4.20	4.70	4.18	
PRISTINE, extremely inhomogeneous	3.20	3.48	3.86	3.07	
POLLUTED, homogeneous	3.48	4.53	4.18	4.10	5.70
POLLUTED, extremely inhomogeneous	2.91	3.71	3.48	3.77	4.40

Cloud droplet lifetime.

- For base simulation, timescale is in the range of 3-5 minutes.
- Lower values for the extremely inhomogeneous mixing than for the homogeneous mixing.
- Larger values and differences in timescale for cases without cloud droplet activation above 700m.
- Lower value for the POLLUTED case than for the PRISTINE case, although not for cases that differ with precipitation.
- Cloud droplet concentration is either constant or slightly increasing with height.
- Besides a peak at the cloud base, there is an **additional peak** of activation slightly above z=1.2 km

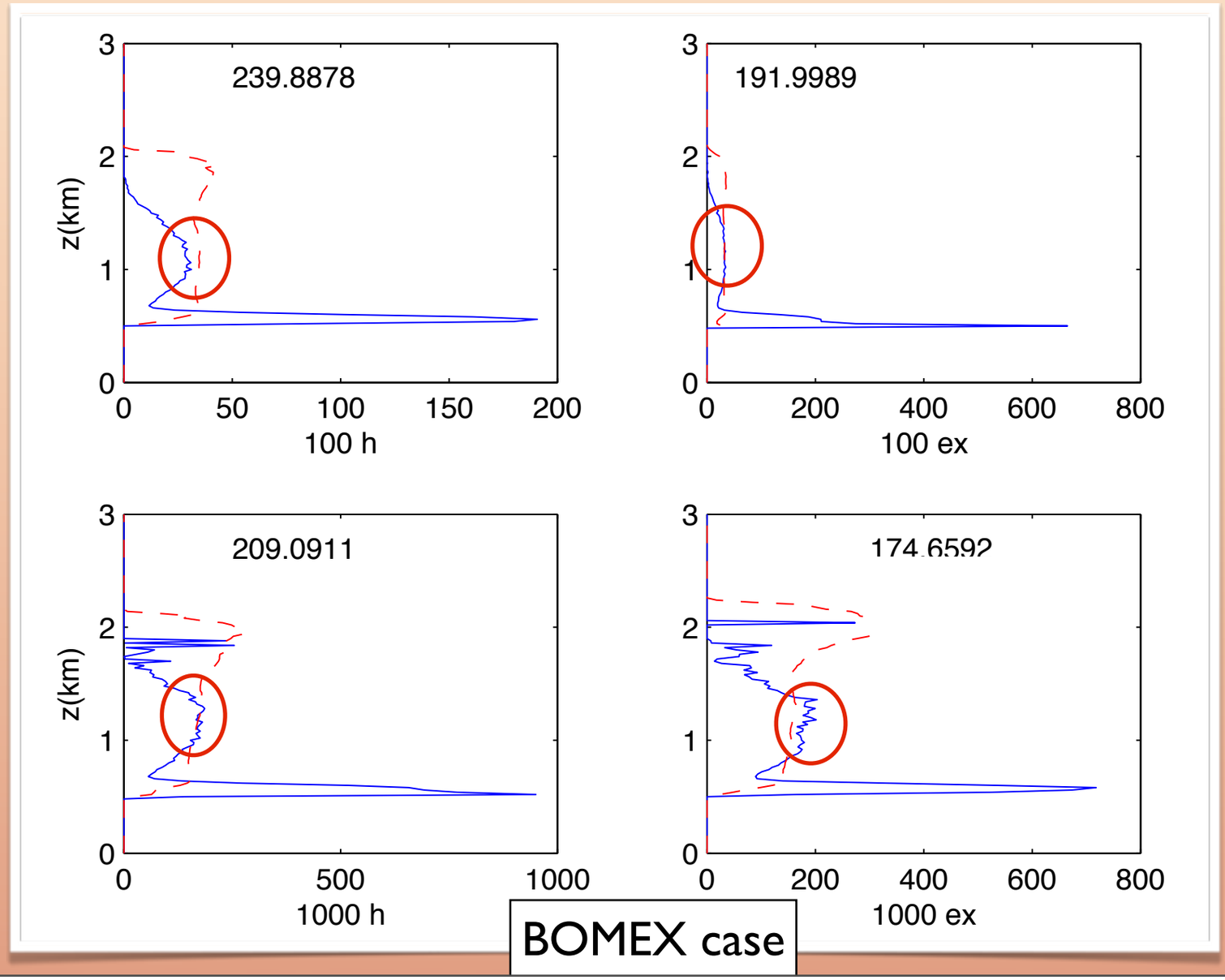

BOMEX case

Activation level versus cloud droplet fate

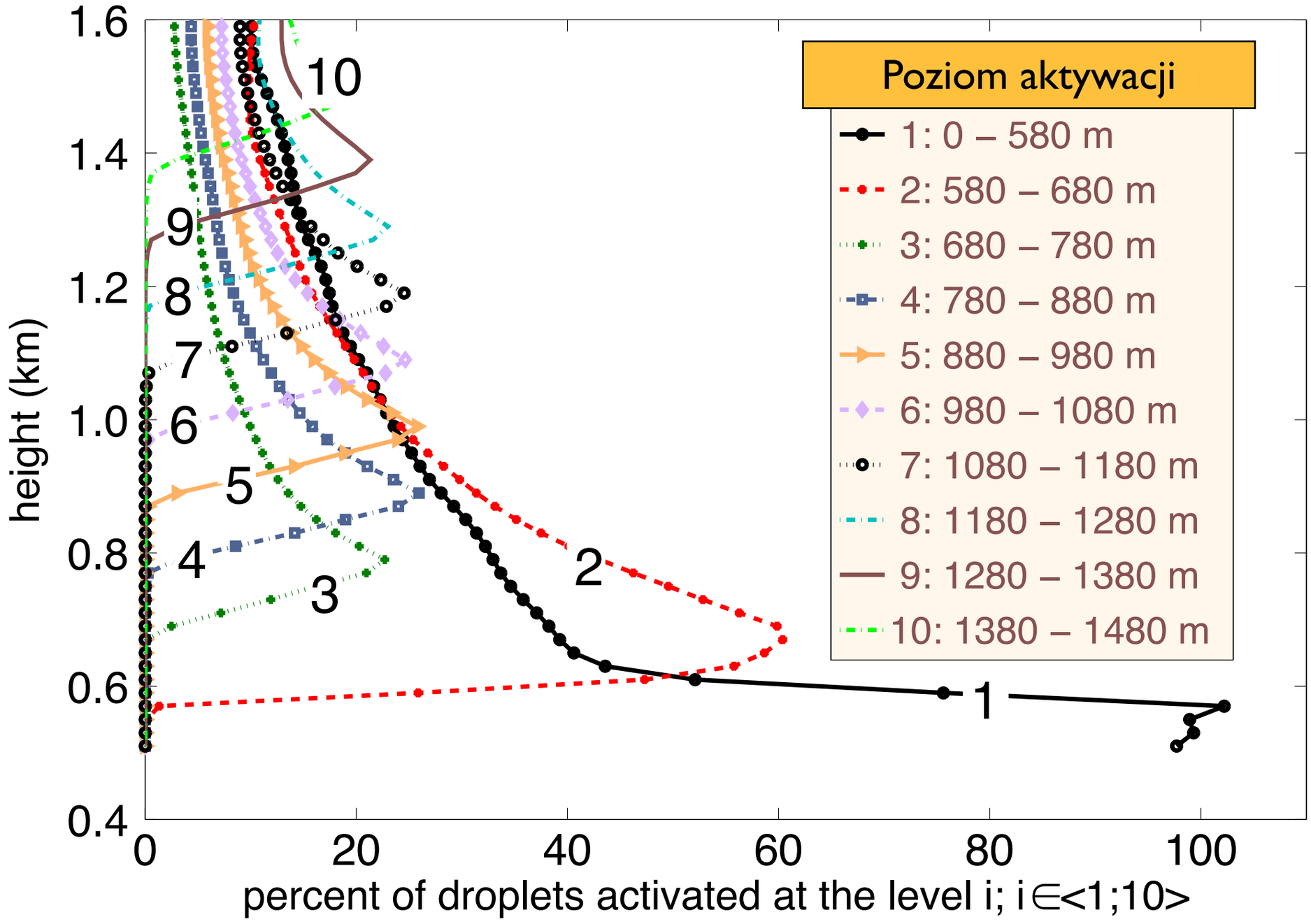

Activation level versus cloud droplet fate

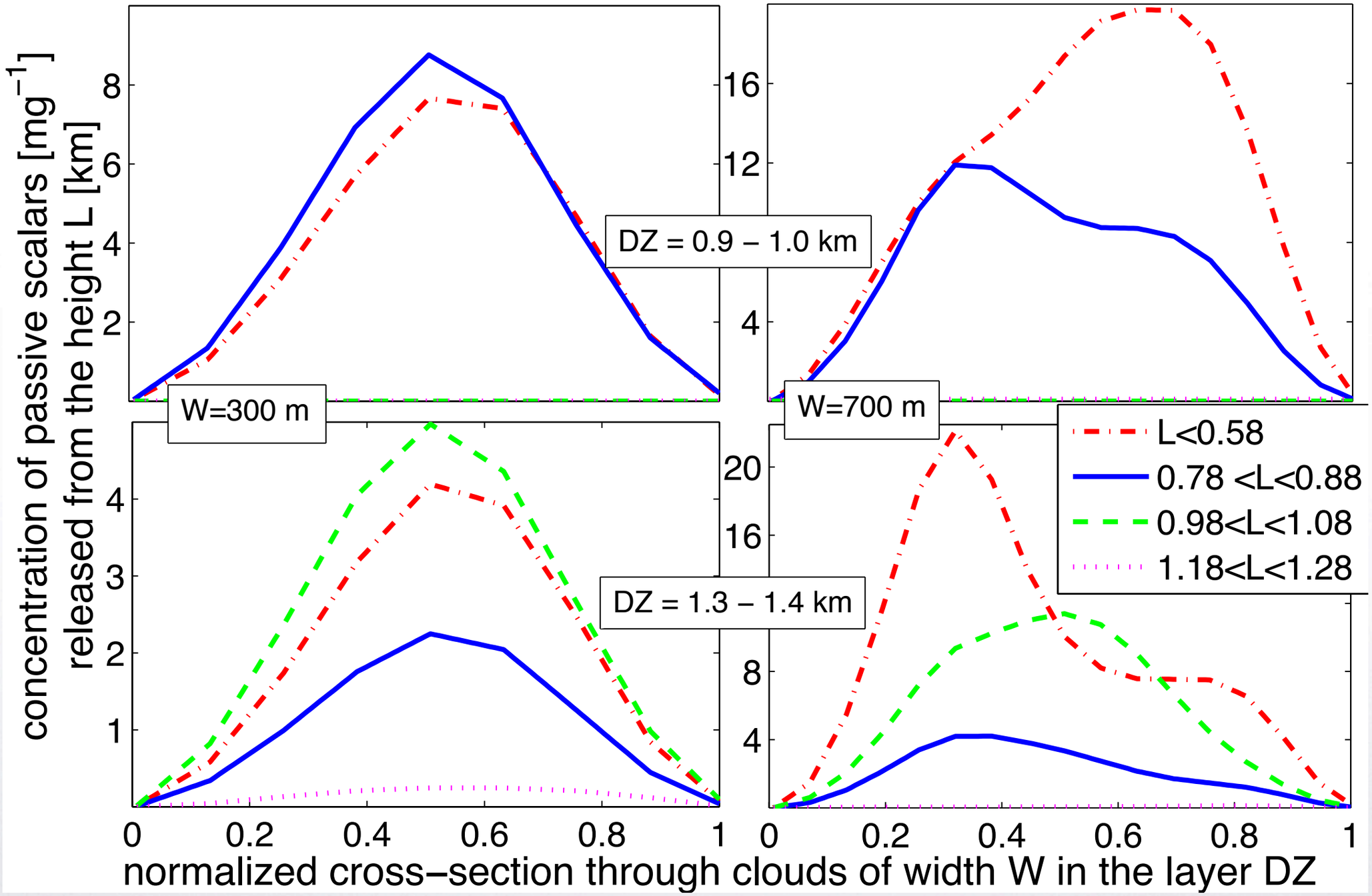

Radiative effects

- EULAG is not coupled with a radiative transfer model.
- Radiative cooling is taken into account through prescribed forcing, corresponding to clear-sky radiative cooling (given in setup).
- Data, with effective radius being calculated, allows for the estimation of radiative effects.
- The two-stream radiation transfer model was applied column-by-column to model output.
- This model comes from the NCAR Community Climate System Model (CCSM; Kiehl et al. 1994), so called independent-column approximation.
- With this model, shortwave and longwave radiative transport is calculated for every column.
- Clear-sky as well as cloud droplet effects are included.
- Annual and diurnal cycle are neglected and a constant value of incoming solar flux is taken as 436 W m^{-2}, with zero zenith angle assumed.
- The surface albedo, here set as the albedo of the ocean surface (0.05).

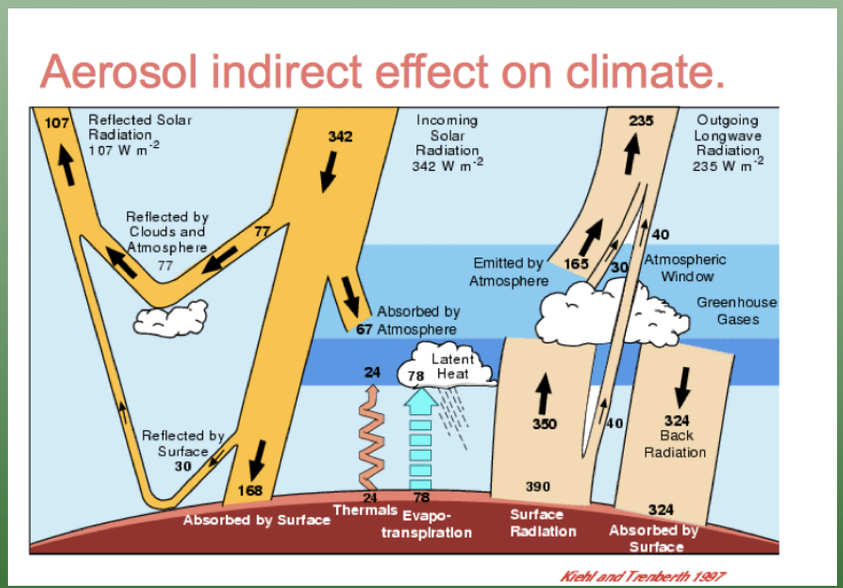

Radiative effects

- EULAG is not coupled with a radiative transfer model.
- Radiative cooling is taken into account through prescribed forcing, corresponding to clear-sky radiative cooling (given in setup).
- Data, with effective radius being calculated, allows for the estimation of radiative effects.
- The two-stream radiation transfer model was applied column-by-column to model output.
- This model comes from the NCAR Community Climate System Model (CCSM; Kiehl et al. 1994), so called independent-column approximation.
- With this model, shortwave and longwave radiative transport is calculated for every column.
- Clear-sky as well as cloud droplet effects are included.
- Annual and diurnal cycle are neglected and a constant value of incoming solar flux is taken as 436 W m^{-2}, with zero zenith angle assumed.
- The surface albedo, here set as the albedo of the ocean surface (0.05).

Top of the atmosphere (TOA) albedo (for model columns with LWP greater than $5*10^{-3}$ kg m^{-2})	BOMEX 3-6	BOMEX 3-6 without activation	RICO 3-6	RICO 18-21	RICO 18-21 without activation
PRISTINE homogeneous	0.270	0.238	0.286	0.315	
PRISTINE extremely inhomogeneous	0.265	0.233	0.282	0.330	
POLLUTED homogeneous	0.347	0.308	0.357	0.372	0.350
POLLUTED extremely inhomogeneous	0.338	0.289	0.357	0.406	0.315

Radiative effects

- EULAG is not coupled with a radiative transfer model.
- Radiative cooling is taken into account through prescribed forcing, corresponding to clear-sky radiative cooling (given in setup).
- Data, with effective radius being calculated, allows for the estimation of radiative effects.
- The two-stream radiation transfer model was applied column-by-column to model output.
- This model comes from the NCAR Community Climate System Model (CCSM; Kiehl et al. 1994), so called independent-column approximation.
- With this model, shortwave and longwave radiative transport is calculated for every column.
- Clear-sky as well as cloud droplet effects are included.
- Annual and diurnal cycle are neglected and a constant value of incoming solar flux is taken as 436 W m^{-2}, with zero zenith angle assumed.
- The surface albedo, here set as the albedo of the ocean surface (0.05).

Top of the atmosphere (TOA) albedo (for model columns with LWP greater than $5*10^{-3}$ kg m^{-2})	BOMEX 3-6	BOMEX 3-6 without activation	RICO 3-6	RICO 18-21	RICO 18-21 without activation
PRISTINE homogeneous	0.270	0.238	0.286	0.315	
PRISTINE extremely inhomogeneous	0.265	0.233	0.282	0.330	
POLLUTED homogeneous	0.347	0.308	0.357	0.372	0.350
POLLUTED extremely inhomogeneous	0.338	0.289	0.357	0.406	0.315

Radiative effects

- EULAG is not coupled with a radiative transfer model.
- Radiative cooling is taken into account through prescribed forcing, corresponding to clear-sky radiative cooling (given in setup).
- Data, with effective radius being calculated, allows for the estimation of radiative effects.
- The two-stream radiation transfer model was applied column-by-column to model output.
- This model comes from the NCAR Community Climate System Model (CCSM; Kiehl et al. 1994), so called independent-column approximation.
- With this model, shortwave and longwave radiative transport is calculated for every column.
- Clear-sky as well as cloud droplet effects are included.
- Annual and diurnal cycle are neglected and a constant value of incoming solar flux is taken as 436 W m^{-2}, with zero zenith angle assumed.
- The surface albedo, here set as the albedo of the ocean surface (0.05).

Top of the atmosphere (TOA) albedo (for model columns with LWP greater than $5*10^{-3}$ kg m^{-2})	BOMEX 3-6	BOMEX 3-6 without activation	RICO 3-6	RICO 18-21	RICO 18-21 without activation
PRISTINE homogeneous	0.270	0.238	0.286	0.315	
PRISTINE extremely inhomogeneous	0.265	0.233	0.282	0.330	
POLLUTED homogeneous	0.347	0.308	0.357	0.372	0.350
POLLUTED extremely inhomogeneous	0.338	0.289	0.357	0.406	0.315

Radiative effects

- EULAG is not coupled with a radiative transfer model.
- Radiative cooling is taken into account through prescribed forcing, corresponding to clear-sky radiative cooling (given in setup).
- Data, with effective radius being calculated, allows for the estimation of radiative effects.
- The two-stream radiation transfer model was applied column-by-column to model output.
- This model comes from the NCAR Community Climate System Model (CCSM; Kiehl et al. 1994), so called independent-column approximation.
- With this model, shortwave and longwave radiative transport is calculated for every column.
- Clear-sky as well as cloud droplet effects are included.
- Annual and diurnal cycle are neglected and a constant value of incoming solar flux is taken as 436 W m^{-2}, with zero zenith angle assumed.
- The surface albedo, here set as the albedo of the ocean surface (0.05).

Top of the atmosphere (TOA) albedo (for model columns with LWP greater than $5*10^{-3}$ kg m^{-2})	BOMEX 3-6	BOMEX 3-6 without activation	RICO 3-6	RICO 18-21	RICO 18-21 without activation
PRISTINE homogeneous	0.270	0.238	0.286	0.315	
PRISTINE extremely inhomogeneous	0.265	0.233	0.282	0.330	
POLLUTED homogeneous	0.347	0.308	0.357	0.372	0.350
POLLUTED extremely inhomogeneous	0.338	0.289	0.357	0.406	0.315

Mixing scenario impact

Cloud droplet lifetime (τ), mean effective radius (r_{eff}) and mean cloud TOA albedo (A_{cloudy}) for the PRISTINE (100) and POLLUTED (1000) case with homogeneous (h) or extremely inhomogeneous (ex) mixing scenario with in-cloud activation turn on (ACT ON) or turn off (ACT OFF).

	τ [min]	r_{eff} [μm]	A_{cloudy} [1]
100 h; ACT ON	4.00	11.20	0.270
100 ex; ACT ON	3.20	11.97	0.265
1000 h; ACT ON	3.48	6.97	0.347
1000 ex; ACT ON	2.91	7.33	0.338
100 h; ACT OFF	4.20	15.51	0.238
100 ex; ACT OFF	3.48	17.74	0.233
1000 h; ACT OFF	4.53	9.80	0.308
1000 ex; ACT OFF	3.71	11.23	0.289

Mixing scenario impact

Cloud droplet lifetime (τ), mean effective radius (r_{eff}) and mean cloud TOA albedo (A_{cloudy}) for the PRISTINE (100) and POLLUTED (1000) case with homogeneous (h) or extremely inhomogeneous (ex) mixing scenario with in-cloud activation turn on (ACT ON) or turn off (ACT OFF).

	τ [min]	r_{eff} [μm]	A_{cloudy} [1]
100 h; ACT ON	4.00	11.20	0.270
100 ex; ACT ON	3.20	11.97	0.265
1000 h; ACT ON	3.48	6.97	0.347
1000 ex; ACT ON	2.91	7.33	0.338
100 h; ACT OFF	4.20	15.51	0.238
100 ex; ACT OFF	3.48	17.74	0.233
1000 h; ACT OFF	4.53	9.80	0.308
1000 ex; ACT OFF	3.71	11.23	0.289

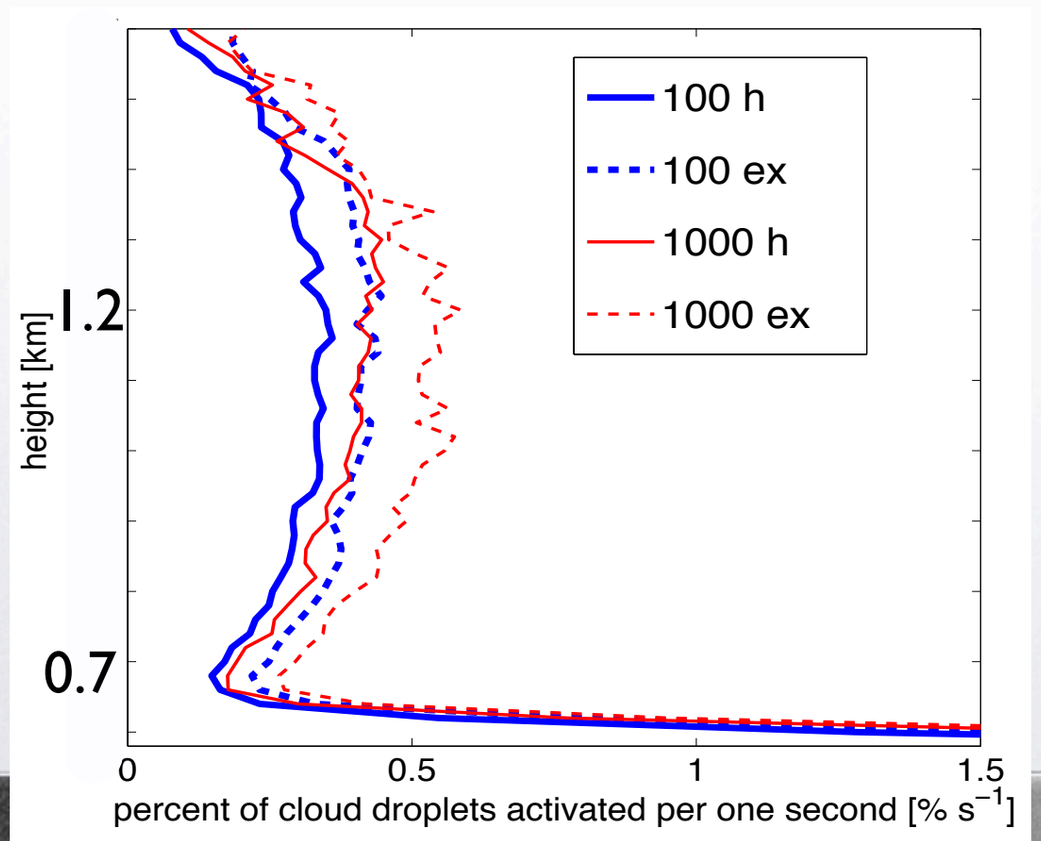

IMPACT OF EXTREMELY INHOMOGENEOUS MIXING (IN COMPARISON TO HOMOGENEOUS MIXING):

- Ratio of activation tendency is larger (left plot)
- Cloud droplet lifetime, τ, is shorter (Table)
- This is because cloud droplets disappear faster and thus in-cloud activation can happen more intensively
- This is because there is more CCN can be activated after being entrained into a cloud.

in other words....

activation decreases differences in between mixing scearios.

Properties of entrained air

- Assumption that initially the cloud is adiabatic.
- Final, i.e., after mixing, properties of the cloud are given from the model output.
- The impact of mixing is expressed by the following relations:

$$q_{t,c} = (1 - X) \times q_{t,ad} + X \times q_{t,env},$$

$$T_{l,c} = (1 - X) \times T_{l,ad} + X \times T_{l,env},$$

Subscripts c, ad and env correspond to: cloudy, adiabatic, and environmental state.

X - dilution ratio

q_t – total water mixing ratio (consisting only of water vapour mixing ratio in the environment)

T_l - liquid water potential temperature

- For simulations without in-cloud activation, the depletion of in-cloud droplet concentration relates to the mixing that is enabled throughout the cloud.
- Thus, a similar relation can be written for cloud droplet concentration, Nc , depletion.
- Lack of cloud droplets in the environment allows for simplification of the equation:

$$N_c = N_{ad} \times (1 - X)$$

Properties of entrained air

- Dilution ratio

$$X = 1 - \frac{< N_c >}{< N_{ad} >},$$

- Diagnostic water vapour mixing ratio of entrained air

$$q_{v,env} = \frac{< q_{t,c} > -(1 - X) \times < q_{t,ad} >}{X},$$

- Diagnostic liquid water potential temperature of entrained air

$$T_{l,env} = \frac{< T_{l,c} > -(1 - X) \times < T_{l,ad} >}{X},$$

Properties of entrained air

Dilution ratio

$$X = 1 - \frac{< N_c >}{< N_{ad} >},$$

dashed-dotted line - adiabatic fraction
dashed line - mean profile of locally calculated dilution
solid line - dilution calculated from mean profiles
red line - homogeneous mixing scenario
green line - extremely inhomogeneous mixing scenario

Diagnostic water vapour mixing ratio of entrained air

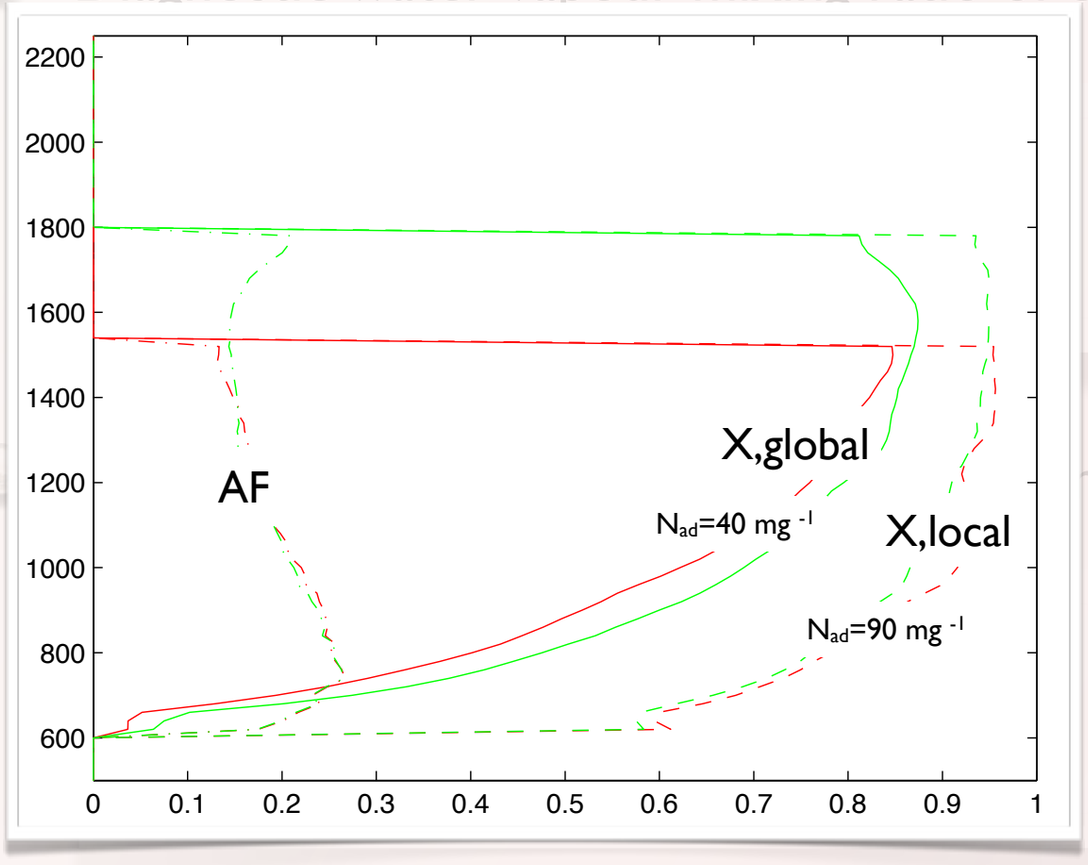

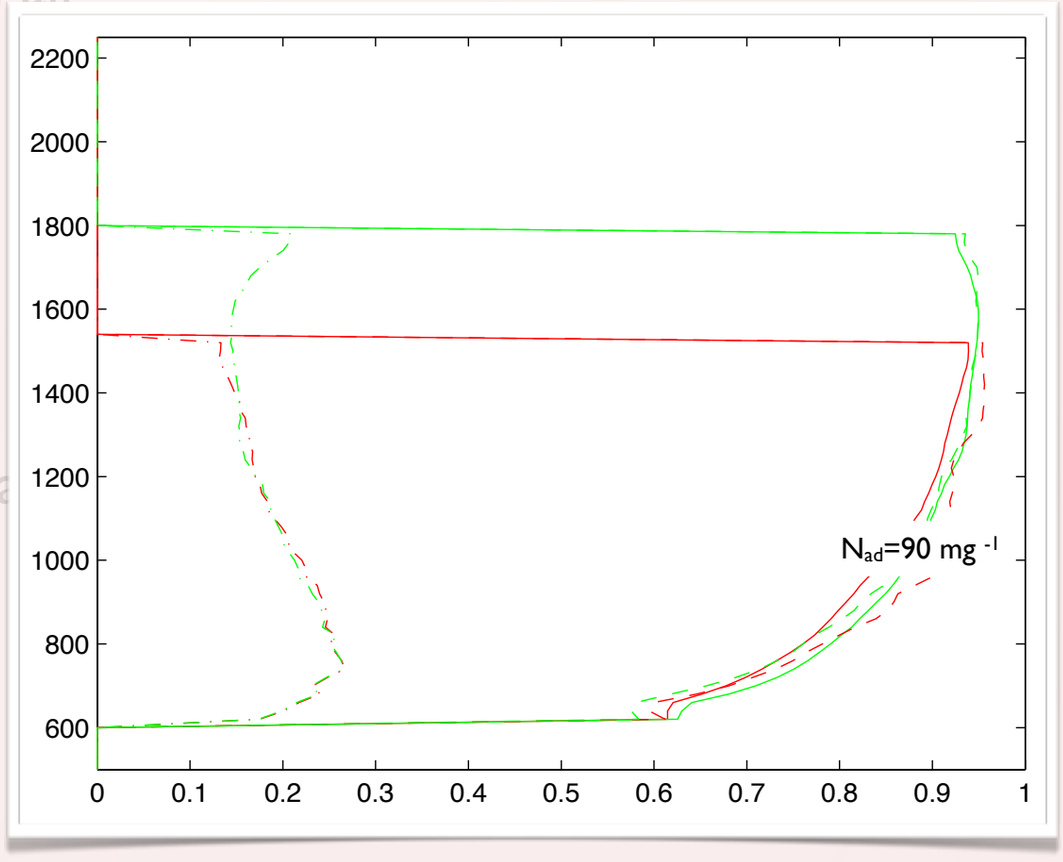

BOMEX, 3-6

Properties of entrained air

Dilution ratio

$$X = 1 - \frac{< N_c >}{< N_{ad} >},$$

dashed-dotted line - adiabatic fraction
dashed line - mean profile of locally calculated dilution
solid line - dilution calculated from mean profiles
green line - homogeneous mixing scenario
red line - extremely inhomogeneous mixing scenario

Diagnostic water vapour mixing ratio of entrained air

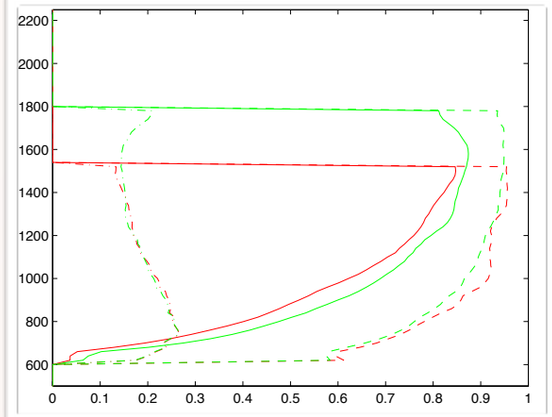

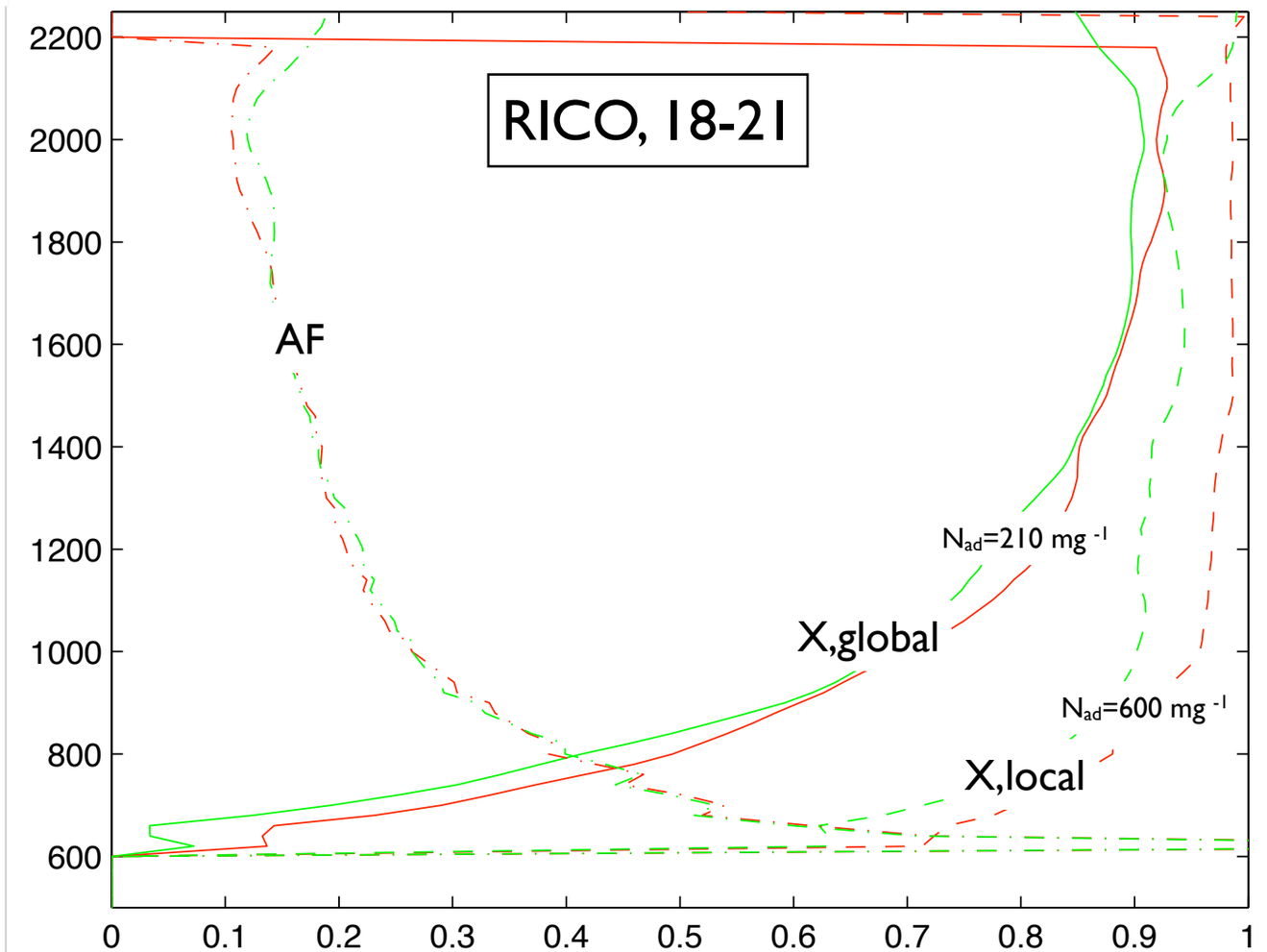

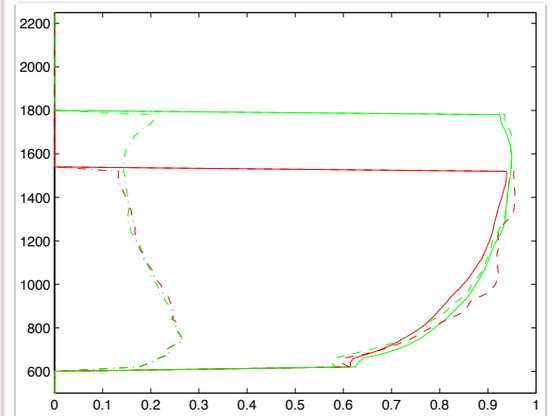

Diagnostic liquid w

$$T_{l,env} = \frac{< T_{l,c} >}$$

Properties of entrained air

- Dilution ratio

$$X = 1 - \frac{< N_c >}{< N_{ad} >},$$

- Diagnostic water vapour mixing ratio of entrained air

$$q_{v,env} = \frac{< q_{t,c} > -(1 - X) \times < q_{t,ad} >}{X},$$

- Diagnostic liquid water potential temperature of entrained air

$$T_{l,env} = \frac{< T_{l,c} > -(1 - X) \times < T_{l,ad} >}{X},$$

Properties of entrained air

Diagnostic water vapour mixing ratio

$$q_{v,env} = \frac{< q_{t,c} > -(1 - X) \times < q_{t,ad} >}{X},$$

BOMEX, 3-6

different adiabatic concentration:
40, 50, 60, 70, 80, 90 mg^{-1}

Properties of entrained air

Diagnostic water vapour mixing ratio

$$q_{v,env} = \frac{< q_{t,c} > -(1-X) \times < q_{t,ad} >}{X},$$

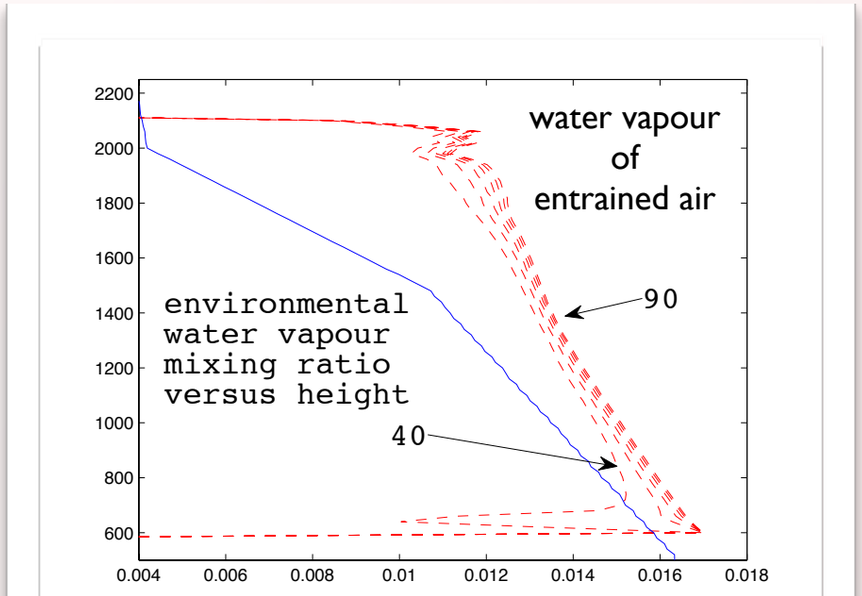

BOMEX, 3-6

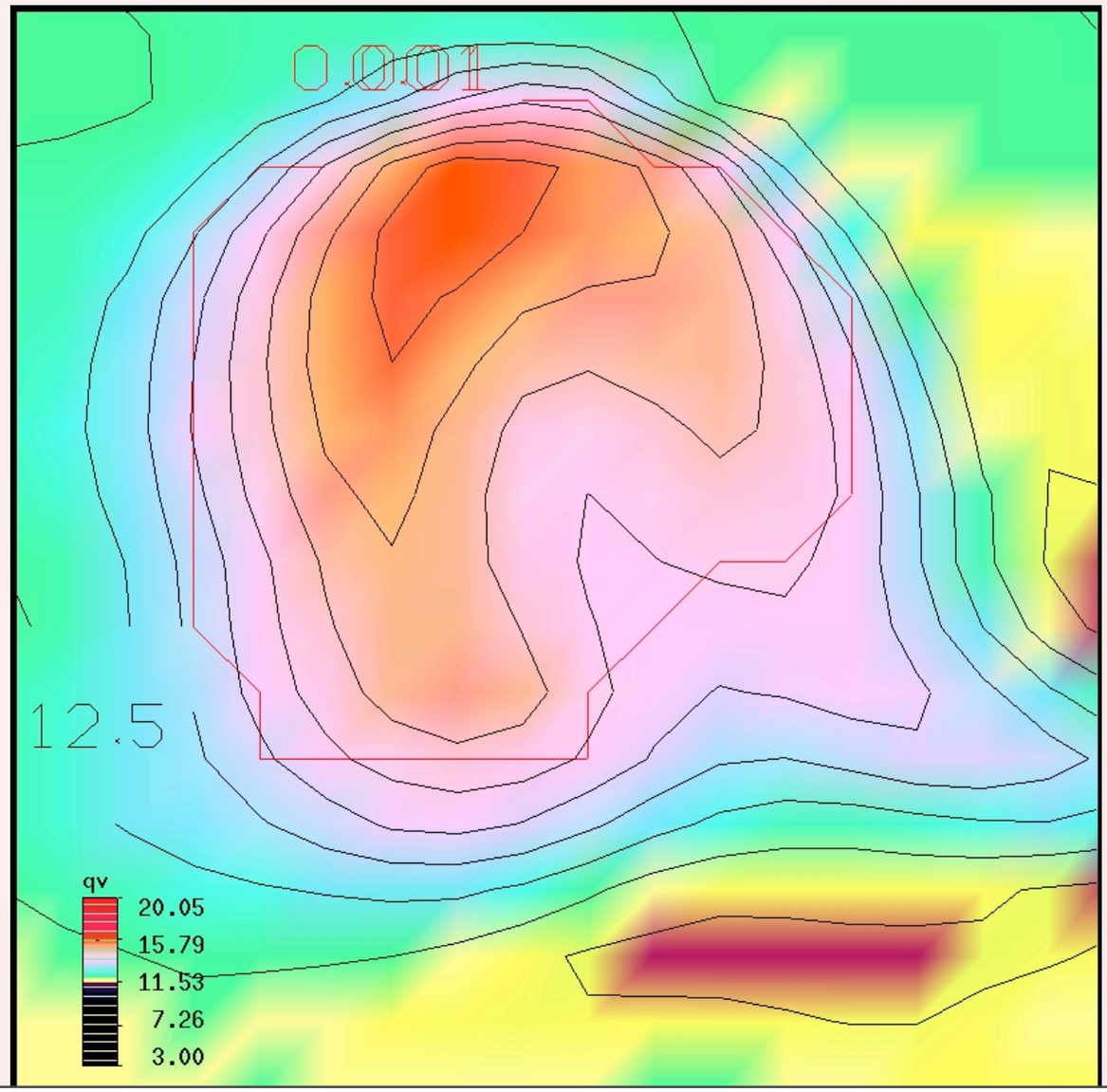

background color - water vapour mixing ratio
black isolines - water vapour mixing ratio
red contours - isolines of qc=0.001 g kg^{-1}
z=1200 m

Properties of entrained air

Diagnostic relative humidity

$$q_{v,env} = \frac{< q_{t,c} > -(1 - X) \times < q_{t,ad} >}{X},$$

blue line - environmental profile
dashed line - mean profile of locally calculated dilution
solid line - dilution calculated from mean profiles
red line - homogeneous mixing scenario
green line - extremely inhomogeneous mixiing scenario

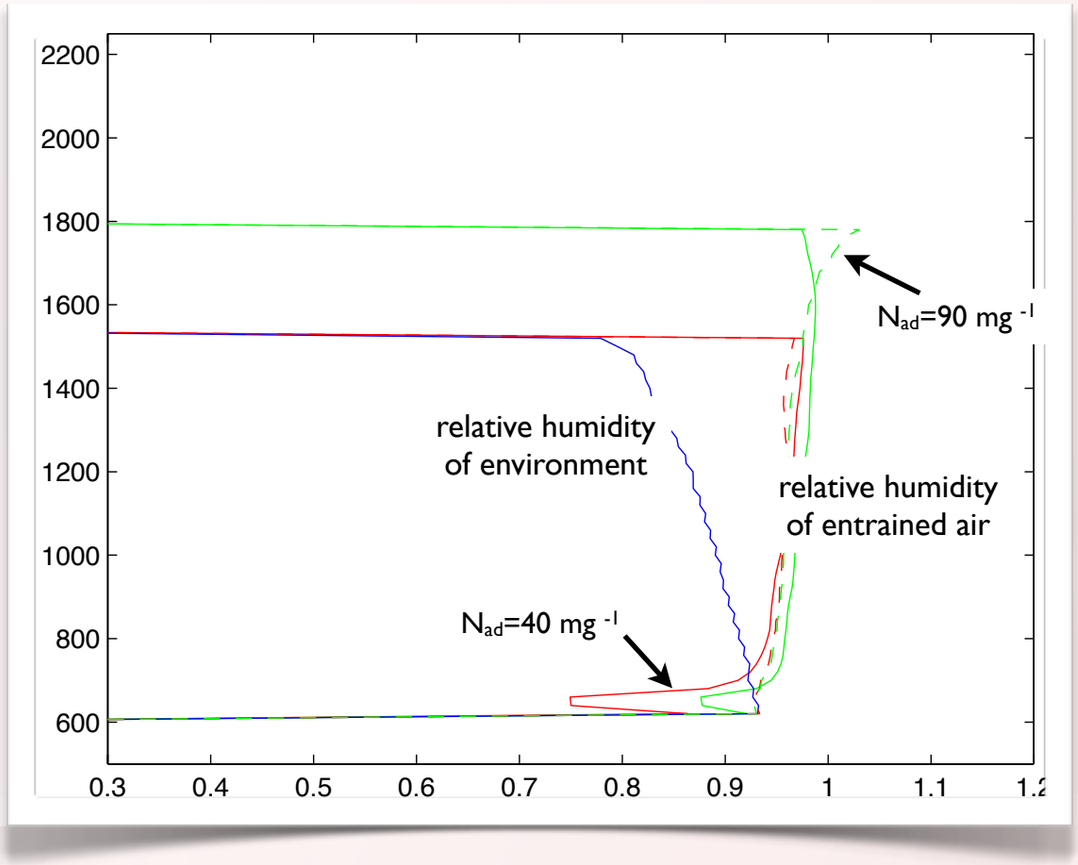

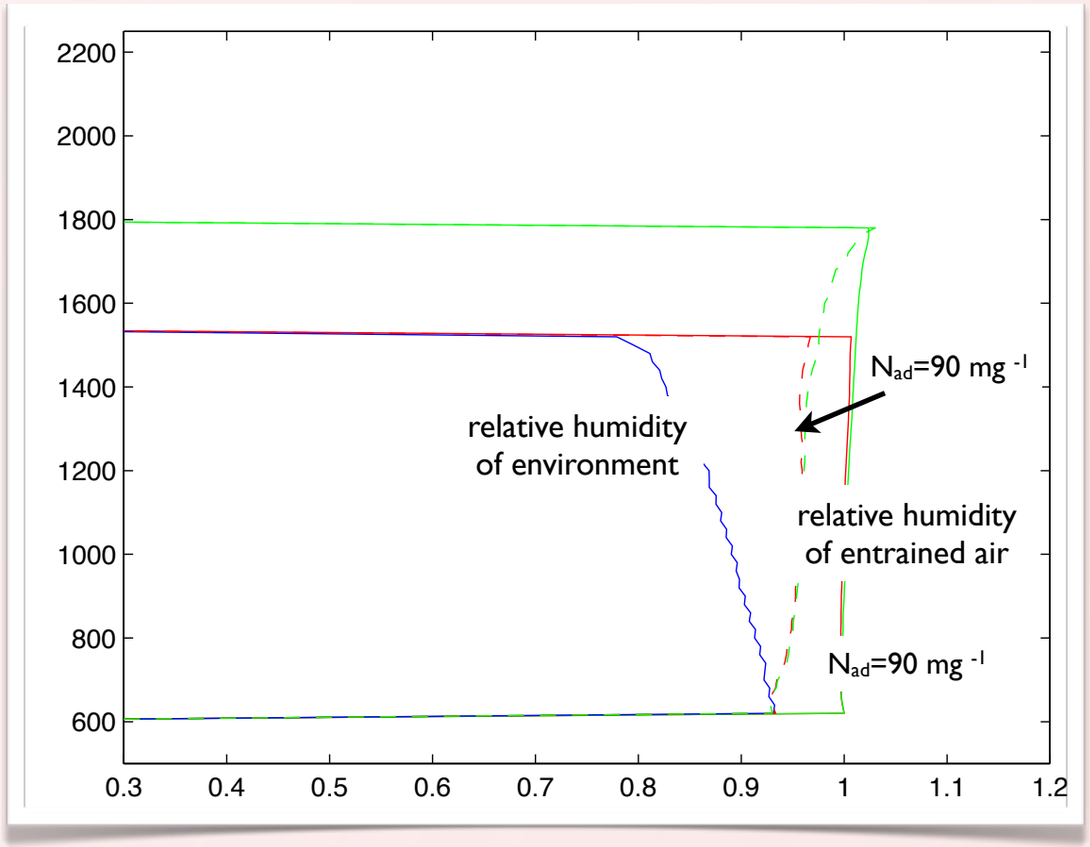

BOMEX, 3-6

Properties of entrained air

Diagnostic relative humidity

$$q_{v,env} = \frac{< q_{t,c} > -(1 - X) \times < q_{t,ad} >}{X},$$

blue line - environmental profile
dashed line - mean profile of locally calculated dilution
solid line - dilution calculated from mean profiles
green line - homogeneous mixing scenario
red line - extremely inhomogeneous mixiing scenario

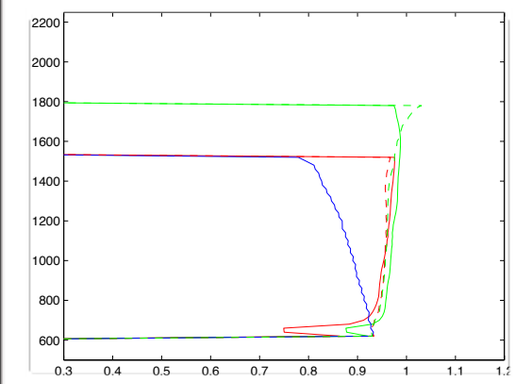

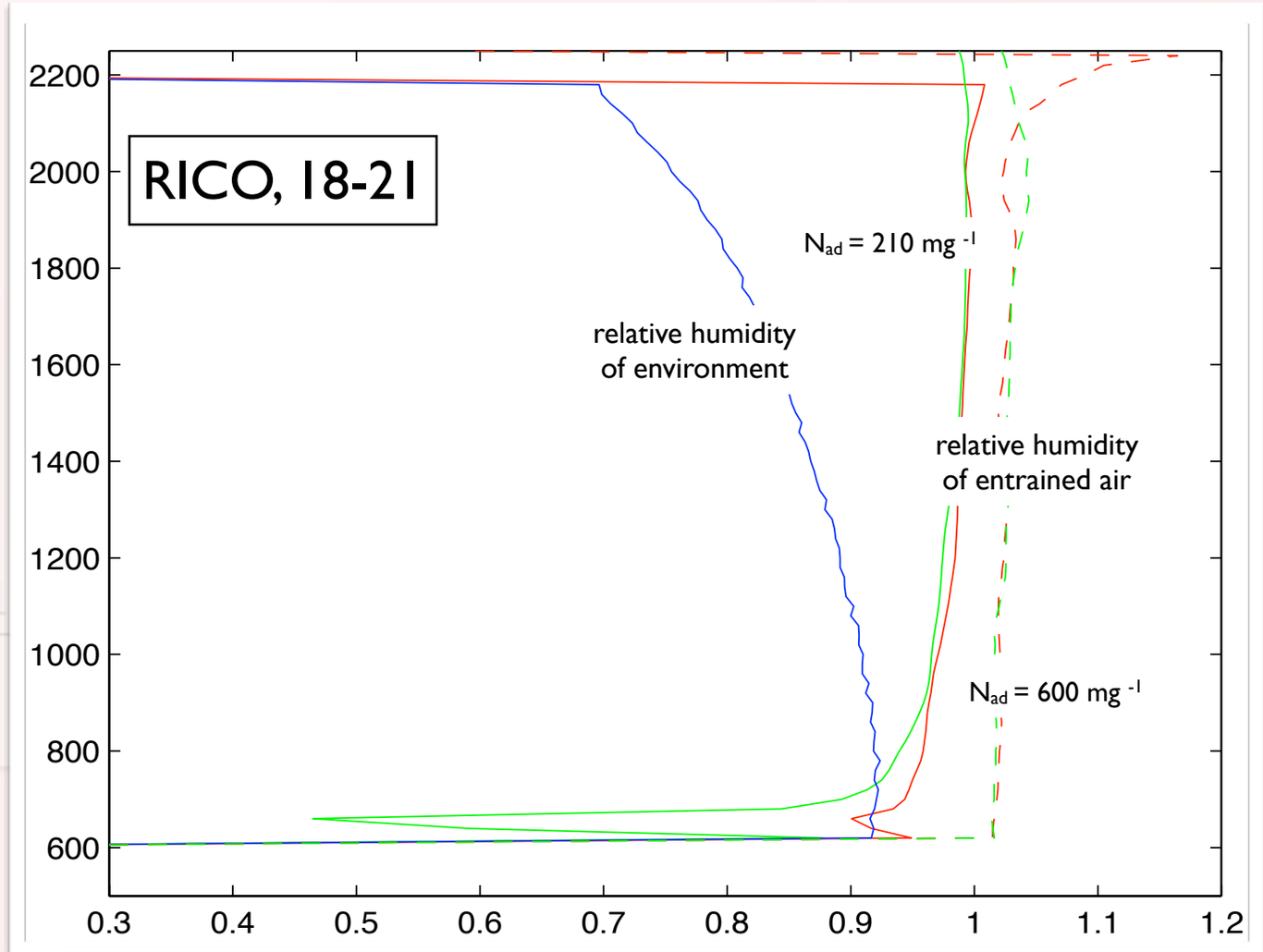

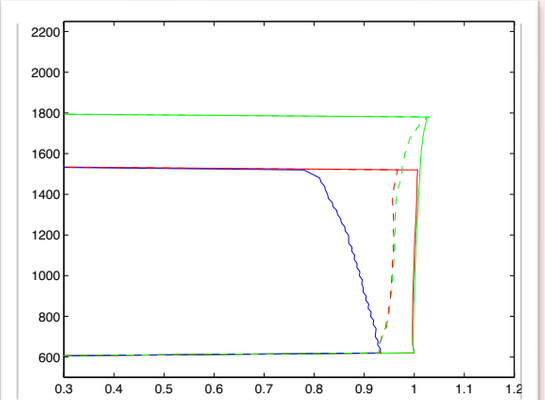

Properties of entrained air

- Dilution ratio

$$X = 1 - \frac{< N_c >}{< N_{ad} >},$$

- Diagnostic water vapour mixing ratio of entrained air

$$q_{v,env} = \frac{< q_{t,c} > -(1 - X) \times < q_{t,ad} >}{X},$$

- Diagnostic liquid water potential temperature of entrained air

$$T_{l,env} = \frac{< T_{l,c} > -(1 - X) \times < T_{l,ad} >}{X},$$

Properties of entrained air

Diagnostic liquid water potential temperature

$$T_{l,env} = \frac{< T_{l,c} > -(1 - X) \times < T_{l,ad} >}{X},$$

blue line - environmental profile
dashed line - mean profile of locally calculated dilution
solid line - dilution calculated from mean profiles
red line - homogeneous mixing scenario
green line - extremely inhomogeneous mixiing scenario

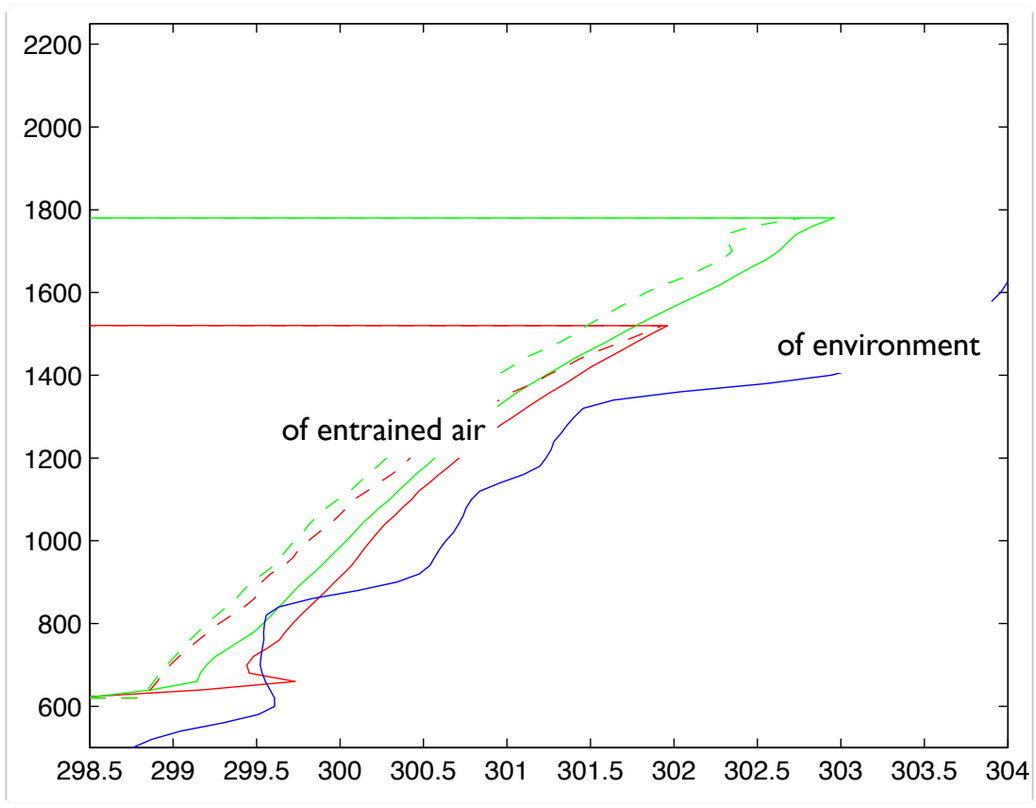

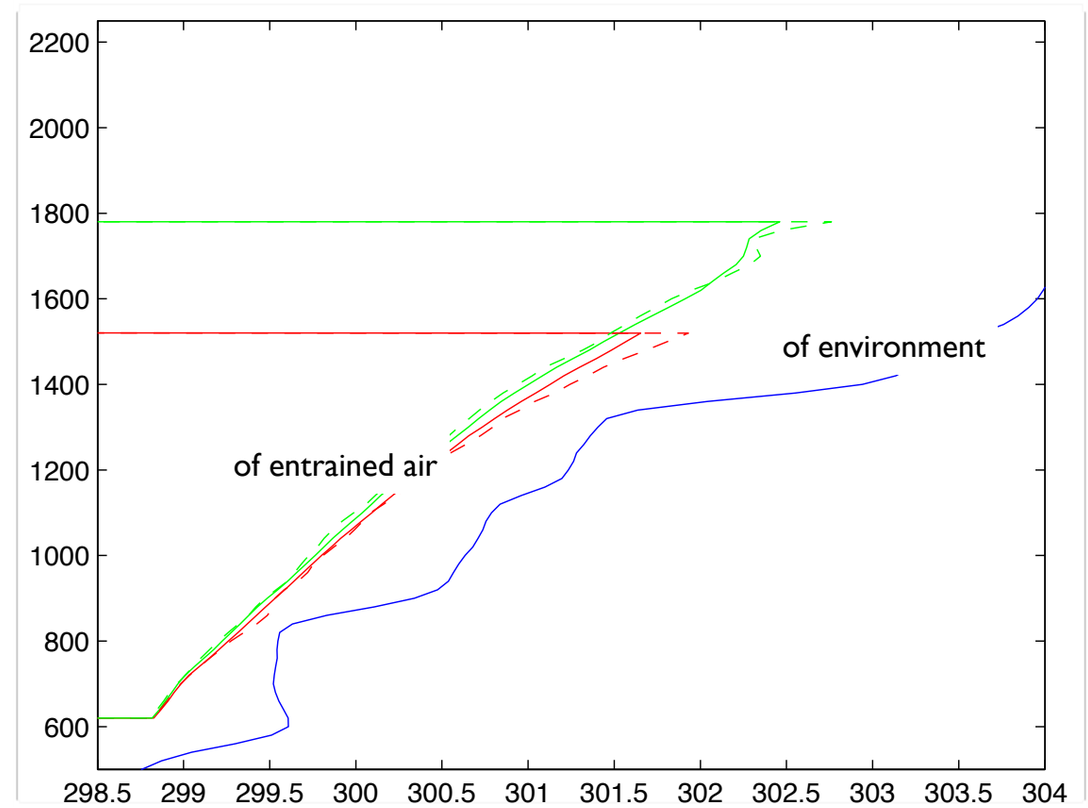

BOMEX, 3-6

Properties of entrained air

Diagnostic liquid water potential temperature

$$T_{l,env} = \frac{< T_{l,c} > -(1 - X) \times < T_{l,ad} >}{X},$$

blue line - environmental profile
dashed line - mean profile of locally calculated dilution
solid line - dilution calculated from mean profiles
green line - homogeneous mixing scenario
red line - extremely inhomogeneous mixiing scenario

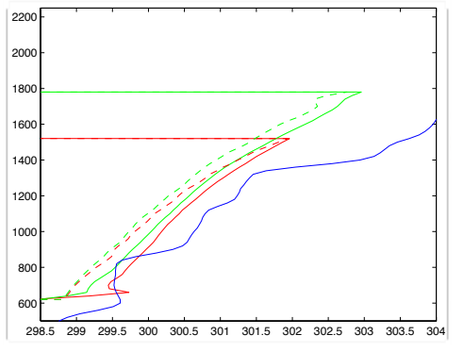

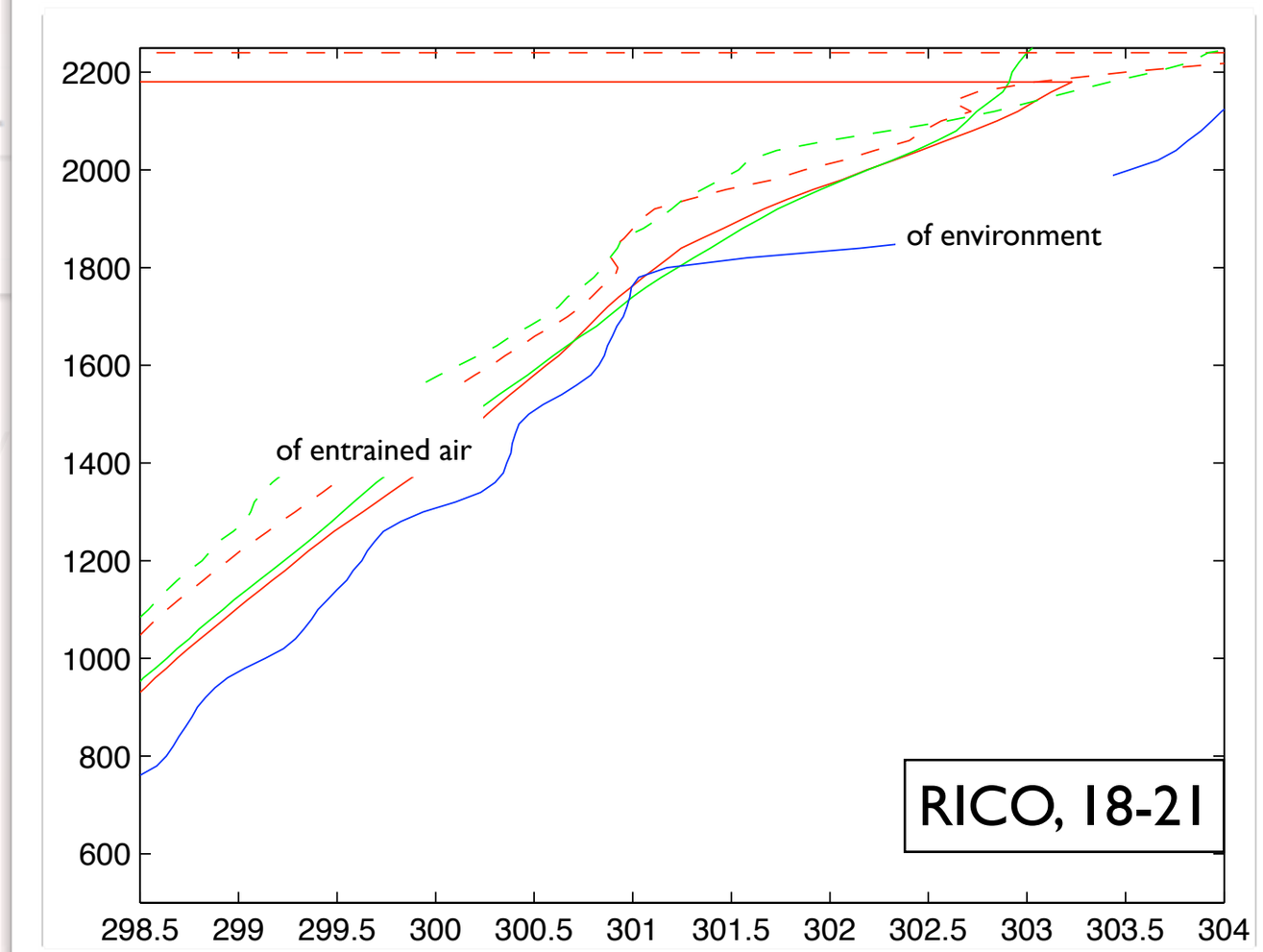

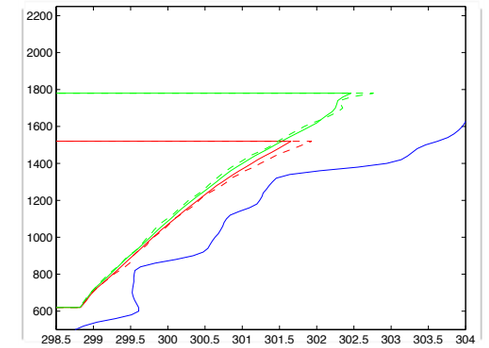

Properties of entrained air

Diagnostic liquid water potential temperature

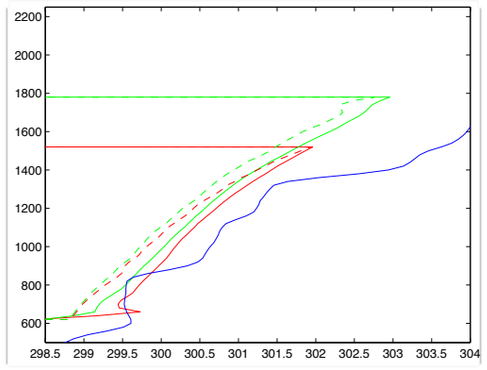

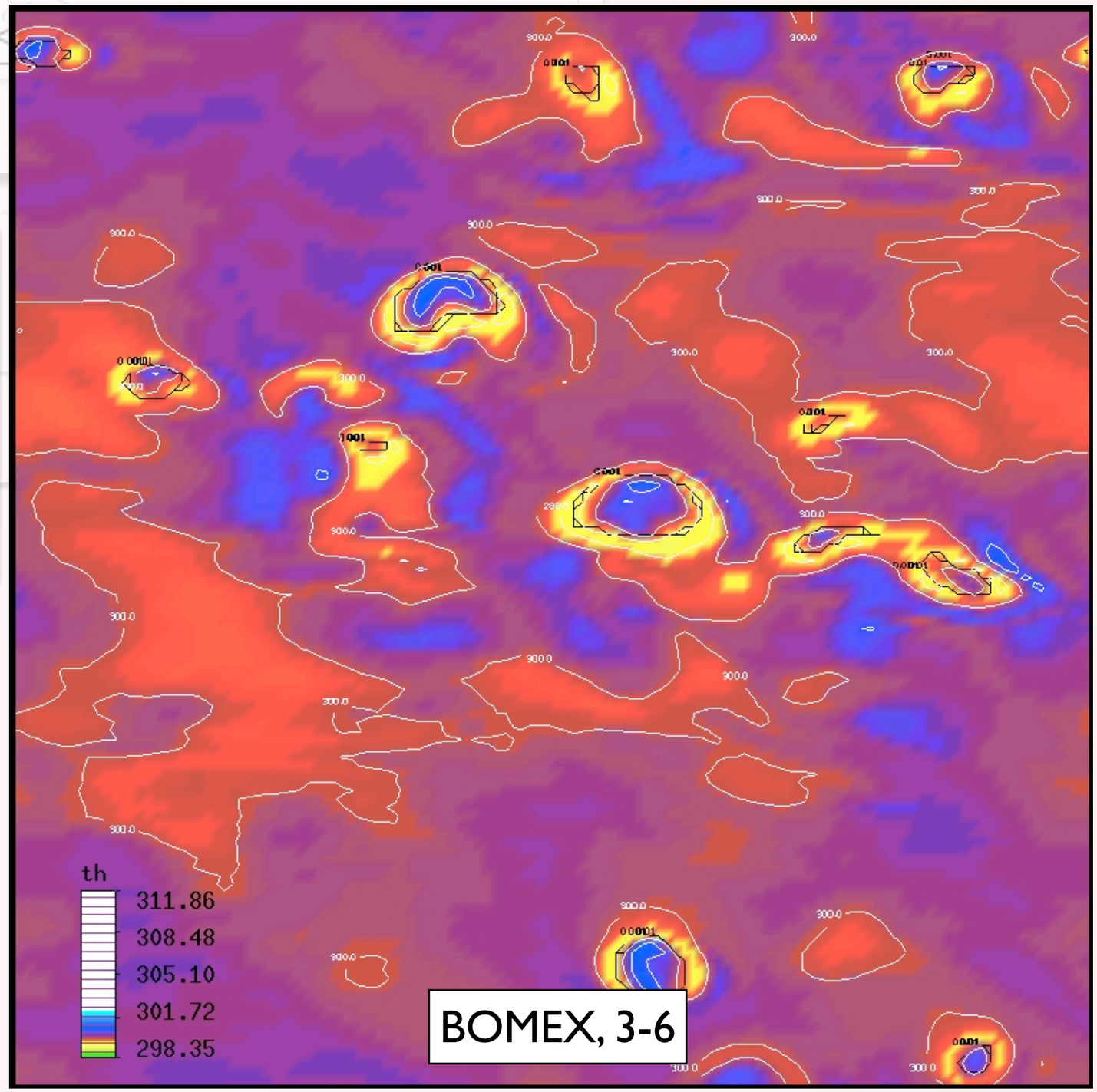

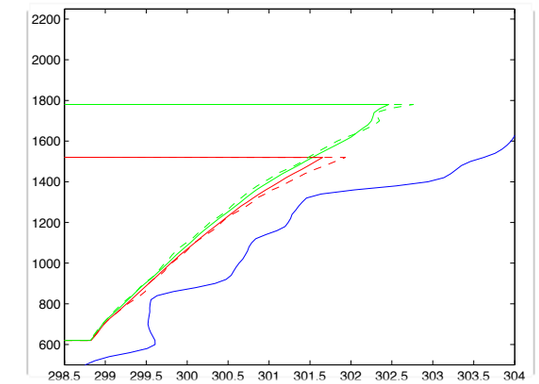

background color - potential temperature
white contours - isoline of potential temperature
black contours - isoline of qc=0.1 and 0.01 g kg $^{-1}$
z = 890 m

Conclusions

- In-cloud activation is a significant process for shallow cumulus convection
- In-cloud activation occurs at the edge of cloud core, in the region of strong increase of vertical velocity as well as supersaturation
- Differences in between mixing scenarios are mitigated by in-cloud activation
- Entrained air is close to saturation

RICO intercomparison

- The interplay between cloud micro and macro-structure remains poorly understood, is more subtle than often appreciated.

- Do aerosol or other microphysical perturbations meaningfully regulate the development of precipitation, and how does precipitation influence the macroscopic evolution of clouds?

- A total of twelve research groups successfully simulated the case using LES, with different microphysics.

JAMES-D
JOURNAL OF ADVANCES IN MODELING EARTH SYSTEMS - DISCUSSION

Controls on precipitation and cloudiness in simulations of trade-wind cumulus as observed during RICO

Margreet C. vanZanten [1], Bjorn Stevens [2,3], Louise Nuijens[2,3], A. Pier Siebesma [1,4], A. Ackerman [5], F. Burnet [6], A. Cheng [7], F. Couvreux [6], H. Jiang [8], M. Khairoutdinov [9], Y. Kogan [10], D. C. Lewellen [11], D. Mechem [12], K. Nakamura [13] A. Noda [14], B. Shipway [15], J .Slawinska [16], S. Wang [17], and A. Wyszogrodzki [18]

LES name	scientist	SGS	mom. adv.	scal. adv.	microph. scheme	P_{srf} [W m^{-2}]
1 Moment Schemes						
2DSAM	A. Cheng	HoT	M	C	KK_s	31.2
EULAG	J. Slawinska	SL	M	M		13.8
MESO-NH	F. Couvreux	DL	C	C		25.9
NHM	A. Noda	DL	C	C		12.7
SAM	M. Khairoutdinov	DL	M	C	KK_s	11.1
COAMPS	S. Wang	DL	C	M	KK	5.5
DALES	M.C. van Zanten	DL	C	C	SB	2.5
MetO	B. Shipway	SL	C	C		26.7
UCLA	B. Stevens	SL	C	M	SB	2.3
WVU	D.C. Lewellen	DL	C	M	KK	0.0
DHARMA	A.S. Ackerman	DS	M	M	25	5.9
RAMS	H. Jiang	DL	C	M	66	0.1
SAMEX	D. Mechem	DL	M	C	34	7.5

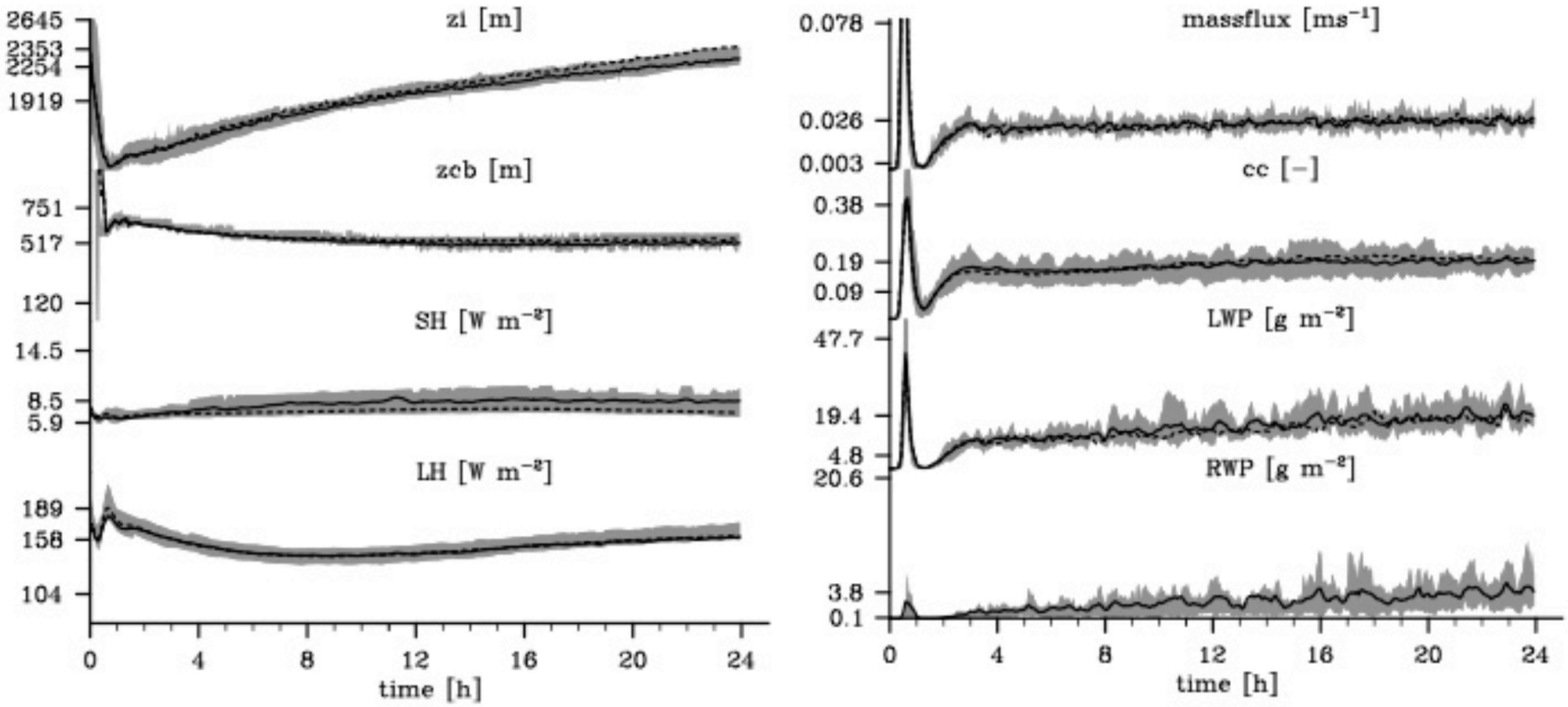

The first couple of hours of simulation time are dominated by the spin-up of the turbulence and the initial development of the cloud layer.

A longer adjustment timescale is also evident in the thermodynamics state of the subcloud layer: latent heat fluxes initially decrease, reaching a minimum after about eight hours, and cloud base height evolves more markedly over the first twelve hours than it does thereafter.

In the second half of the simulation period the temporal evolution is modest but secular.

The layer deepens continuously, latent heat fluxes increase, the mass flux and cloud cover remain relatively constant, while the liquid water path and the rain water path increase in association with the deepening cloud layer.

Values of cloud cover, surface fluxes, and the general depth of the convective layer are consistent with observations during RICO

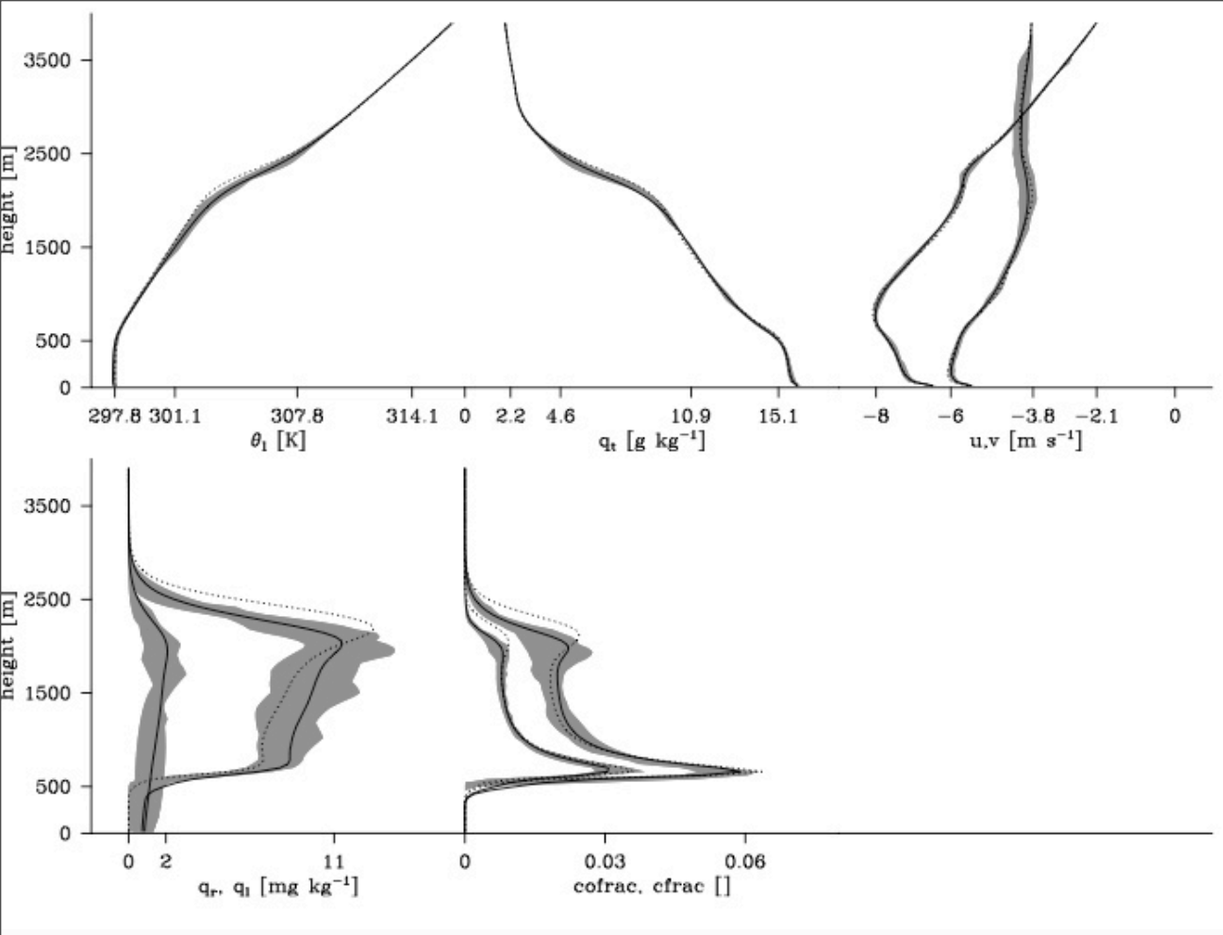

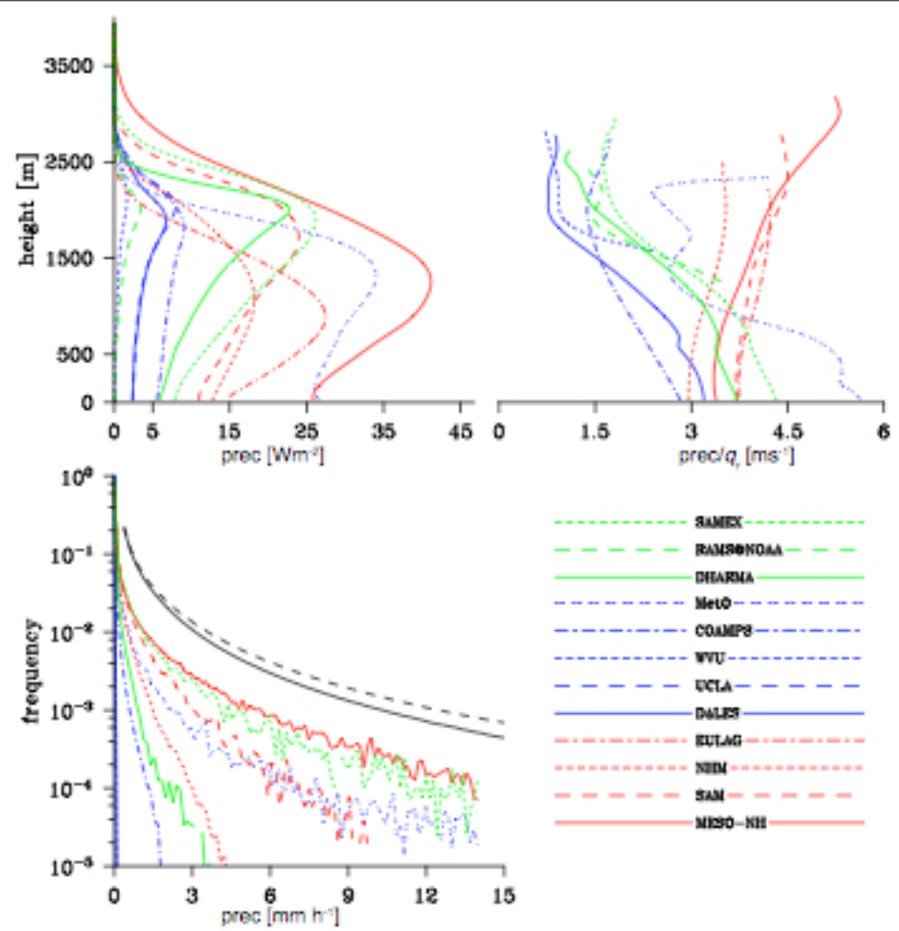

- Although the general evolution and structure of the cloud field is quite similar among models, the same cannot be said about the development of precipitation.

- The vertical structure and character of the precipitation field among the simulations differ more markedly. Some similarities: the tendency of the precipitation flux to maximize at cloud top.

- Microphysical differences appear to be more decisive than dynamical differences in our simulations ensemble no relation found in between rain rate in the precipitating case, and cloud water in the non-precipitating case.

- The effect of allowing precipitation to develop: a marked (100 m) reduction in the growth of the cloud layer; and a cooling of the sub-cloud layer, larger stability, less vigorous clouds.

- This result supports the hypothesis, that the principal mechanism through which the trade-wind layer deepens is through the evaporation of liquid water in the stable air within, and above, the trade inversion, thus gradually imbuing these layers with the properties of the cloud layer below.